Targeting Regulatory T Cells for Therapeutic Gain in Cancer Therapy

UCL Cancer Institute

University College London

A thesis presented for the Degree of Doctorate in Philosophy

Isabelle Solomon

October 2019

DECLARATION

I, Isabelle Solomon, confirm that the work presented in this thesis is my own. Where information has been derived from other sources, I confirm that this has been indicated in the thesis.

ABSTRACT

Regulatory T cell (Treg) abundance associates with diminished anti-tumour immunity and poor prognosis in human epithelial cancers, underscoring their value as an immunotherapy target. There has been limited clinical success in targeting this cell population likely due to a lack of consensus on the most selective targets for depletion of Treg cells, and the limited mechanistic insight into the activity of these antibodies *in vivo*. Recent work from our lab (Vargas et al., 2017) demonstrates that CD25 (the high affinity alpha receptor subunit for IL-2) is a selective target for the depletion of regulatory T cells in mouse and human malignancies. However, despite being a selective target, αCD25^{PC61} lacks single agent activity against tumours. Based on this, two projects were developed, both focusing on CD25 as a target for Treg depletion.

The first project focused on the development of a bispecific antibody targeting both CD25 and PD-L1, with the rationale being that Treg depletion would be targeted to the tumour (due to PD-L1 upregulation in the tumour microenvironment). The bispecific antibody was developed in the lab, and its production, characterisation and activity *in vitro* and *in vivo* is discussed in depth in Chapter 4.

The second project was initiated as a hypothesis that the *in vivo* activity of available anti-CD25 mAbs targeting human and mouse Treg cells, is likely limited by their IL-2 blocking activity. By developing a CD25 antibody which does not block IL-2 signalling, this hypothesis was tested *in vivo* in various mouse tumour models. The work presented in this thesis demonstrates the critical importance of endogenous IL-2 to the function of the CD4 and CD8 effector compartments in the context of Treg depletion and that this is key for the superior anti-tumour activity of αCD25^{NIB}.

IMPACT STATEMENT

The manipulation of the immune system to promote cancer rejection is the premise of cancer immunotherapy (Peggs, Quezada and Allison, 2008). This includes various strategies, all aiming to tilt the balance towards tumour elimination rather than escape, based on the intervention of different components of the immune response. Over the last decade, immunotherapy has revolutionised the clinical management of multiple tumours. However, the proportion of patients responding to these remain low and the search remains to develop improved agents with increased survival rates and minimal toxicity.

Regulatory T cells (Treg) are key players within the tumour's immune suppressive environment. Their presence is correlated with a bad prognosis in multiple cancer types (Shang *et al.*, 2015) while a greater ratio of effector T cells (Teff) to Tregs is associated with improved control of established tumours and a better response to immunotherapy both in humans and in mice (Quezada *et al.*, 2006; Mihm *et al.*, 2008). Therefore, developing effective strategies for Treg depletion is an important consideration in current immunotherapy approaches. There has been limited clinical success in targeting this cell population likely due to a lack of consensus on the most selective targets for depletion of Treg cells, and the limited mechanistic insight into the activity of these antibodies *in vivo*.

Whilst recent work demonstrates that CD25, the high affinity alpha receptor subunit for IL-2, is a selective target for depletion of regulatory T cells in mouse and human malignancies, anti-human CD25 antibodies have failed to deliver significant responses against solid tumours. As these antibodies were originally developed to prevent transplant rejection via IL-2 receptor blockade, we hypothesised that this particular feature could potentially limit the activity of anti-CD25 antibodies. Targeting CD25 whilst preserving IL-2 signalling should promote more potent and durable responses.

We demonstrate, for the first time, potent single agent activity of mouse anti-CD25 antibodies optimised for Treg depletion, but with preserved IL-2 signalling, and the characterization of an ADCC-enhanced anti-human CD25 (developed by Roche) with equivalent features. The data supports further development of the anti-human CD25 and pre-clinical evaluation of novel combination therapies incorporating non-IL-2 blocking anti-CD25 antibodies.

Acknowledgments

First of all, I would like to express my sincere gratitude to Professor Sergio Quezada for giving me the opportunity to work in his laboratory and for believing in me, at a time when I did not. His support and enthusiasm for science has kept me going and made this thesis possible. I would like to express my gratitude to my co-supervisor, Professor Karl Peggs, for his friendly advice and guidance throughout this project.

I would like to thank CRUK for funding this PhD.

A massive thank you to TUSK Therapeutics and Roche, as collaborating with these companies gave me the tools and support needed to get this project done quickly and efficiently.

A special thanks goes to Frederick Arce Vargas, for always being there for me and for his patient guidance, support and motivation throughout this PhD as well as my MSc.

Then I would like to specially thank Dimitrios Zervas, without whose day-to-day help with experiments, I would not be able to finish this project.

Huge thank you and lots of love to Dafne Franz, Emine Hatipoglu, Anna Sledzinska, and Mariana Werner Sunderland. Our close friendship has kept me going during difficult times and I'll forever be grateful for all of you being there by my side.

Thank you to Enrique from Kerry Chester's lab for all his help with antibody production.

Thank you to the UCL Cancer Institute that has actually turned into a home for me these past few years. This has been an amazing experience, with many ups and downs, but one that I would never change.

An enormous thank you to my family, who have always supported me in my studies. I am especially grateful to my mom, for her unwavering belief in me and for standing by my side throughout all these years.

Table of contents

LIST OF FIGURES

LIST OF TABLES

ABBREVIATIONS

2-MEA: 2-mercaptoethylamine HCl

4-1BBL: 4-1BB ligand

Ab: Antibody

ADCC: Antibody-dependent cell-mediated cytotoxicity

ADCP: Antibody-dependent cellular phagocytosis

APC: Antigen presenting cell

ATP: Adenosine triphosphate

BFP: Blue fluorescent protein

BsAb: Bispecific antibody

BTLA: B and T lymphocyte attenuator

CAR: Chimeric antigen receptor

CD: Cluster of differentiation

CEX: Cation exchange chromatography

cFAE: Controlled fab arm exchange

CTL: Cytotoxic T lymphocyte

CTLA-4: Cytotoxic T lymphocyte antigen-4

DC: Dendritic cell

EGFR: Epidermal growth factor receptor

ESI-MS: Electrospray ionisation mass spectrometry

Fab: Fragment, antibody binding

Fc: Fragment, crystallizable

FcγR: Fc gamma (γ) receptor

GFP: Green fluorescent protein

GITR: Glucocorticoid-induced tumour necrosis factor receptor family related protein

GITRL: GITR ligand

GM-CSF: Granulocyte-Macrophage colony stimulating factor

GVHD: Graft-versus-host disease

GzmB: Granzyme B

HC: Heavy chain

HIC: Hydrophobic interaction chromatography

HNSCC: Head and neck squamous cell carcinoma

ICOS: Inducible T-cell Co-stimulator

ICOSL: Inducible T-cell Co-stimulator ligand

IDO: Indoleamine 2,3-dioxygenase

IgG: Immunoglobulin G

IgSF: Immunoglobulin super-family

IFNγ: **I**nterferon γ

IL-2: Interleukin 2

ITAM: Immunoreceptor tyrosine-based activating motif

ITIM: Immunoreceptor tyrosine-based inhibitory motif

irAE: Immune related adverse events

Kd: Dissociation constant

LAG3: Lymphocyte activation gene 3

LC: Light chain

LN: Lymph node

mAb: Monoclonal antibody

MAPK: Mitogen-activated protein kinase

MDSC: Myeloid-derived suppressor cells

MHC-I: Major Histocompatibility complex class I

MHC-II: Major Histocompatibility complex class II

mOS: Median overall survival

MSI-H: Microsatellite instability-high

nAb: Neutralising Antibody

NK: Natural Killer cell

NSCLC: Non-small cell lung cancer

OS: Overall survival

OX-40L: OX-40 ligand

PCR: Polymerase chain reaction

PBMC: Peripheral blood mononuclear cell

PD-1: Programmed death-1

PD-L1: Programmed death-ligand 1

PD-L2: Programmed death-ligand 2

PEI: Polyethylenimine

PI3K: Phosphatidylinositol-3-Kinase

PFS: Progression free survival

SDS-PAGE: Sodium dodecyl sulfate polyacrylamide gel electrophoresis

TCR: T-cell receptor

Teff: Effector T-cell

TGFβ: Transforming growth factor-β

Th1: Type 1 T helper

Th2: Type 2 T helper

TIGIT: T cell Immunoglobulin and ITIM (immunoreceptor tyrosine-based inhibitory motif) domain

TIL: Tumour infiltrating lymphocyte

TIM-3: T-cell Immunoglobulin- and mucin-domain-containing 3

TME: Tumour microenvironment

TNFα: Tumour necrosis factor α

TNFR: Tumour necrosis factor receptor

TNFRSF: Tumour necrosis factor receptor superfamily

Treg: Regulatory T-cell

UCOE: Ubiquitous chromatin opening element

WT: Wild-type

1 GENERAL INTRODUCTION

1.1 BASICS OF IMMUNOLOGY

The main role of the immune system is defence against pathogens. The immune system consists of two parts; the innate immune system, which is our body's first line of defence against pathogens, and the adaptive immune system, which is more specialised and characterised by antigen-specific responses and the ability to mount immunological memory. The innate immune system is made up of epithelial barriers, the complement system, natural killer (NK) cells, mast cells, eosinophils, basophils, macrophages, neutrophils and dendritic cells (DC). This branch of the immune system recognises structures which are common to many pathogens but are absent in normal host cells and is responsible for providing immediate protection against a broad variety of pathogens. The adaptive immune system, in contrast to the innate immune system, generates immunological memory, which means that once an individual is exposed to a pathogen, a re-exposure to the same antigen will lead to a quicker and more powerful response. The adaptive immune system is further classed into two groups; humoral immune responses and cell-mediated immune responses, and begin when a B or T lymphocyte is exposed to its cognate antigen. In the humoral immune response, B cells bind its cognate antigen which stimulates their proliferation and differentiation into plasma cells which secrete antibodies against the antigen. Cell-mediated responses, on the other hand, refer to T cells, which eliminate pathogens themselves (Murphy, 2017).

Upon exposure to its antigen, a T cell can proliferate and differentiate into different types of effector T cells; cytotoxic T cells, helper T cells, regulatory T cells and memory cells. Cytotoxic T cells kill cells which are infected with viruses or other intracellular pathogens containing the antigen. Helper T cells activate the functions of other cells, such as production of antibody by B cells and killing of engulfed pathogens by macrophages. Regulatory T cells control

steady state immunity and limit excessive immune responses by suppressing the activity of other lymphocytes (Abbas, Lichtman and Pillay, 2015). The various ways by which Tregs suppress the immune response against tumours are discussed in detail in 1.2.3 – “The role of Tregs in the TME”.

The part of the antigen which is recognised by a T Cell Receptor (TCR) or antibody is known as an antigenic determinant or epitope. As opposed to antibodies, T cell receptors are able to recognise epitopes which are buried within antigens. However, these must first be degraded by proteases and the resulting epitope delivered onto a self molecule – Major Histocompatibility Complex (MHC) molecule, of which there are two main types; MHC Class I and MHC Class II. These differ in their structures, but both bind peptide using a groove present on the outer surface, following which the complex is transported to the surface of the cell and exposed to T cells. Internal peptides are usually loaded and presented by MHC Class I molecules, while extracellular peptides are phagocytosed by specialised antigen presenting cells (APC), processed inside the cell, bound and presented via MHC Class II. $CD8^+$ T cells recognise peptides that are bound to MHC class I molecules whereas $CD4^+$ T cells recognise peptides presented by MHC Class II (Murphy, 2017). How these cells recognise and eliminate tumour cells is discussed in more detail below in “1.2.2 - Generation of an immune response against tumours”.

1.2 ROLE OF THE IMMUNE SYSTEM IN THE CONTROL OF TUMOUR GROWTH

The six hallmarks of cancer, proposed by Hanahan and Weinberg in 2000, define a particular set of characteristics that a normal cell must acquire to become malignant. These features include self-sufficiency in growth signals, evasion of apoptosis, lack of anti-growth signals, limitless replication, the induction of angiogenesis, as well as the activation of tissue invasion and metastasis. Significant advancement in cancer research over the last fifteen years led to two new general characteristics being considered as the hallmarks

of cancer, namely the reprogramming of energy metabolism and the evasion of immunosurveillance, the latter of which was validated by Schreiber and colleagues in 2004 (Dunn, Old and Schreiber, 2004b). It is now clear that the alterations which occur in the process of the transformation of a normal cell into a neoplastic cell are part of a multistep process which is controlled at every step by both cell-intrinsic anti-tumour mechanisms—such as the control of proliferation by tumour suppressors—and cell-extrinsic checkpoints, which includes the control of the tumour by the immune system, also known as the cancer immunosurveillance theory (Zitvogel, Tesniere and Kroemer, 2006). This theory was originally proposed by Burnet and Thomas in the late 1950s and suggested that cells and tissues are continuously being monitored by the immune system and that this so-called surveillance is able to detect and eliminate most of the tumours that are developing before these become clinically apparent. Therefore, any tumours that have arisen, have succeeded in not being detected by the immune system or have suppressed the immune system in one way or another (Burnet, 1957; Dunn *et al.*, 2002).

1.2.1 Immunoediting model

Further research into the cancer immunosurveillance theory both in murine models and in human cancers led to the idea that the immune system not only protects the host against the development of cancers, but also has the ability to promote the development of tumours which have a lower immunogenicity (i.e. a lower ability of the tumour antigen to elicit an immune response) and allows them to escape the immune system (Shankaran *et al.*, 2001). This led to the principle of cancer immunosurveillance being further characterised and broadened to include several aspects of the role of the immune system in the eradication of cancer as well as its promotion, the so-called “sculpting”. This model was proposed by Ikeda, Old and Schreiber in 2002 and consists of three different phases: elimination, equilibrium and escape (**Figure 1.1**).

The model is based on the fact that the immune system has the ability to either stop or promote tumour growth by altering the immunogenicity of the tumour or by modulating the anti-tumour response (Dunn *et al.*, 2002; Ikeda, Old and

Schreiber, 2002). The first phase involves the detection and elimination of transformed cells by the molecules of the innate and adaptive immune system (Dunn, Old and Schreiber, 2004a). During the process of transformation, cells acquire the expression of tumour-associated antigens and of molecules that can initiate an immune response and favour their elimination, such as natural killer (NK)-cell activating receptor NKG2D (NK group 2, member D) (Bauer *et al.*, 2018). If the tumour cells are not eradicated during the elimination phase, the process continues to a phase of equilibrium in which the tumour is held under pressure of the immune system and neither grows nor regresses. This balance can be disrupted by inhibition of the immune response as a result, for example, of T cell exhaustion or accumulation of regulatory T cells. It can also be altered by the acquisition of new mutations in the tumour cells that cannot be recognized by the immune system. When this balance is broken, the tumour "escapes" the immune pressure and can continue to grow (Dunn, Old and Schreiber, 2004a). Examples of mechanisms by which tumours manage to escape the immune system are summarised in **Table 1.1.**

Only in the last 30 years has the principle of cancer immunosurveillance been acknowledged due to accumulation of evidence from genetically engineered mice as well as from clinical studies, which support the notion that the immune system does in fact have the ability to stop the development of tumours as well as their progression in both viral and non-viral-related cancers. Amongst the most relevant research pointing out to the fact that the immune system sees but fails to control cancer is the identification and targeting of immune regulatory (or immune checkpoint) pathways. This intensive research led to the Nobel Prize in physiology or medicine being awarded in 2018 to James P. Allison and Tasuku Honjo for their discovery of cancer therapy by inhibition of negative immune regulation, i.e. immune checkpoint blockade (Nobel Media AB, 2018), which has revolutionised cancer treatment and is discussed in detail in the "Tumour Immunotherapy" section in 1.4.4.

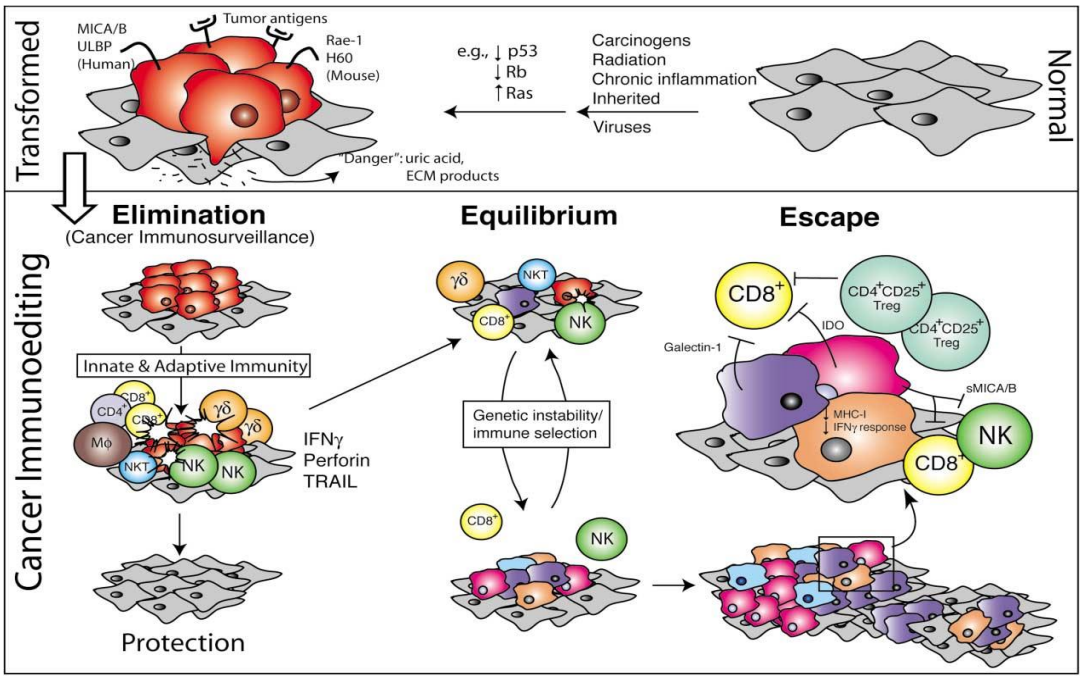

Figure 1.1. The Three Phases of the Cancer Immunoediting Model.

Normal cells (gray) undergo transformation and become tumour cells (red) (top). In the elimination phase, the tumour may be eradicated by the molecules of the innate and adaptive immunity. However, if the tumour is not eliminated in this phase, the tumour cells enter an equilibrium phase. The escape phase begins when tumour variants are produced and are able to evade the immune system by a number of different mechanisms, described in the text (Dunn, Old and Schreiber, 2004a)

ESCAPE MECHANISM	EXAMPLES	REFERENCE
Initiated by tumour cells		
Becoming undetectable	Decreased expression or loss of expression of MHC class I molecules (e.g. in melanoma)	(So *et al.*, 2005)
	Decreased expression of molecules that are involved in the processing of antigens and their presentation by MHC class I molecules, such as transporter associated with antigen processing 1 (TAP1) and tapasin (e.g. in colorectal carcinoma)	(Atkins *et al.*, 2004)
Inhibition of cytotoxicity	Overexpression of the serine-protease inhibitor PI9, which leads to the inhibition of the granzyme B/perforin pathway involved in the lysis and killing of target cells	(Medema *et al.*, 2001)
	Decreased expression or mutation of death receptors	(Ochsenbein, 2005)
Dependent on immune cells		
T cell exhaustion	Chronic antigen exposure in the absence of co-stimulatory molecules	(Antonia, Extermann and Flavell, 1998)
Decrease of the T cell effector/regulators ratio in the TME	Increase in $CD4^+CD25^+$ regulatory T cells which leads to the inhibition of immune responses against tumours	(Onizuka *et al.*, 1999)
Direct suppression of the immune response by tumours	Increased production of nitric oxide by tumours and greater arginase-1 function	(Bronte and Zanovello, 2005)
	Expression of TGF-β which stimulates angiogenesis and inhibits the function of CTL and NK cells	(Beck, Schreiber and Rowley, 2001)

Table 1.1. The different mechanisms by which tumours are able to escape the immune system, both from the tumour and immune cells' perspective.

1.2.2 Generation of an immune response against tumours

For successful T cell activation as part of an immune response, the cells must receive three signals. The first signal involves the recognition of an antigen in the form of peptide-MHC complexes, which are expressed by antigen presenting cells (APCs) which present the antigen to the T cells. The second signal depends on a balance between the engagement of co-stimulatory or co-inhibitory receptors in the T cells (Schwartz *et al.*, 2002). The third signal comes from cytokines which regulate the type and extent of the immune response that is generated (Jonuleit *et al.*, 2001). A T cell can only be stimulated in the presence of signals 1 and 2, and a lack of either of these signals results in T cell tolerance to the presented antigen, whereby the T cell is rendered unresponsive to the antigen (Sharpe and Freeman, 2002). The balance between co-stimulatory and co-inhibitory signals in the tumour microenvironment is critical as it is needed both for effective immune responses to pathogens and cancer cells as well as for maintaining tolerance to self-molecules (Peggs, Quezada and Allison, 2008).

On one side of this balance are the $CD8^+$ Cytotoxic T Lymphocytes (CTL), Natural Killer (NK) cells, and $CD4^+$ helper T cells, all of which favour the elimination of the tumour (**Figure 1.2).** $CD8^+$ T cells promote tumour elimination through their capacity to directly engage and kill transformed cells by the secretion of Granzyme B and perforin. Perforin is a pore-forming protein, which allows Granzyme to enter the cell, cleave and activate caspases and their substrates, leading to the induction of apoptosis (Barry and Bleackley, 2002; Milstein *et al.*, 2011). NK cells can also promote tumour elimination by the secretion of Granzyme B and perforin, but as opposed to $CD8^+$ T cells, do not need priming or recognition of a certain antigen. They express activating and inhibitory receptors on their surface, with the balance of these signals regulating the recognition of healthy cells. Their effector functions (such as cytotoxicity, cytokine production and proliferation) are triggered by “non-healthy” cells in a number of ways; loss of self molecules such as MHC class I (which bind inhibitory receptors on NK cells), or by the expression of ligands which bind to activatory receptors and by pass the

inhibitory signals. In addition, they express CD16, FcγRIIIa, which upon binding to antibody-antigen complexes can trigger ADCC of those cells (Morvan and Lanier, 2016). A subset of $CD4^+$ T cells, T-helper 1 (Th1) $CD4^+$ T cells are also able to promote tumour rejection. These cells help anti-tumour responses by production of cytokines such as IL-2 and IFNγ (Quezada *et al.*, 2010).

On the other side of the balance (**Figure 1.2**) are the regulatory T cells (T_{reg} cells), which suppress the immune response, mechanisms of which will be discussed in detail in the next section in 1.2.3 – "Role of Tregs in the TME". Myeloid Derived Suppressor Cells (MDSC) are also present in the tumour microenvironment (TME), and can greatly suppress anti-tumour activity in a variety of ways, such as induction of apoptosis of T cells and NK cells, damaging antigen recognition by T cells as well as their proliferation and migration. In addition, they produce immunosuppressive cytokines such as IL-10 and TGFβ (Umansky *et al.*, 2016) and their presence is thought to promote tumour angiogenesis as well as metastasis (Gabrilovich and Nagaraj, 2009). These cells express co-stimulatory and co-inhibitory receptors on their surface, which modulate TCR-mediated T cell activation and are discussed below (Schwartz *et al.*, 2002).

1.2.3 Co-inhibitory and Co-stimulatory receptors

There are two main families of co-stimulatory and co-inhibitory receptors: the immunoglobulin (Ig) superfamily (Esensten *et al.*, 2016) and the tumour-necrosis factor (TNF) superfamily (Ward-Kavanagh *et al.*, 2016). Co-stimulatory molecules belong to both the Ig superfamily and the TNF superfamily. The first co-stimulatory receptor described on T cells was CD28. This receptor is constitutively expressed on the surface of T cells and binds to ligands B7-1 and B7-2, which are expressed on B cells, monocytes, dendritic cells (DCs) and T cells (Lenschow, Walunas and Bluestone, 2002; Esensten *et al.*, 2016). This pathway signals via the phosphatidyl-inositol-3-kinase (PI3K)/Akt/Nuclear Factor kappa B (NF-kB) and the mitogen-activated kinase

(MAPK) pathway, both of which promote cellular proliferation, survival as well as memory development and the production of cytokines (Song *et al.*, 2008).

We now know there are many other co-stimulatory receptors on T cells including ICOS, 4-1BB, OX40, GITR (**Figure 1.2**). The latter three are part of the TNF superfamily, which upon high affinity binding to their ligands leads to receptor clustering and initiation of signal transduction pathways (either via their death domain, by engaging TRAF family of ubiquitin E3 ligases or by acting as decoy receptors) leading to various cellular responses, including survival, death or differentiation (Ward-Kavanagh *et al.*, 2016).

Amongst co-inhibitory molecules, CTLA-4 and PD-1 are the most characterised targets. They belong to the B7-CD28 family of receptors. Cytotoxic T-Lymphocyte Antigen 4 (CTLA4) is a cell surface receptor which is rapidly upregulated following T cell activation and binds the B7-1 and B7-2 ligands with much greater affinity than the CD28 receptor, leading to downregulation or termination of T cell responses. CTLA4 ligation by B7 ligands leads to a decreased secretion of cytokines as well as the inhibition of proliferation of T cells. It therefore acts as a regulator of naive and effector antigen-specific T cell activation to prevent aberrant effector responses (Walunas *et al.*, 1994; Lenschow, Walunas and Bluestone, 2002). PD-1 is expressed on T cells after activation, and its ligands (PD-L1 and PD-L2) are expressed on the surface of antigen presenting cells as well as tumour cells. Ligation of the PD-1 receptor with its ligands results in inhibitory signalling in T cells and thus limits their effector functions (Latchman *et al.*, 2001).

Antibodies blocking the interaction of these receptors with their natural ligands are now routinely used in the treatment of specific cancers and will be discussed in 1.4.4 - Tumour Immunotherapy chapter; “Immune checkpoint blockade”.

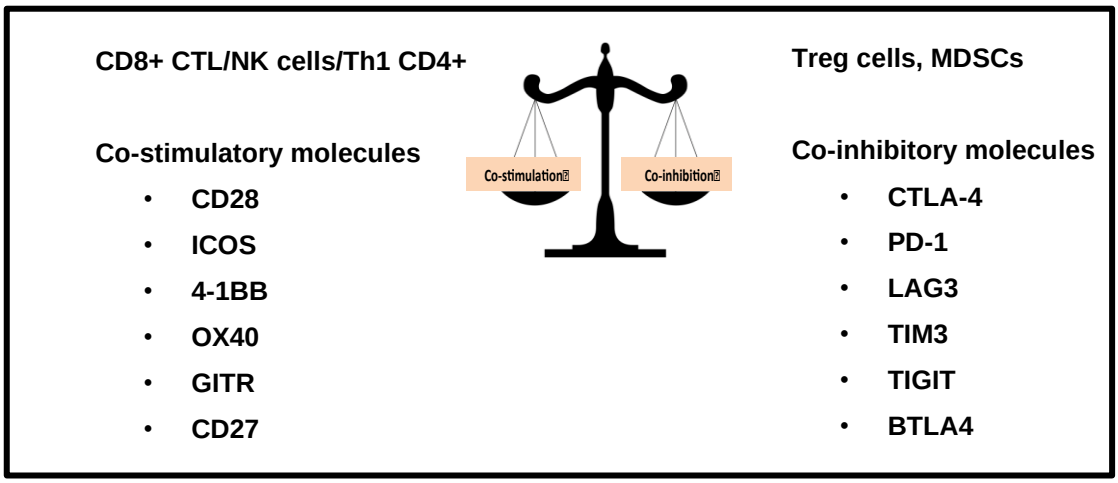

Figure 1.2. Balance between co-stimulatory and co-inhibitory signals in the tumour microenvironment.

Summarised from (Capece *et al.*, 2012; Pardoll, 2012; Śledzińska *et al.*, 2015)

1.2.4 Role of Regulatory T cells (Tregs) in the TME

As mentioned above, regulatory T cells (Treg) are key players within the tumour's immune suppressive environment. Their presence is correlated with a bad prognosis in multiple cancer types (Shang *et al.*, 2015) while a greater ratio of effector T cells (Teff) to Tregs is associated with improved control of established tumours and a better response to immunotherapy both in humans and in mice (Quezada *et al.*, 2006; Mihm *et al.*, 2008). Therefore, developing effective strategies for Treg depletion is an important consideration in current immunotherapy approaches, which will be discussed in more detail further on in the thesis in the Immunotherapy Chapter: 1.4.5 – "Targeting Tregs for anti-cancer therapy".

Tregs act in a number of ways to suppress the immune response against cancer, which is summarised in **Figure 1.3** below. Firstly, Tregs compete for IL-2 binding, as well as its consumption, thereby limiting the availability of IL-2 to other cells (Takahashi *et al.*, 1998; Thornton and Shevach, 1998). This is due to the fact that Tregs are highly dependent on IL-2 for survival and proliferation, but are unable to produce it in enough quantities to sustain themselves. However, as they constitutively express high levels of CD25, they are able to bind and compete for IL-2 with neighbouring effector cells.

There is some research which argues against IL-2 scavenging as a major mechanism of suppression. This includes studies showing that Tregs from $CD25^{-/-}$ mice continue to be suppressive *in vitro* (Fontenot *et al.*, 2005), as well as others showing that mice which carry a deletion of CD122 in peripheral Tregs do not suffer from autoimmune illnesses (Malek *et al.*, 2002). However, further studies have diminished these arguments by illustrating that Tregs lacking CD122 are still able to respond to IL-2 (Bayer, Yu and Malek, 2007). This was further supported by research showing that Tregs from $CD25^{-/-}$ mice are unable to stop encephalomyelitis from occurring in these mice (Furtado *et al.*, 2002).

Evidence for IL-2 depletion as a mechanism for Treg suppression came from a few studies which showed that the depletion of IL-2 or blocking of its binding replicated the effect of Treg cells on activated T cells. Moreover, adding IL-2 or blocking its uptake by Treg cells was shown to be enough to remove the suppressive capacities of Tregs *in vitro* (de la Rosa *et al.*, 2004; Barthlott *et al.*, 2005; Brandenburg *et al.*, 2008). Research by the Lenardo group went on to show that Tregs induced apoptosis of effector $CD4^+$ T cells *in vitro* and *in vivo* in a mouse model of inflammatory bowel disease. This was attributed to the lack of common-gamma chain cytokines and showed that cytokine-deprivation-induced apoptosis is an important mechanism by which Tregs inhibit effector T cell responses. They also looked at the supernatant of Teff-Treg co-cultures and compared those to cultures containing Teff-only. Lower IL-2 concentrations were shown in the co-cultures and this was attributed to Treg consumption rather than less production by Teff cells. Taken all the data into account, they strengthened the view that IL-2 depletion by Treg cells is an important mechanism by which Tregs are able to be suppressive (Pandiyan *et al.*, 2007).

Other mechanisms include Tregs inhibiting the maturation of APCs and therefore the consequent activation of T cells. This is due to the expression of high levels of CTLA4, which as explained previously, binds to the B7 molecules B7-1 and B7-2 on antigen presenting cells, not only competing with the CD28 receptor for binding, but also triggering inhibitory signalling in APCs

(Walker and Sansom, 2011). Moreover, Tregs produce immunosuppressive cytokines such as IL10, IL35 and TGFβ (Jarnicki *et al.*, 2006) suppressing the immune response. Furthermore, Tregs produce high amounts of ATP which they are able to convert into adenosine via the expression of CD39 and CD73 (Deaglio *et al.*, 2007) which inhibits proper T cell activation by binding to the adenosine A2A receptor (A2AR), leading to the immune suppression of Teff cells as well as APCs. Tregs are also able to secrete Granzyme as well as perforin, which is an important mechanism by which Tregs suppress the function of effector T cells (Grossman *et al.*, 2004).

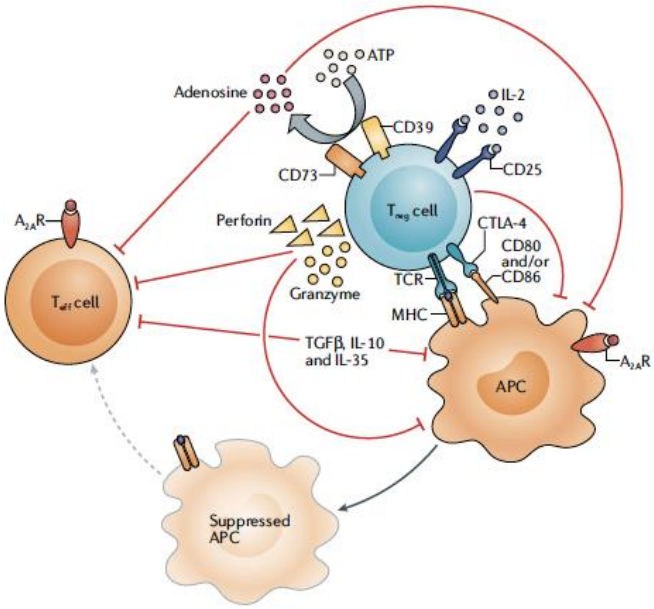

Figure 1.3. Variable mechanisms of Treg cell-mediated immunosuppression.

(Togashi, Shitara and Nishikawa, 2019)

1.3 ANTIBODY STRUCTURE AND FUNCTION

As mentioned above, antibodies are produced by the immune system to bind and neutralise a variety of foreign targets. Of those, IgG antibodies are the main class of immunoglobulins produced during an immune response against foreign antigens (Bournazos and Ravetch, 2017).

Whole mAbs are large molecules (140-160kDa) and consist of 4 polypeptide chains; two identical heavy and 2 identical light chains, bound together by disulphide bonds and interchain non-covalent interactions. Heavy and light chains each have variable and constant regions, which combine to form an antigen-binding site that determines the antigen-binding specificity of the antibody. Therefore, each antibody has two identical variable regions, and so has two identical antigen-binding sites. The variable region (Fab region) of the antibody binds to a specific target on a cell and thus confers specificity and affinity to the antibody. The constant region of the antibody contains an Fc domain (**Figure 1.4**) which is able to bind to different Fc receptors (FcRs), receptors that are present on immune cells, and are able to trigger antibody-mediated effector functions by different cells of the innate and adaptive immune system (DiLillo and Ravetch, 2015). Due to both regions of the antibody having a function, IgG antibodies are referred to as bifunctional molecules. After years of research, the importance of the interactions between the Fc domain and FcγRs is very well-known and this will be discussed in further detail below in the following section in 1.3.1 – “The role of FcγRs”.

Figure 1.4. Structure of an antibody molecule.

(Genmab, 2019)

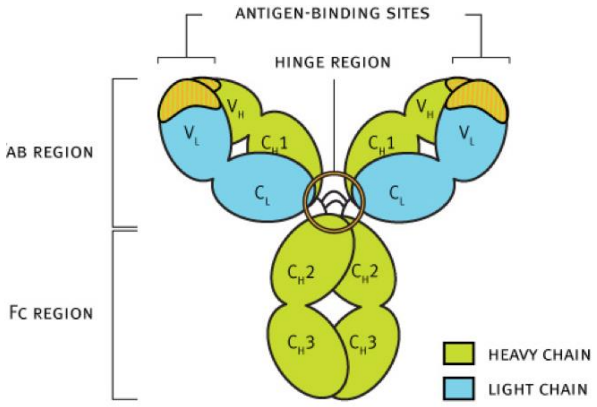

Antibody binding to its target on tumour cells can lead to a number of different effects (Barnhart and Quigley, 2017).

- block protein-protein receptor interactions
- deplete suppressive subsets
- act as agonists of co-stimulatory receptors to increase activation of target cells
- blocking of certain growth survival signals
- activation of apoptosis
- decrease in angiogenesis in the TME
- killing of tumour cells via different mechanisms initiated by the Fc region (discussed in more detail below in 1.3.1)

1.3.1 Role of FcγRs

As stated above, the Fc domain of an IgG molecule mediates a variety of effector functions by interacting specifically with different FcγRs expressed on immune cells. There are 2 types of FcγRs which differ in terms of their functionality; activating FcγRs or inhibitory FcγRs. The activating group includes murine FcγRI, FcγRIII and FcγRIV, as well as human FcγRI, FcγRIIa and FcγRIIIa. These all signal via their intracellular immunoreceptor tyrosine-based activation motif (ITAM). On the other hand are the inhibitory FcγRs, of which there's only one of both human and mouse subtypes, the FcγRIIb, which signals inhibitory signals via its intracellular immunoreceptor tyrosine-based inhibitory motifs (ITIM) (**Figure 1.5**) (Nimmerjahn and Ravetch, 2010). All of these receptors apart from FcγRI, do not bind to monomeric IgG at normal physiological levels, as they are of low/intermediate affinity. Therefore, these receptors will only bind to immune complexes or targets coated with an antibody, which then leads to cross-linking of the receptors and the activation of cellular signalling. Binding of these IgG immune complexes to activating FcγRs leads to receptor clustering and aggregation. This leads to the recruitment of Syk and Src family kinases to the intracellular domains (Bournazos and Ravetch, 2017). Interaction of these kinases with the ITAMs of activating FcγRs leads to the phosphorylation and activation of various pro-inflammatory signalling pathways that includes phosphorylation of different

kinases, remodelling of actin, influx of Ca+ and increased expression of pro-inflammatory and pro-survival genes (Odin *et al.*, 1991; Swanson and Hoppe, 2004). This then leads to changes in the functional activity of innate leukocytes. For this reason, FcγR activation is strictly controlled by FcγRIIb, which antagonises the signalling of activating FcγRs. FcγRIIb receptor cross-linking leads to phosphorylation of the ITIMs which leads to the recruitment of SHIP family phosphatases which hydrolyse phosphatidylinositol 3,4,5-triphosphate to phosphatidylinositol 4,5-biphosphate, whose production prevents recruitment of Src kinases and PLCγ and thus limits further activation (Ono *et al.*, 1996).

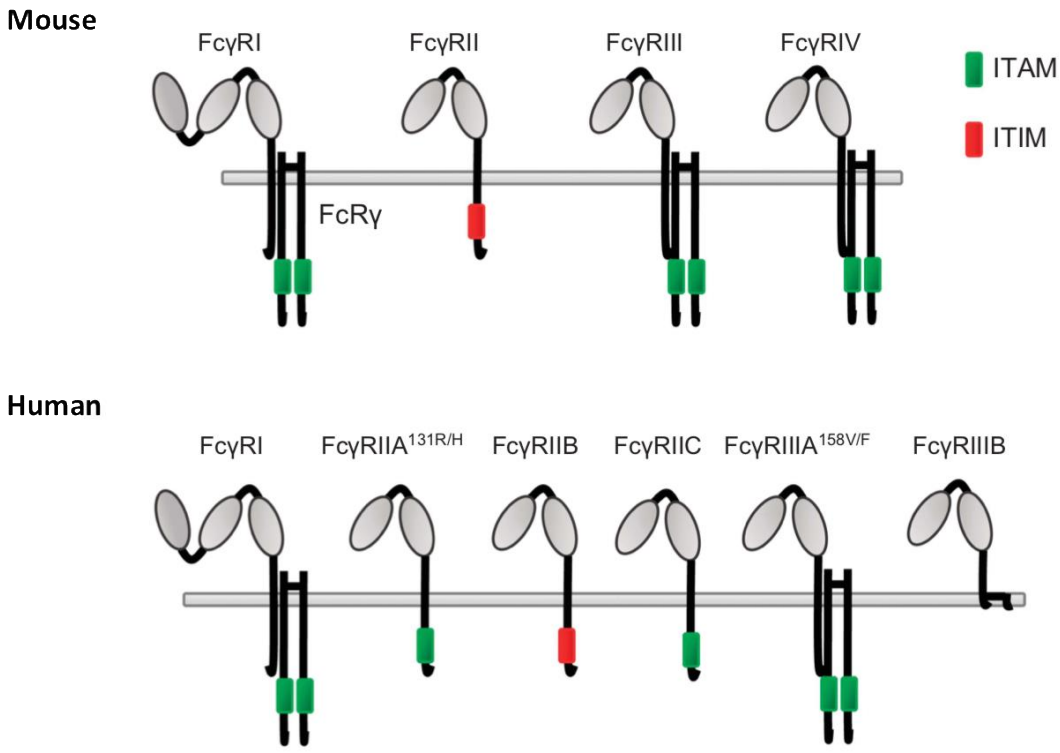

Figure 1.5. Activating and inhibitory FcgRs in Mouse and Humans.

(Barnhart and Quigley, 2017)

FcγRs are expressed on a variety of cells in a characteristic pattern as is shown in **Table 1.2**. Different cell types often express more than one FcγR at a given time. In addition, expression of these can be changed by chemokines and cytokines which affect this profile (e.g. IFNγ leads to expression of FcγRI on myeloid cells and FcγRIIb on eosinophils) (Boruchov *et al.*, 2005; Dhodapkar *et al.*, 2007). Most effector cells express both activating and

inhibitory receptors on its surface, which will bind to these Fc domains on antibodies. Therefore, the outcome of the interaction between an antibody Fc region and FcγR depends on the relative ratio of the binding affinities to these receptors. Classic examples of these are the mIgG2a and mIgG1 antibody which differ greatly in their affinities to activating receptors; with mIgG2a binding very strongly to activating FcγRIV versus inhibitory receptor FcγRIIB, and mIgG1 preferentially binding to the inhibitory receptor FcγRIIB (Nimmerjahn and Ravetch, 2005). Based on these affinities, each antibody subtype has an activating: inhibitory ratio, known as the A:I ratio, which needs to be considered when designing an antibody for therapy. mIgG2a antibodies have a ratio of approximately 70, with mIgG1 being 0.1. These translate *in vivo*, where mIgG2a isotype antibodies are very capable of killing target cells bound by antibody, as opposed to mIgG1 which shows very little killing activity in vivo (Nimmerjahn and Ravetch, 2007b).

Table 1.2. Human and mouse FcgR homologues.

+ indicates expression, +i inducible expression, - no expression, +/- minimal expression. [a]Memory CD8 T cells intrinsically express functional FcgRIIβ in mice. [b]FcgRIIβ is expressed by a subset of human NK cells. (Furness *et al*., 2014).

Mouse	FcgRI	FcgRIII	FcgRIV	FcgRIIb
Distribution:				
B cells	-	-	-	+
Dendritic cells	+	+	+	+
Macrophages	-	+	+	+
Neutrophils	-	+	+	+
NK cells	-	+	+	-
T cells	-	-	-	+/- [a]

Human	FcgRI	FcgRIIa	FcgRIIIa	FcgRIIb
Distribution:				
B cells	-	-	-	+
Dendritic cells	+	+	-	+
Macrophages	+	+	+	+/-
Neutrophils	+i	+	+	+/-
NK cells	-	-	+	+/- [b]
T cells	-	-	-	-

Similar trends are seen with human IgGs, but these show either very strong binding affinity to FcγRs or low, with no differential affinities between the activating and inhibitory receptors. Examples of these are the hIgG1 and hIgG3 which are known to bind with high affinity to FcγRs, versus hIgG2 and hIgG4 which bind weakly to these receptors (Nimmerjahn and Ravetch, 2007a). However, by studying these genes in humans, researchers have found that there are allelic variants in human of the hFcγRIIa and hFcγRIIIa. These variants (FcγRIIA131H and FcγRIIIa158V) show a much greater affinity to human IgG1 than their original alleles FcγRIIa131R and FcγRIIIa158F respectively (Dijstelbloem, Kallenberg and Van De Winkel, 2001). This increased binding to hIgG1 translates functionally in vivo where patients harbouring these mutations do better post-therapy with anti-tumour antibodies (Cartron *et al.*, 2002; Weng and Levy, 2003).

These different binding affinities of antibodies to FcγRs mentioned above depend on the composition of the Fc domain within the IgG molecule. This affinity is determined by two main factors: the amino acid sequence of the IgG Fc subclass and the N-linked glycan pattern of the IgG Fc domain. The glycan structure is composed of a heptasaccharide core of mannose and N-acetylglucosamine residues. Other saccharide units can be added to it, such as fucose, galactose and N-acetylglucosamine which changes its interaction with FcγRs (Anthony, Wermeling and Ravetch, 2012). An example of this is the lack of a fucose molecule at the core, which confers a higher affinity to FcγRIIa, and has shown to lead to increased effector function by the stronger activation of FcγRIIa-expressing leukocytes such as NK cells and macrophages (Lux and Nimmerjahn, 2011; Liu *et al.*, 2015).

Binding of the Fc region to FcγRs on immune cells can lead to different effects and consequences, examples of which are summarised in **Table 1.3** below. This depends on the expression of these FcγRs, the balancing activity between activatory and inhibitory receptors, and the type of cell it's expressed on. Other than these immediate effects, FcγR crosslinking also has some later effects, such as up-regulation of proinflammatory gene expression which results in various chemokines and cytokines to be produced and released.

These then further influence cellular differentiation and levels of FcγRs as well as the survival of cells (Wang *et al.*, 2017).

Table 1.3. Effects observed upon binding of Fc domains to FcγRs.

Summarised from (Barnhart and Quigley, 2017; Bournazos and Ravetch, 2017).

CELL TYPE	EFFECT
Effector leucocytes	Cellular activation
Natural killer cells	Activation and release of enzymes such as perforin and granzymes, which leads to the activation of pro-apoptotic pathways and cell death in the targets coated by IgG
Antigen presenting cells	IgG coated targets internalised and transferred to endosomal compartments to be degraded in lysosomes Better processing of antigens and their presentation on MHC-II molecules, leading to strong T-cell responses
Dendritic cells only	DC activation and maturation, antigen processing and loading onto major histocompatibility complex class II and class I molecules and subsequent presentation and cross-presentation to CD4 and CD8 T cells, respectively (known as the vaccinal effect)

1.4 TUMOUR IMMUNOTHERAPY

The manipulation of the immune system to promote cancer rejection is the premise of cancer immunotherapy (Peggs, Quezada and Allison, 2008). Different strategies have been used to tilt the balance towards tumour elimination rather than escape based on the intervention of different components of the immune response. These include the use of vaccines and cytokines, which will be briefly discussed in the following pages. Two types of immunotherapy that have proven to be very successful over the past 10 years have been immunomodulatory monoclonal antibodies (mAbs) and adoptive cell therapy (ACT) (Khalil *et al.*, 2016). These immunomodulatory mAbs target molecules on the surface of immune cells, altering their function and leading

to durable remissions as a result of invigorated effector function and the establishment of immunological memory (Pedicord *et al.*, 2010).

1.4.1 Cytokines

Cytokines are major players in the regulation of the immune system as they are able to provide growth, differentiation and inflammatory or anti-inflammatory signals to various cells. Cytokines are one of the first immunotherapies that were approved for clinical use and was the first time that an immunotherapy led to anti-tumour immune responses and durable objective responses (Berraondo *et al.*, 2018).

Tumour necrosis factor (TNF)-α, IFNs and IL-12 have all shown at least some success in clinical trials although their use has been limited by their toxicity when used at high effective doses. This led to the consideration of these cytokines being used as adjuvants, at lower doses, in other forms of immunotherapy, with more effective anti-tumour activities being observed as a result (Kirkwood, 1998; Colombo and Trinchieri, 2002). IL-2, a growth factor for antigen-specific T cell and NK cells, has been used extensively and following years of animal data, IL-2 got FDA approved for the treatment of renal cell carcinoma (1992) and melanoma (1998), with objective response rates between 5 and 15% being recorded (Rosenberg, 2014). IL-2 binds to the IL-2R, which consists of three subunits, α, β, and γ chains, with the signalling via this receptor being discussed in Chapter 3. Even though IL-2 is able to stimulate an anti-tumour response in some patients, the issue is that in most patients IL-2 has been shown to cause significant toxicity in many organs and tissues, with most of these being associated with general capillary leak syndrome (Atkins *et al.*, 1999). Therefore, it seemed IL-2 led to a general stimulation of the immune system rather than a specific anti-tumour response. More recently, new versions of IL-2 receptor agonists have been developed, amongst these are engineered versions of IL-2 that preferentially bind CD8 and NK IL-2Rs (low affinity IL-2 receptor consisting of β and γ chains) over Treg IL-2Rs (high affinity IL-2R consisting of the α, β, and γ chains) (Charych *et al.*, 2017) as well as bispecific constructs which target tumour antigens, thus

directing the IL-2 activity into the tumour microenvironment (Klein *et al.*, 2017) with the aim of increasing the efficacy as well as reducing the toxicity. The role of IL-2, as well as its signalling pathway is discussed in more detail in Chapter 3.

Due to immune checkpoint inhibitors revolutionising cancer immunotherapy, and new combinations being used in the treatment of cancer (such as αCTLA4 and αPD-1 in melanoma) there is now a great interest for new combinations. This led to many cytokines being incorporated into combination clinical trials, mainly in combination with αPD1 and αPD-L1 (Melero *et al.*, 2015)

1.4.2 Tumour vaccines

Different vaccination strategies against cancer have been tested over the past few years. These vaccinations aim to induce an optimal immune response against cancer cells by delivering tumour antigens in the context of the right co-stimulation. Examples include cell-based vaccines, DNA-based, and protein/peptide based. Despite being tested in multiple types of tumours, there is only one cancer vaccine to date that has been approved for therapeutic use in patients; Sipuleucel in prostate cancer (Kantoff *et al.*, 2010). Thus far, the use of tumour vaccines has not led to any durable anti-tumour responses. However, more recently, with sequencing techniques becoming more routinely used, the identification of neoantigens (antigens exclusively expressed by the tumour), has become easier. This has led to the invention of neoantigen tumour vaccines, which have revived the popularity of vaccines, as these focus on new antigens which do not induce central tolerance and have a high affinity to T cells. Clinical trials in melanoma have been encouraging (Carreno *et al.*, 2015; Ott *et al.*, 2017; Sahin *et al.*, 2017) and it will be interesting to follow whether these neoantigen vaccines manage to lead to durable anti-tumour responses in the future.

1.4.3 Adoptive Cell Therapy

Adoptive Cell Therapy (ACT) involves the transfer of T cells from a patient, post-manipulation in the lab, making these cells better at targeting the tumour, back into the patient. The main types of ACT that have been explored include; Tumour Infiltrating Lymphocyte (TIL) therapy, T-Cell Receptor (TCR) therapy and Chimeric Antigen Receptor (CAR)-T cell therapy.

TIL therapy: involves the harvest of naturally occurring T cells, with anti-tumour activity, from the patient's tumour. In order for these cells to be effective and remain active *in vivo*, post-transfer, they are first activated *ex vivo* using IL-2 and expanded. Large numbers of these cells are then re-introduced into the patient with high doses of IL-2, to make sure they persist and are active *in vivo*. TIL therapy in metastatic melanoma has shown to lead to tumour regression in 10-20% of patients (Rosenberg *et al.*, 2011; Besser *et al.*, 2013).

Some patients however may not have T cells which recognise the tumour. In order to identify tumour specific antigens in patients, tumours need to be sequenced. With whole exome sequencing now being routinely used, the identification of tumour specific antigens has become easier and newer generations of T cell therapies; (TCR therapy and CAR-T cell) make use of this by genetically engineering T cells to recognise a specific tumour antigen.

TCR therapy and CAR-T cell therapy: Both of these methods involve the harvesting of T cells from patients and engineering them in the lab to target specific tumour antigens. The main difference between these two therapies is that TCR engineered T cells can only recognise their antigen if bound and correctly presented by MHC molecules. As tumours use MHC downregulation to escape immune control, this method can be ineffective. CAR-T cells, however, do not need the antigen to be presented by MHC molecules and thus have revolutionised adoptive cell therapy (Dudley *et al.*, 2002).

CAR-T cells are genetically engineered T cells which have an antigen binding domain (single chain variable fragment [scFv] against a specific antigen

expressed on malignant cells, as well as more intracellular co-stimulatory domains from receptors such as CD28 and/or CD137. The CAR-T is therefore able to recognize antigen in the absence of MHC expression. CAR-T cells recognise and destroy the cells expressing the target. However, the problem is if other cells express the target, which is the case in B cell lymphoma and leukaemia cells expressing CD19, which means the CAR-T therapy also eliminates all the normal $CD19^+$ B cells. As well as having off-target toxicity, a critical irAE arising from this therapy is acute cytokine release syndrome (CRS) which occurs due to supraphysiologic levels of cytokines between produced upon antigen recognition (Brudno and Kochenderfer, 2016; Namuduri and Brentjens, 2016). Nonetheless, results from clinical trials have underscored the power of CAR-T cells and led to FDA approval of Kymriah™ and Yescarta™, both anti-CD19 CAR-T for non-Hodgkin Lymphoma and Lymphoblastic leukaemia (Zheng, Kros and Li, 2018).

1.4.4 Immune checkpoint blockade in cancer immunotherapy

As mentioned previously, immune evasion is one of the hallmarks of cancer cells. Cancer cells exploit the action of checkpoints such as CTLA-4, PD-1 and its ligand, PD-L1 to evade immune surveillance and promote tumour growth rather than control.

Immune checkpoint blockade involves the use of antibodies which bind to these inhibitory receptors expressed on T cells, or their ligands, preventing the ligands from binding to their receptors, and thus preventing inhibitory signals within the cells, leading to enhanced anti-tumour immunity. The most commonly used targets have been the immune checkpoint molecules, CTLA4 and PD1 (Schildberg *et al.*, 2016).

As described above, CTLA-4 acts as a regulator of naïve and effector antigen-specific T cell activation to prevent aberrant effector responses (Walunas *et al.*, 1994; Lenschow, Walunas and Bluestone, 2002). Use of antibodies blocking the CTLA4 receptor provided the first evidence that immune checkpoint blockade can increase survival in late stage cancer and led to the

development of the αCTLA4 blocking antibody Ipilimumab, which is approved in the clinic for metastatic melanoma and renal cell carcinoma (Peggs and Quezada, 2010).

Similarly, ligation of the PD-1 receptor with its ligands (PD-L1 and PD-L2) results in inhibitory signalling in T cells and thus limits their effector functions (Latchman *et al.*, 2001), which led to the development of αPD-1 antibodies. There are two blocking αPD-1 antibodies currently approved in the clinic; Pembrolizumab and Nivolumab, both of which have shown very strong responses in patients, with up to 40% of patients with advanced melanoma responding versus a mere 12% seen with Ipilimumab-treated patients (Ibrahim *et al.*, 2015). In addition, combination of Nivolumab and Ipilimumab has been tested in advanced stage melanoma with greater response rates and progression-free survival seen in combo-treated patients compared to monotherapy alone (Bastholt *et al.*, 2015). αPD-1 therapy is the first FDA approved immunotherapy which shows a greater percentage of objective immune responses than severe treatment-related adverse events. It has shown success in many different cancers as well as late stage tumours, broadening the use of immune therapy, to other, less immunogenic tumours such as – metastatic melanoma, lung cancer, head and neck cancer, renal cell carcinoma, urothelial carcinoma, liver cancer, gastric cancer, Hodgkin's lymphoma, Merkel cell carcinoma, large B cell lymphoma, cervical cancer and any MSI^+ tumours (Ribas and Wolchok, 2018). In addition, the development of Atezolizumab (αPD-L1 antibody) followed these and has been FDA approved for advanced urothelial carcinoma, metastatic NSCLC as well as advanced triple-negative breast cancer (Akinleye and Rasool, 2019).

These immune checkpoint blocking Abs have revolutionised cancer immunotherapy and led to responses in patients previously untreatable. However, this is not without consequences. The use of these antibodies has been shown to cause a different form of toxicity, called immune-related adverse events (irAEs), which differ from those toxicities observed post-chemo/radio therapy. Common irAEs include: gastrointestinal toxicity (such as

diarrhoea and colitis), hepatotoxicity, dermatologic toxicity (such as rash and pruritus) and endocrine toxicity (such as hypo- and hyperthyroidism). Even though early detection of these symptoms allows patients to be treated, if left too late, these irAEs can also lead to severe complications and even death (Villadolid and Amin, 2015).

1.4.5 Targeting Tregs for anti-cancer therapy

Regulatory T cells (Treg) are considered key players in the control of immune homeostasis, autoimmunity and anti-tumour immune responses (Plitas and Rudensky, 2016). Several studies have linked Treg infiltration of tumours with poor prognosis in multiple cancer types (Onizuka *et al.*, 1999; Golgher *et al.*, 2002; Jones *et al.*, 2002; Elpek *et al.*, 2007) whilst complementary work has demonstrated that, within tumours, the balance between effector (Teff) and regulatory T (Treg) cells associates with tumour progression and response to immunotherapy (Quezada et al., 2006; Mihm et al., 2008). Whilst these studies underscore the potential value of Treg cells as targets in cancer immunotherapy, there has been limited clinical success in targeting this cell population likely due to a lack of consensus on the most selective targets for depletion of Treg cells, and the limited mechanistic insight into the activity of these antibodies in vivo.

Various ways of controlling suppression by Tregs include

- Depletion of Tregs
- Targeting immune receptors expressed on Tregs
- Targeting kinase signalling in Treg cells
- Targeting Treg modulating factors in the TME

Depletion of Tregs

Depletion of Tregs for cancer therapy has been tested for many years using anti-CD25 targeting antibodies and is discussed in detail in Chapter 3. Briefly, a lack of in vivo therapeutic activity of CD25 targeting mAbs in mice has been observed for many years and was later shown by our group (Vargas *et al.*,

2017) that this was associated to poor binding to activating FcγRs required for antibody dependent cell cytotoxicity/phagocytosis (ADCC/P). Our group demonstrated that by using a different isotype of antibody, a mouse IgG2a backbone, this Fc optimised anti-CD25 could synergise with anti PD-1 to drive complete responses in mouse models of cancer (Vargas *et al.*, 2017).

Targeting immune receptors expressed on Tregs

As mentioned previously, Treg cells constitutively express co-stimulatory and co-inhibitory molecules. Amongst those, OX40, ICOS and GITR are being investigated in the clinic (Shimizu *et al.*, 2002; Griseri *et al.*, 2010). By targeting these molecules on Treg cells, it is thought that activation of these receptors on Treg cells decreases their ability to suppress the immune response, and increases the activation of T cells (Valzasina *et al.*, 2005). These mAbs are thought to have a dual mode of action – depletion of Tregs while activating antigen specific $CD4^+$ T effector cells. However, it is not yet known whether these Tregs within the TME are being inhibited or depleted post-treatment and more immune monitoring is needed to draw proper conclusions from these studies (Togashi, Shitara and Nishikawa, 2019).

Targeting kinase signalling in T cells

Other forms of therapy focus on targeting signals which are essential for the survival and function of Tregs. As Tregs are dependent on PI3Kδ signalling a PI3Kδ inhibitor has been developed. This has proven to have positive effects on tumour growth and survival in various mouse models of cancer, as well as progression and metastasis (Ali *et al.*, 2014) and is currently being evaluated in early phase clinical trials (NCT02646748) (Togashi, Shitara and Nishikawa, 2019).

Targeting Treg modulating factors in the TME

Furthermore, Treg survival and activity is highly dependent on many factors present within the TME, making room to indirectly target these cells. An example includes indoleamine 2,3-dioxygensase (IDO), which is known to be expressed in different types of cancer and whose levels increase upon tumour progression and metastasis (C. Smith *et al.*, 2012). IDO has two mechanisms

of action; firstly it depletes tryptophan, an essential amino acid needed for T cell activation, and secondly, by metabolising tryptophan, it results in production of tryptophan catabolites, which are immunosuppressive and promote the differentiation and activation of not only Tregs but also MDSCs (Holmgaard *et al.*, 2015). Taking these into account, an IDO1 inhibitor was developed, named epacadostat, and showed promising results in phase I and phase II in combination with pembrolizumab studies. However, this combination failed to lead to longer PFS in melanoma patients compared to pembrolizumab alone (Long *et al.*, 2019).

VEGFA – VEGF receptor 2 (VEGFR2) signalling is also known to promote an immunosuppressive TME as it has been shown to increase the migration of Tregs into the tumours in animal models (Terme *et al.*, 2013). In mouse models of breast cancer, blocking VEGF signalling reduced the numbers of immunosuppressive cells such as Tregs, MDSCs and M2 macrophages inside the tumour, while increasing the number of mature DCs, and led to an inhibition of tumour growth (Roland *et al.*, 2009).

1.5 AIMS

Whilst recent work demonstrates that CD25 is a selective target for depletion of regulatory T cells in mouse and human malignancies, anti-human CD25 antibodies have failed to deliver significant responses against solid tumours. Based on this, two projects were undertaken, both focusing on CD25 as a target for Treg depletion, but using different, novel methods of targeting this receptor.

- Development and characterisation of an anti-CD25 antibody which does not block IL-2R signalling
    - Presented in Chapter 3
- Production and characterisation of a BsAb targeting CD25 and PD-L1
    - Presented in Chapter 4

2 MATERIALS AND METHODS

2.1 CELL LINES

The cell lines HEK 293T (human embryonic kidney 293), CT26 (mouse colon carcinoma) and SupT1 (human T lymphoblast) were kindly donated by Dr Martin Pule from the UCL Cancer Institute.

MCA205 (mouse fibrosarcoma) cell line, was kindly donated by Dr Lorenzo Galluzzi.

MC38 (mouse colon adenocarcinoma) cell line was kindly donated by Dr Burkhard Becher.

HEK 293-F cells were purchased from Thermofisher scientific (#R79007)

2.2 CELL CULTURE

MCA205 tumour cells and HEK293T were cultured in Dulbecco's modified Eagle medium (DMEM, Sigma) supplemented with 10% fetal calf serum (FCS, Sigma), 100U/mL penicillin, 100µg/mL streptomycin and 2mM L-glutamine (all from Gibco). CT26, MC38 AND SupT1 tumour cells were cultured in Roswell Park Memorial Institute medium (RPMI, Sigma) supplemented with 10% fetal calf serum (FCS, Sigma), 100U/mL penicillin, 100µg/mL streptomycin and 2mM L-glutamine (all from Gibco). All of these cells were maintained at 37C with 5% CO2.

HEK-293F cells were cultured in serum-free, antibiotic-free FreeStyle™ 293 Expression Medium (Gibco) and incubated at 37°C in a humidified atmosphere of 8% CO_2 in air on an orbital shaker rotating at 125 rpm.

2.3 *IN VITRO* FUNCTIONAL ASSAYS

2.3.1 PhosphoSTAT5 evaluation

Pan T cells were isolated from splenocytes using the Dynabeads FlowComp™ Mouse Pan T (CD90.2) kit. 200,000 mouse T cells, in complete RPMI were plated and rested for 2-3 hours at 37°C. Antibodies (mouse: αCD25^{PC61} mIgG2a (Evitria), αCD25^{7D4} mIgG2a (Evitria), αIL-2 nAb (JES6-1A12, BioXcell) were added at 50µg/ml and were incubated with the cells for 30 mins at 37°C, following which cells were stimulated with IL-2 (50U/ml Peprotech) for 10 mins at 37°C. IL-2 induced STAT5 phosphorylation was stopped when the cells were fixed and permeabilized with the eBioscience™ Foxp3 / Transcription Factor Staining Buffer Set and treated with the BD Phosflow Perm Buffer III. % blocking was calculated as follows: % blocking = 100 x [(% STAT5$^+$ cells No Ab group - % STAT5$^+$ cells 50ug/ml Ab group) / (% STAT5$^+$ cells No Ab group)].

2.3.2 CFSE / Cell Trace Violet labelling of cells

For CFSE/Cell Trace Violet labelling, cells (5-10 x 10^6 cells/mL) were incubated at 37°C for 10 minutes with carboxyfluorescein succinimydil ester (CFSE, Invitrogen #C34554)/ Cell Trace Violet (Invitrogen #C34557) at a final concentration of 5µM. At the end of the incubation, the reaction was quenched with cold medium for 5 minutes and the cells were washed 5 times with medium.

2.4 MICE

7-8-week-old female C57BL/6 and BALB/c *wild-type* (WT) mice were obtained from Charles River Laboratories.

All animals were maintained in individually ventilated cages and pathogen-free conditions at UCL Biological Service Unit (BSU) following arrival, in accordance with Home Office and institutional guidelines. Animal protocols were approved by local institutional research committees and in accordance

with the Animal (Scientific Procedures) Act 1986 guidelines by UK Home Office.

2.5 THERAPEUTIC ANTIBODIES

The production of the anti-CD25 mouse IgG2a antibodies (clone PC61 and 7D4) was outsourced to Evitria AG (Switzerland).

The production of the parental antibody for the bispecific; αPD-L1 on a human IgG1 backbone containing the F405L mutation was produced in the lab and described in the antibody production section. The second parental antibody, αCD25 hIgG1 K409R was outsourced to Evitria AG (Switzerland).

2.6 TUMOUR MODELS

2.6.1 Subcutaneous Tumours

C57BL6 mice were injected subcutaneously with 500,000 MCA205 or MC38 cells in the right flank. BALBc mice were injected subcutaneously with 500,000 cells CT26 cells in the right flank. Cells were trypsinised, washed and resuspended in PBS pre-injection.

For **tumour growth and control** experiments, tumours were measured twice weekly and volumes calculated as the product of three orthogonal diameters. Mice were euthanised when any diameter reached 150mm.

For **tumour microenvironment evaluation** experiments, mice were treated with therapeutic antibodies at the dose indicated in each figure by intraperitoneal injection on day 5 after tumour injection, unless indicated otherwise. Mice were euthanised on the day indicated in the figure, and tumours and draining lymph nodes (LN) were collected for further analysis by flow cytometry.

2.6.2 Single cell suspensions for flow cytometry analysis

For functional experiments, tissues were harvested and processed at the time points indicated in the legends. Lymph nodes were collected and mashed through a 70μM cell strainer (BD Falcon). For extraction of tumour-infiltrating lymphocytes (TILs), tumour tissue was cut into pieces and incubated for 30 minutes at 37°C in a solution containing 0.33 mg/ml DNase (Sigma-Aldrich) and 0.27 mg/ml Liberase TL (Roche) in serum-free RPMI. The tissues were homogenised in an automated tissue dissociator (OctoMACS, Miltenyi Biotech) and filtered through a 70μM cell strainer. The cell suspension was gradient-centrifuged using Histopaque 1119 (Sigma) at 700g for 10 minutes at room temperature. Cells were collected from the interphase, washed and resuspended in FACS buffer (2% FBS, 2mM EDTA in PBS) for further staining.

2.7 FLOW CYTOMETRY STAINING AND ANALYSIS

2.7.1 Staining

All antibody staining for flow cytometry was done according to the following protocol. Antibodies employed for flow cytometry are listed below in Table 2.1.

Extracellular staining: A master mix was created for extracellular staining antibodies in a “superblock” solution (HBSS, 2% FCS, 2% anti-Fc receptor, 5% mouse serum and 5% rat serum) in a volume of 40-50 μl per sample. Samples were incubated for 30 minutes on ice in the dark and then washed twice with FACS buffer (HBSS, 2% FCS, 2 mM EDTA).

Secondary staining: When using biotin-conjugated antibodies, streptavidin-conjugated fluorochromes were added after surface staining in 40-50μL of superblock, incubated for 15 minutes on ice and washed with FACS buffer.

Intracellular staining: Following extracellular staining, cells were fixed and permeabilised with 100μL of the Fixation/Permeabilization solution (Fixation/Permeabilization Concentrate diluted in Fixation/Permeabilization Diluent) (ThermoFisher Scientific) for 20 minutes at 4°C in the dark. Cells were

washed twice with Permeabilization buffer (ThermoFisher Scientific) and stained in 40-50µL of a mix of Permeabilization buffer with intracellular antibodies for 30 minutes at 4°C in the dark. Cells were then washed twice with Permeabilization buffer and resuspended in FACS Buffer prior to data acquisition. Counting beads were added in 50µL PBS prior to data acquisition.

For **pSTAT5 staining**, TILs and LN were rested for 2 hours in FCS-free media followed by 10 min stimulation with 50 IU/ml of IL-2 (Peprotech) and fixed for 30 min with Fixation/Permeabilization buffer (ThermoFisher) and Perm Buffer III (BD Phosphlow) followed by the staining.

Table 2.1. Antibodies used for flow cytometry

Antigen	Clone	Conjugate	Company	Catalogue #	Dilution
FoxP3	FJK-	PE	ThermoFisher	12-5773-82	1:100
FoxP3	FJK-	efluor450	ThermoFisher	48-5773-82	1:100
4-1BB	17B-5	biotin	ThermoFisher	13-1371	1:200
CD3	145-	PECy.7	ThermoFisher	25-0031	1:200
CD3	17A2	BUV737	BD Biosciences	564380	1:300
CD4	RM4-5	V500	BD Biosciences	560782	1:300
CD4	GK1.5	BUV496	ThermoFisher	564667	1:300
CD45	30-	BUV563	BD Biosciences	565710	1:300
CD8	53-6.7	BUV805	BD Biosciences	564920	1:300
CD8	53-6.7	BV650	ThermoFisher	100742	1:300
CTLA-4	UC10-	BV605	ThermoFisher	106323	1:100
Granzyme B	GB11	APC	ThermoFisher	GRB05	1:100
GITR	DTA-1	efluor450	ThermoFisher	48-5874	1:200
CD25	PC61	BV510	BioLegend	102041	1:200
CD25	PC61	AF488	Biolegend	102017	1:200
CD25	7D4	AF488	BD Biosciences	553071	1:200
Lag3	C9B7	BV650	BioLegend	125227	1:200
CD45	30-	BUV563	BD Biosciences	565710	1:300
Ki67	SolA1	eFluor450	ThermoFisher	48-5698	1:400
NK1.1	PK136	eFluor450	ThermoFisher	48-5941	1:200
NK1.1	PK136	Alexafluor700	ThermoFisher	56-5941	1:200
PD-1	29F.1	PE-Dazzle594	BioLegend	135228	1:200
IFNg	XMG1	AF488	Ebioscience	505813	1:100
pSTAT5	-	AF647	Ebioscience	612599	20µl/test
Streptavidin	-	BV650	BioLegend	405232	1:200
Streptavidin	-	BV711	BioLegend	405241	1:200
Viability dye	-	eFluor780	ThermoFisher	65-0856	1:1000

2.7.2 Quantification of tumour-infiltrating lymphocytes

For quantification of absolute number of cells, a defined number of fluorescent beads (Cell Sorting Set-up Beads for UV Lasers, ThermoFisher) was added to each sample before acquisition and used as counting reference.

2.8 MOLECULAR BIOLOGY TECHNIQUES

2.8.1 Molecular buffers and bacterial media

The buffers and bacterial media used for the molecular biology procedures are summarised in Table 2.2.

Table 2.2. Buffers and media used for molecular biology experiments.

BUFFERS/MEDIA	COMPOSITION
1X phosphate-buffered saline (PBS)	137 mM NaCl, 2 mM KCl, 10 mM sodium hydrogen phosphate (dibasic), 2 mM potassium hydrogen phosphate (dibasic), pH 7.4
1X tris-acetate EDTA buffer (TAE)	40 mM Tris (pH 7.8), 20 mM sodium acetate, 1mM EDTA
6X gel loading buffer	0.25% bromophenol blue, 0.25% xylene cyanol FF, 30% glycerol in water
EB buffer	10 mM Tris.Cl, pH 8.5
Luria Bertani agar	LB broth plus bacto-agar 15g/l
Luria Bertani broth	1% bacto-tryptone, 0.5% bacto-yeast extract, 10% NaCl, pH 7.0
Tris-EDTA buffer (TE)	10 mM Tris.Cl, 1 mM EDTA, pH 8.0

2.8.2 Fusion PCR

In order to produce the anti-PD-L1 human IgG1 construct required (amongst other constructs), a fusion PCR reaction was performed using Phusion High-

Fidelity DNA Polymerase and the Phusion HF buffer (NEB). Principles of a fusion PCR are illustrated below in Figure 2.1.

The variable region (PCR1) and constant region (PCR2) are amplified separately, their size confirmed by running the fragments on an agarose gel and the DNA extracted for a third round of amplifications which produce the full length construct.

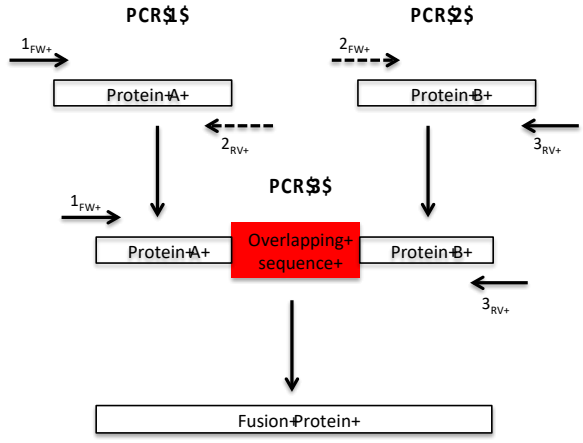

Figure 2.1. Schematic representation of the use of overlapping primers to generate a fusion protein.

Schematic representation of the use of overlapping primers to generate a fusion protein. The two fragments to be fused together are made separately in two different PCRs: PCR 1 and PCR 2. The primers 2_{fw} and 2_{rev} are designed in such a way to create an overlapping sequence between the products of the first two PCR reactions. The primers 1_{FW} and 3_{RV} are used to introduce restriction sites and to fuse the two proteins together by means of their overlapping sequence in a third PCR reaction (PCR 3).

2.8.3 Agarose gel electrophoresis

Electrophoreses were performed in 1% agarose (Invitrogen) gels with 5 µg/mL ethidium bromide (Dutscher Scientific). All gels were run at 130V. Samples were loaded onto the gel with 6X loading dye (5µL of dye/25µL of reaction). A 1kB Plus ladder (Invitrogen) was run alongside the samples to identify band sizes.

2.8.4 Purification of DNA from agarose gels

DNA on the agarose gel was visualised using a transilluminator (Clare Chemical Research). Bands of the right sizes were excised using a sterile scalpel and the DNA was purified using the QIAquick Gel Extraction Kit (Qiagen) according to the manufacturer's instructions.

2.8.5 DNA digestion with restriction enzymes and ligations

All restriction enzymes used were obtained from New England Biolabs (Ipswich). For checking small amounts of DNA, digestions were carried out for at least 30 minutes at 37°C. For purification of DNA fragments for cloning, digestions of at least 10 µg of DNA were carried out for one hour. All digestions with restriction enzymes were performed according to the conditions suggested by the manufacturer for the different combinations of enzymes.

For ligations of DNA fragments into vector plasmids, a ligation mix was prepared using 4 µL of digested and purified DNA insert, 4 µl of digested and purified vector backbone, 1 µL of 10X buffer for T4 DNA ligase (New England Biolabs) and 1 µL (100,000 U) of T4 DNA ligase (New England Biolabs). The mixture was incubated for 15 minutes at room temperature and used for the transformation of competent bacteria.

2.8.6 Transformation of competent bacteria

For transformation of bacteria, a vial of NEB5α chemically competent E. coli bacteria (NEB) was thawed on ice for 20 minutes prior to their use. 3-5 µL of the ligation mix was added to the bacteria, gently swirled and incubated on ice for 30 minutes. Bacteria were then heat shocked at 37°C for exactly 2 minutes, followed by incubation on ice for 2 minutes. They were then cultured on LB agar with ampicillin (50 µg/mL) and grown overnight at 37°C. Colonies were then picked and grown overnight at 37° C in a shaker in 4 mL or 150 mL of LB broth with ampicillin (50 µg/mL) for mini or midipreps, respectively.

2.8.7 DNA purification and quantification

DNA was purified from mini and midipreps using QiaPrep Spin Miniprep and Plasmid Midi kits (Qiagen) according to the manufacturer's instructions. The former typically gave small yields of DNA (<100μg) and were used to select positive clones after ligations, while the latter were used to purify larger amounts of DNA (150-200μg) for further use. ZymoPURE™ Plasmid Maxiprep kits were used for the production of ultra-pure low-endotoxin plasmid DNA, which is critical for transfection quality.

The concentration of the purified DNA was measured using the NanoDrop 1000A Spectrophotometer. Purified plasmid DNA was kept in solution in EB buffer at 1μg/μL.

2.8.8 DNA Sequencing

DNA sequences were validated by Sanger sequencing. Purified plasmid DNA samples (100ng/μL) were sent to GATC with the appropriate sequencing primer (5μM). The sequencing results were analysed and aligned to the reference map using SnapGene 3.0.

2.8.9 Transfection and transduction for binding tests and virus production

HEK 293T cells were transfected using FuGENE 6 Transfection Reagent (Promega). Fugene was added to plain RPMI medium and incubated for 5 minutes. DNA was added to the Fugene-RPMI mix, incubated for another 15 minutes at room temperature and added dropwise to HEK 293T plate. Conditions used for the transfection of 293T cells are shown below in Table 2.3.

For antibody binding tests, 293T cells were co-transfected with two different plasmids containing either construct (heavy or light chain) to produce a small amount of the antibody and check its binding by flow cytometry.

For murine CD25 and PD-L1 virus production after transfection of the HEK293T cells with the plasmid containing the sequence for CD25/PD-L1, the supernatant was collected 48 and 72 hours after transfection and snap frozen immediately for further use.

Table 2.3. Conditions used for transfection of 293T cells.

Plain RPMI	470µL
Fugene	30µL
Envelope plasmid (only for virus production)	3.125µg
Gag-pol plasmid (only for virus production)	4.69µg
Retroviral construct	4.69µg

Transduction of cell lines

To transduce SupT1 cells to make them express murine CD25 or PD-L1 on the surface, SupT1 cells were plated onto a non-tissue culture treated plate (pre-coated with retronectin – 25µg/mL). The viral supernatant collected from the transfection of the HEK293T cells added onto the SupT1 cells and centrifuged with no brake at 1000g for 40 minutes at room temperature. Percentage of cells transduced was verified by flow cytometry 3 days post-transduction. Cells expressing murine CD25/PD-L1 were electronically sorted and named SupT1 mCD25/mPD-L1.

Antibody binding test

For testing binding of cells to their target, SupT1-PD-L1 and SupT1-CD25 cells were harvested and counted. 1 x 10^5 – 3 x 10^5 target-expressing cells were seeded in a 96 well-plate. The cells were centrifuged at 2000 rpm 4°C for 2 minutes and washed twice with 200 µL FACS buffer. 200 µL of concentrated supernatants of the transfected 293T cells were added to corresponding wells and incubated on ice for 30 minutes. Cells were stained and analysed for binding by flow cytometry.

2.8.10 Large scale transfection of 293F cells for antibody production

MAX - mediated

Approximately 24 hours before transfection, FreeStyle 293F cells were passed at 6-7 × 10^5 /mL. On the day of transfection, cells were counted and diluted to 1 × 10^6 /mL. Viability of the cells was confirmed (>90%). 30mL of the cells were added into each 125-mL shake flask. The tube of FreeStyle™ MAX Transfection Reagent was inverted several times to mix. 37.5µg of plasmid DNA was diluted into OptiPRO™ SFM to a total volume of 0.6 mL and mixed. In a separate tube, 37.5µL of FreeStyle™ MAX Reagent was diluted in OptiPRO™ SFM to a total volume of 0.6mL and mixed gently by inverting the tube (taking care not to vortex). Diluted FreeStyle™ MAX Reagent was immediately added to the diluted DNA solution to obtain a total volume of 1.2 mL and mixed gently. The DNA-lipid mixture was incubated for 10 minutes at room temperature to allow complexes to form. 1.2mL of DNA-lipid mixture was slowly added into the 125-mL flask containing cells while slowly swirling the flask. For scaling up and optimisation, Invitrogen guidelines were followed.

PEI - mediated

293F cells were thawed, cultured and expanded for about 2 weeks. 24 hours before transfection, the cells were pooled and centrifuged at 100 x g for 5 minutes. Approximately 6 x 10^5 cells/mL were seeded in 300 mL FreeStyle™ 293 Expression Medium (Gibco). When the density reached 1 x 10^6 cells/mL, the DNA mix containing 225µg of plasmid DNA encoding antibody the light chain and 75µg of plasmid DNA encoding antibody the heavy chain (in case of 3:1 ratio) was mixed with 14.1 mL Freestyle Medium. 600 µL of sterile linear 25 kDa PEI solution (1mg/mL) was added dropwise to the DNA mix and incubated for 10 minutes, after which, the mixture was slowly added to 293F cells.

Harvesting the antibody

The cells were incubated at 37°C for 6 days prior to harvest of antibodies by centrifuging the culture at 3000 x g at 4°C for 10 minutes. Supernatants were

collected and filtered using a 0.22μm filter. EMD Millipore Labscale TFF System was used to concentrate the supernatants collected from the cells that were transfected. Manufacturer's instructions were followed. 250mL of supernatants were concentrated to approximately 50mL, which was then purified using rProtein A or rProtein G GraviTrap™ (GE Healthcare Life Sciences) according to manufacturer's instructions.

2.9 Production of bispecific antibody

The duobody technology, developed by Genmab was used for the fab arm exchange between the two parental antibodies, following the step by step protocol published in Nature (Labrijn *et al.*, 2014). Briefly, the antibodies were mixed in equimolar amounts (5mg/ml each, calculated using exact extinction coefficients), 75mM 2-MEA was added and topped up with PBS. The mixture was incubated at 31°C for 5 hours, with no shaking. Following this, the antibody was dialysed using dialysis cassettes with 10 MWCO (during which the buffer was changed three times), filtered using 0.22 μm filter and stored in the fridge overnight. The formation of the BsAb was confirmed using Matrix Assisted Laser Desorption/Ionization (MALDI) at UCL School of Pharmacy (Mass Spectrometry Facility). The exchange efficiency was determined using Hydrophobic Interaction Chromatography (HIC) analysis.

2.10 SDS-PAGE

To check the expression of antibodies, the supernatants of cells transfected with the corresponding vectors were used for sodium dodecyl sulphate polyacrylamide gel electrophoresis (SDS-PAGE) analysis. Laemmli buffer was added to the samples at a ratio of 1:5. The mixture was heated in a heatblock at 97°C for 10 minutes. The samples were then separated by SDS-PAGE using a 4% stacking gel and a 12% separation gel with SDS. The gels were run at 120V for about 1 hour.

For Coomassies, gels were stained for 1 hour with Coomassie blue and then de-stained with de-stain buffer for about 24 hours

For Western blots, proteins were blotted onto a polyvinylidene fluoride (PVDF) membrane (Amersham), activated with methanol (1 minute) and transfer buffer (5 minutes) for 1.5 hours at 90V. The membranes were blocked for 1 hour with blocking buffer at room temperature. The membrane was incubated overnight with a polyclonal anti-human Fc antibody (1 in 5000 in milk) at 4°C. Following overnight incubation, the membrane was washed three times with PBS containing 0.1% Tween 20. Finally, the membrane was briefly incubated in ECL development solution and exposed on x-ray film (Fujifilm), followed by development of the film in a chemiluminescent camera. The buffers and solutions used for the SDS-PAGE are shown in Table 2.4 below.

Table 2.4. Buffers and gels used for SDS-PAGE.

BUFFER/GEL	COMPOSITION
4% stacking gel	4% acrylamide/bis, 125 mM Tris.HCl (pH 6.8), 10% SDS, 0.1% TEMED, 1% ammonium persulphate (APS)
11% polyacrylamide gel	11% acrylamide/bis, 125 mM Tris. HCl (pH 8.8), 10% SDS, 0.1% TEMED, 1% APS
Blocking buffer	5% semi-skimmed milk, 0.1% Tween 20 in PBS
Laemmli buffer	2% sodium duodecylsulphate (SDS), 10% glycerol, 5% 2-mercaptoethanol, 0.2 mg/mL bromophenol blue, 0.1M DTT 50 mM Tris (pH 6.8)
Running buffer	25mM Tris (pH 8.5), 200mM glycine, 0.1% SDS
Transfer buffer	100 mM Tris, 200 mM glycine, 20% methanol
Coomassie stain	0.1% Coomassie R250, 10% acetic acid, 40% methanol
Coomassie de-stain	20% methanol, 10% acetic acid

2.11 Data acquisition and analysis

Flow cytometry data was obtained using LSR-Fortessa analyser (BD Biosciences) and BD FACSymphony (BD Biosciences). Electronic cell sorting was performed using FACS Aria III sorter (BD Biosciences) by the Flow Cytometry Core Facility (Flow Cytometry Translational Technology Platform) of the UCL Cancer Institute. Flow cytometry data was analysed using FlowJo v10.5.0. PCR reactions and primers were designed using Snapgene 3.3.2. Statistical analysis was performed using GraphPad Prism 6.0; p values were calculated using one or two-way ANOVA with Tukey post-tests (ns=$p>0.05$, *$p<0.05$, **$p<0.01$, ***$p<0.001$, ****$p<0.0001$). Analysis of Kaplan-Meier survival curves was done with log-rank test.

3 REJECTION OF ESTABLISHED TUMOURS WITH CD25-TARGETING ANTIBODIES PRESERVING IL-2 SIGNALLING ON EFFECTOR T CELLS

3.1 OVERVIEW

In this chapter, the development of a non-IL-2 blocking anti-CD25 antibody is presented. The rationale that led to the production of this antibody is discussed, followed by its characterisation *in vitro* and *in vivo*.

3.2 INTRODUCTION

3.2.1 Importance of targeting regulatory T cells as targets in cancer immunotherapy

Regulatory T cells (Treg) are considered key players in the control of immune homeostasis, autoimmunity and anti-tumour immune responses (Plitas and Rudensky, 2016). Several studies have linked Treg infiltration of tumours with poor prognosis in multiple cancer types (Onizuka *et al.*, 1999; Golgher *et al.*, 2002; Jones *et al.*, 2002; Elpek *et al.*, 2007) whilst complementary work has demonstrated that, within tumours, the balance between effector (Teff) and regulatory T (Treg) cells associates with tumour progression and response to immunotherapy (Quezada et al., 2006; Mihm et al., 2008). Whilst these studies underscore the potential value of Treg cells as targets in cancer immunotherapy, there has been limited clinical success in targeting this cell population likely due to a lack of consensus on the most selective targets for depletion of Treg cells, and the limited mechanistic insight into the activity of these antibodies *in vivo*. In mice, anti CTLA-4 antibodies have shown to preferentially deplete tumour infiltrating Treg cells via the engagement with activating Fc Receptors (FcγRs) (Selby *et al.*, 2013; Tyler R Simpson *et al.*, 2013; Wilson *et al.*, 2013). Evidence suggests that it is the local intra-tumoural Treg depletion that is important for tumour control

and that depleting Tregs only in the periphery is not efficient (Coe *et al.*, 2010; Selby *et al.*, 2013; Tyler R. Simpson *et al.*, 2013; Bulliard *et al.*, 2014), indicating that the role of Tregs is more likely inhibiting T effector cells rather than T cell priming. In humans, the Treg depleting activity of current anti-CTLA-4 antibodies remains controversial with some studies failing to show a reduction in Treg numbers in patients treated with anti-CTLA-4 (Sharma *et al.*, 2019) and others suggesting that enhancing the affinity of anti-human CTLA-4 mAbs to FcγRs could potentially increase clinical outcomes (Vargas *et al.*, 2018; Waight *et al.*, 2018; Ha *et al.*, 2019).

3.2.2 CD25 as a target for Treg depletion

Beyond CTLA-4, a target that has been recently revisited demonstrating selective expression on Treg over Teff cells in mice and humans is CD25 (Chevrier *et al.*, 2017; Vargas *et al.*, 2017; Azizi *et al.*, 2018). Also known as the interleukin-2 receptor alpha chain (IL-2Rα), CD25 was the first surface marker used to identify, isolate and target Tregs in vivo in a variety of mouse models of autoimmunity (Sakaguchi *et al.*, 1995; Shimizu, Yamazaki and Sakaguchi, 1999). However, in cancer, lack of *in vivo* therapeutic activity of CD25 targeting mAbs in mice and humans thwarted enthusiasm around this molecule. In mouse models of cancer, our lab recently demonstrated that the lack of therapeutic activity of the most common anti-CD25 mAb (clone PC61) was associated to poor binding to activating FcγRs required for antibody dependent cell cytotoxicity/phagocytosis (ADCC/P). The data published by Vargas et al., 2017, showed that Fc optimised anti-CD25 could synergise with anti PD-1 to drive complete responses in mouse models of cancer. Importantly, whilst Fc-optimised anti mouse CD25 boosted the activity of anti PD1, it lacked potent single agent activity in these models. In keeping, anti-CD25 mAbs in the clinic have also failed to deliver significant responses against solid malignancies as a single agent or in combination with vaccines (Onizuka *et al.*, 1999; Golgher *et al.*, 2002; Jones *et al.*, 2002; Jacobs *et al.*, 2010; Rech *et al.*, 2012). Of relevance, both anti-CD25 antibodies currently in the clinic, Daclizumab and Basilixumab (Kapic, Becic and Kusturica, 2004; Baldassari and Rose, 2017), have been developed to prevent acute organ

rejection and for treatment of multiple sclerosis through the blockade of IL-2 signalling required by autoreactive T cells. Coincidently, IL-2 blockade is also a feature of the anti-mouse CD25 mAb (Clone PC61) currently used to deplete Tregs in mouse models of cancer (Moreau *et al.*, 1987).

3.2.3 IL-2 and IL-2R signalling

IL-2 is a key growth factor regulating the activation and proliferation of immune cells. It binds to the IL-2R, which exists in 3 different forms – monomeric, dimeric and trimeric IL-2R; most of these are found on the surface of the cells, but are also found in soluble form in the circulation as a result of proteolytic cleavage (mainly from the surface of activated T cells). Monomeric forms of the receptor exist as IL-2Rα (CD25) alone. Dimeric IL-2Rs consist of the IL-2Rβ (CD122) and IL-2Rγ (common γ chain/CD132), with the trimeric IL-2R containing CD25, CD122 and CD132. CD122 also exists as part of the IL-15R, and the common γ chain is shared by many cytokine receptors, including those for IL-2, IL-4, IL-6, IL-9, IL-15 and IL-21. The trimeric IL-2R is considered a high affinity receptor in terms of signalling, with a Dissociation constant (Kd) of approximately 10^{-11}M, compared to the dimeric form which is considered low-affinity, with a Kd of approximately 10^{-9}M. In contrast, CD25 binds IL-2 with a low Kd of approximately 10^{-8}M and is not able to signal on its own. However, CD25 has an important role in improving the binding of IL-2 to the dimeric IL-2R (Arenas-ramirez, Woytschak and Boyman, 2015).

Once IL-2 is bound to the IL-2R, the whole complex is internalised, with IL-2, CD122 and CD132 being degraded, and CD25 being recycled back to the surface of the cell. There are 3 major signalling pathways downstream of the IL-2R (**Figure 3.1**); the Janus kinase (JAK)-signal transducer and activator of transcription (STAT) pathway; the phosphoinositide 3-kinase (PI3K)-AKT pathway and the mitogen-activated protein kinase (MAPK) pathway (Liao, Lin and Leonard, 2013; Arenas-ramirez and Woytschak, 2015; Spolski, Li and Leonard, 2018)

IL-2 is secreted by a variety of activated immune cells, including T cells, natural killer (NK) cells, NKT cells, dendritic cells (DCs), and mast cells. However, in non-activated, resting conditions, $CD4^+$ helper T (Th) cells constantly produce low levels of IL-2. Upon activation, IL-2 production increases quickly by T cells. In addition, activated DCs are thought to provide an early source of IL-2 and therefore support T cell stimulation. At the same time, activated T cells, including $CD4^+$ and $CD8^+$ T cells, start secreting high concentrations of IL-2 for their own (autocrine) use as well as to activate neighbouring $IL\text{-}2R^+$ cells in a paracrine manner. Treg cells on the other hand, are not able to produce IL-2, regardless of stimulation and are only able to do so if they are peripherally derived (induced) Treg cells which are re-differentiating into Th cells (Liao, Lin and Leonard, 2013).

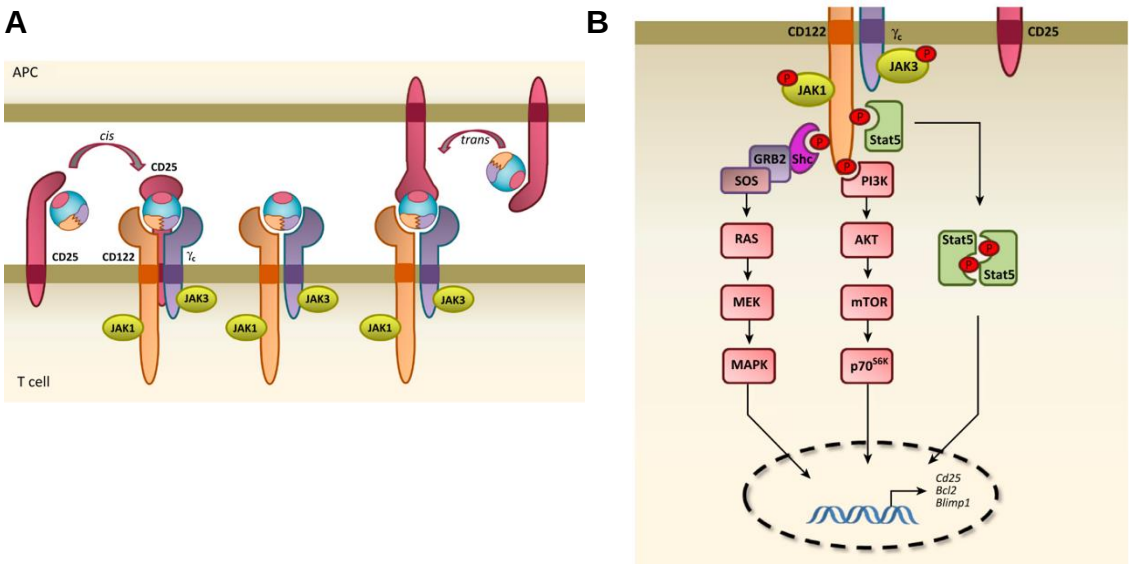

Figure 3.1. IL-2 receptor (IL-2R) Binding and Signalling

Cartoon of **(A)** IL-2 interacting with its receptor subunits, including IL-2R/ (CD25), IL-2Rβ (CD122), and the common γ-chain (CD132), as well as **(B)** signalling pathways following the interaction of IL-2 with various IL-2R subunits (Arenas-ramirez and Woytschak, 2015).

3.2.4 Pleiotropic effects of IL-2

As mentioned above, IL-2 was discovered as a molecule that is capable of sustaining the survival and differentiation of naïve T cells into effector T cells and was considered an essential player in the development of these effector T cell responses. This paradigm was challenged in the early 90s, when IL-2 knockout (KO) mice presented uncontrolled lymphoproliferation and autoimmunity, instead of the predicted immunodeficiency (Sadlack *et al.*, 1993). Similar phenotypes were seen using CD25 KO or IL-2Rβ KO mice (Suzuki *et al.*, 1995; Willerford *et al.*, 1995). These results gave birth to the IL-2 paradox and led to a re-evaluation of the role of IL-2 as simply a positive regulator of effector T cell proliferation and led to the idea that in fact the main role of IL-2 is to suppress immune responses instead. This idea is further supported by data in humans where polymorphisms which change IL-2 signalling are associated with autoimmune diseases such as type I diabetes, multiple sclerosis, Graves' disease, celiac disease, and rheumatoid arthritis (Sharfe *et al.*, 1997; Gregersen and Olsson, 2009; Todd, 2010). Further studies then showed that the severe immune autoreactivity that was seen in these KO mice was due their loss of regulatory T cells (Fontenot *et al.*, 2005; Cheng, Yu and Malek, 2011). It is now known that IL-2 is vital for the development of Tregs in the thymus as well as the regulation, proliferation and maintenance of these cells in peripheral tissues and is key for Treg function by maintaining its transcriptional machinery. Foxp3, the main transcriptional factor which determines Treg identity relies on IL2 for its expression in Tregs. IL-2 KO mice have a very small number of Tregs and those that remain are not functional in preventing autoimmunity (Malek, 2003; Rudensky, 2011).

3.2.4.1 Effects of IL-2 on $CD4^+$ T cell subsets

Naïve CD4+ T cells can differentiate into different functional populations upon exposure to antigen in combination with cytokine signals. These include T_H1, T_H2, T_H17, T_H9, T_{FH}, Treg and T follicular regulatory (T_{FR}) cells. These cells can be distinguished from each other based on the type of cytokine they

produce, which lineage-specific transcriptional master regulators they express and their dependency on cytokines (O'Shea and Paul, 2010). IL-2 has a vital role in the differentiation of these cells as well as their interconversion. For example, IL-2 can promote T_H1 and T_H2 cell fates in $CD4^+$ T cells (Cote-Sierra *et al.*, 2004; Liao *et al.*, 2008, 2011; Liao, Lin and Leonard, 2011) but can suppress the differentiation of T_H17 cells (Laurence *et al.*, 2007; Yang *et al.*, 2011) as well as T_{FH} cells (Ballesteros-Tato *et al.*, 2012; Ray *et al.*, 2015). IL-2 does this by controlling the expression of key cytokine receptors, transcription factors, chromatin regulators and effector cytokines (For example, IL-2 can induce the expression of Eomesodermin, T-bet and Blimp-1, while suppressing BCL6) (Liao *et al.*, 2011).

3.2.4.2 Effects of IL-2 on $CD8^+$ T cells

When naïve $CD8^+$ T cells encounter antigen, they proliferate and differentiate into effector cells as well as long-lived memory cells, with this being affected by multiple co-stimulatory signals from APCs and cytokines from $CD4^+$ T cells (Henning, Roychoudhuri and Restifo, 2018). IL-2 has key roles in influencing these effector activities in $CD8^+$ T cells by stimulating the expression of IFNγ (Reem and Yeh, 1984), TNFα and lymphotoxin (Lin *et al.*, 2012). IL-2 can also induce the expression of cytolytic effector molecules including Granzyme B and perforin (Janas *et al.*, 2005; Pipkin *et al.*, 2010) and stimulates efficient killing of target cells (Pipkin *et al.*, 2010). Even though most of these CTLs die after the pathogen has been removed, some remain as long-lived memory cells. IL-2 can control this balance in effector/memory phenotype of $CD8^+$ T cells. High doses of IL-2 promotes T cell differentiation into effector cells and induces the expression of important effector molecules and cytokines by these cells. Research has shown that this is because IL-2 leads to the expression of Blimp-1, while inhibiting the expression of molecules known to be associated with memory cells, such as BCL6, the IL-7Rα chain (CD127) and L-selectin (CD62L). On the other hand, low levels of IL-2 promote a memory phenotype in these cells. This is because a low dose enables BCL6, IL-7Rα, and L-selectin to be expressed again, enabling the formation of memory cells (Kalia *et al.*, 2010; Pipkin *et al.*, 2010).

3.3 AIMS

Considering that Treg depletion increases local available IL-2 (Scheffold, Murphy and Höfer, 2007), and the critical role that IL-2 plays in effector T cell survival and activity (Liao, Lin and Leonard, 2013; Arenas-ramirez and Woytschak, 2015; Spolski, Li and Leonard, 2018), it was hypothesised (hypothesis illustrated in **Figure 3.2** below) that the *in vivo* activity of available anti-CD25 mAbs targeting human and mouse Treg cells, is likely limited by their IL-2 blocking activity. Therefore, targeting regulatory T cells via CD25 whilst preserving IL-2 signalling on effector T cells within tumours could boost anti-tumour immunity. To test this hypothesis, the main objectives were to:

- Search the literature for a non-IL-2 blocking anti-mouse CD25 mAb
- Characterise the activity of the antibody in terms of blocking of IL-2 signalling, both *in vitro* and *ex vivo* in mouse TILS
- Compare the activity of the non-blocking antibody to the blocking antibody *in vivo* in mouse models of cancer

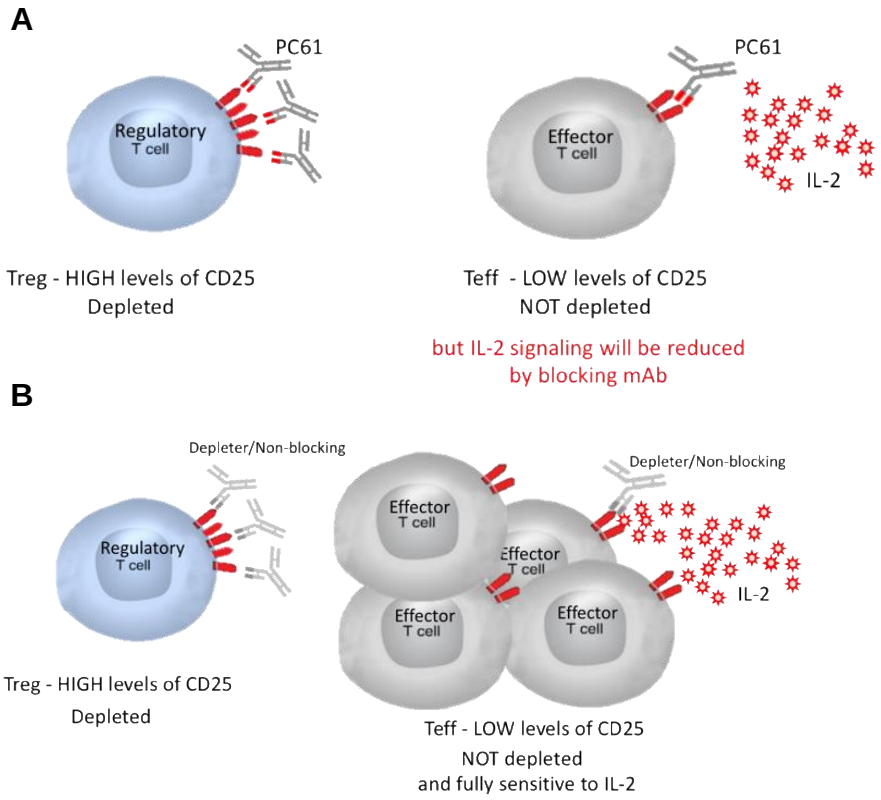

Figure 3.2. Hypothesis of using a non-blocking, depleting anti-CD25 antibody (B) versus a blocking, depleting anti-CD25 antibody (A).

3.4 RESULTS

3.4.1 Characterisation of non-IL-2 blocking anti-mouse CD25 mAbs ($\alpha CD25^{NIB}$)

Our lab has previously demonstrated that when converted to a depleting mIgG2a isotype, the commonly used αCD25 clone PC61 could synergise with anti-PD1 to reject established tumour (Vargas *et al.*, 2017). However, like the clinical antibodies, PC61 also interferes with IL-2 signalling on effector T cells, a feature likely to limit its *in vivo* activity. Anti-CD25 clone 7D4, is a non-depleting IgM which binds to mouse CD25 without blocking IL-2 signalling (Moreau *et al.*, 1987; Kohm and Miller, 2006). By resolving the variable region of 7D4 and cloning it into a mIgG2a backbone (outsourced), a depleting, Non IL-2 Blocking antibody ($\alpha CD25^{NIB}$) was generated, that could be tested *in vitro* and *in vivo* in comparison to the depleting (mIgG2a) but IL-2 blocking $\alpha CD25^{PC61}$.

The IL-2 blocking activity of $\alpha CD25^{NIB}$ and $\alpha CD25^{PC61}$ was compared by quantification of phosphorylated STAT5 (pSTAT5), a critical component of the IL-2 receptor signalling complex (as illustrated in **Figure 3.1**). $CD3^+$ T cells from C57BL6 splenocytes were stimulated with 50U/ml of IL-2 in the presence of IL-2-blocking/non-blocking αCD25 antibody or a control αIL-2 neutralising mAb. No pSTAT5 signalling was observed in $CD8^+$ or CD4 effector T cells (Teff) (as these express low to negative levels of surface CD25 in naïve animals) and thus we focused our analysis on regulatory T cells (Treg), as these constitutively express high levels of CD25. IL-2 stimulation increased pSTAT5 expression by approximately 50% on Treg. Pre-treatment of the cells with $\alpha CD25^{NIB}$ resulted in a similar increase. In contrast, treatment with $\alpha CD25^{PC61}$ resulted in a 50% reduction in pSTAT5 whilst αIL-2 neutralisation completely ablated pSTAT5 signal (**Figure 3.3A and B**).

We next evaluated whether these mAbs would interfere with IL-2 signalling in antigen experienced tumour infiltrating lymphocytes (TILs). To this end, mice where challenged with MCA205 tumour cells, and at days 5, 10 and 14, left

untreated or treated with αCD25^{PC61} or αCD25^{NIB}. One day after the last dose of mAb, mice were sacrificed and TILs isolated for pSTAT5 analysis ex-vivo post re-exposure to IL-2 (**Figure 3.4A)**. In CD8^{+} and CD4^{+} Teff cells, pSTAT5 signalling was significantly reduced by αCD25^{PC61} whereas αCD25^{NIB} did not produce a significant reduction compared to untreated TILS. In the Treg compartment, both αCD25^{PC61} and αCD25^{NIB} reduced pSTAT5 signalling, although to a much lesser extent with the αCD25^{NIB} (**Figure 3.4B**). Considering that binding of anti-CD25 could be reduced during tissue processing, TIL samples were re-incubated with the same antibodies administered *in vivo*. When TILs were re-exposed to αCD25^{PC61} or αCD25^{NIB} post isolation, αCD25^{PC61} completely abolished pSTAT5 signalling in CD8^{+} and CD4^{+} Teff cells as well as in the few remaining Treg cells relative to the untreated control (**Figure 3.4C and D**). In contrast, no significant reduction in pSTAT5 was observed when comparing CD8^{+} and CD4^{+} Teff cells from αCD25^{NIB} treated TILs versus untreated. A small, albeit significant decrease in pSTAT5 was observed in Treg cells treated with αCD25^{NIB}. Of relevance, only a very small number of events were analysed in this treatment group as the αCD25^{NIB} promoted depletion of tumour infiltrating Treg cells (**Figure 3.4D**). The data confirm that the αCD25^{NIB} does not block IL-2 signalling *in vitro* in CD3^{+} T cells as well as *ex vivo* in TILs, whereas the αCD25^{PC61} does significantly interfere with IL-2 signalling at the concentrations used.

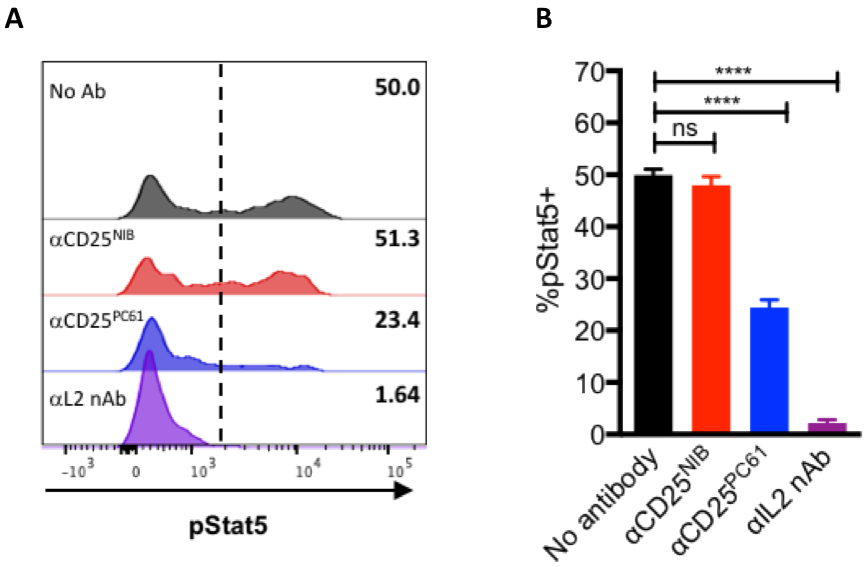

Figure 3.3. *In vitro* characterisation of Non-IL-2 Blocking anti-mouse CD25 mAbs (αCD25^{NIB})

Pan T cells were isolated from splenocytes using the Dynabeads FlowComp™ Mouse Pan T (CD90.2) kit. 200,000 cells were plated and rested for 2 hours at 37°C. Antibodies were added at 50μg/ml and incubated with the cells for 30 mins at 37°C, following which cells were stimulated with IL-2 (50U/ml) for 10 mins at 37°C. Cells were fixed and stained for pSTAT5 as described in the materials and methods section. **(A)** Representative histograms showing percentage of STAT5 phosphorylation observed in Tregs post-incubation with the antibodies listed. **(B)** Graph showing percentage of STAT5 phosphorylation observed in Tregs post-incubation with the antibodies listed.

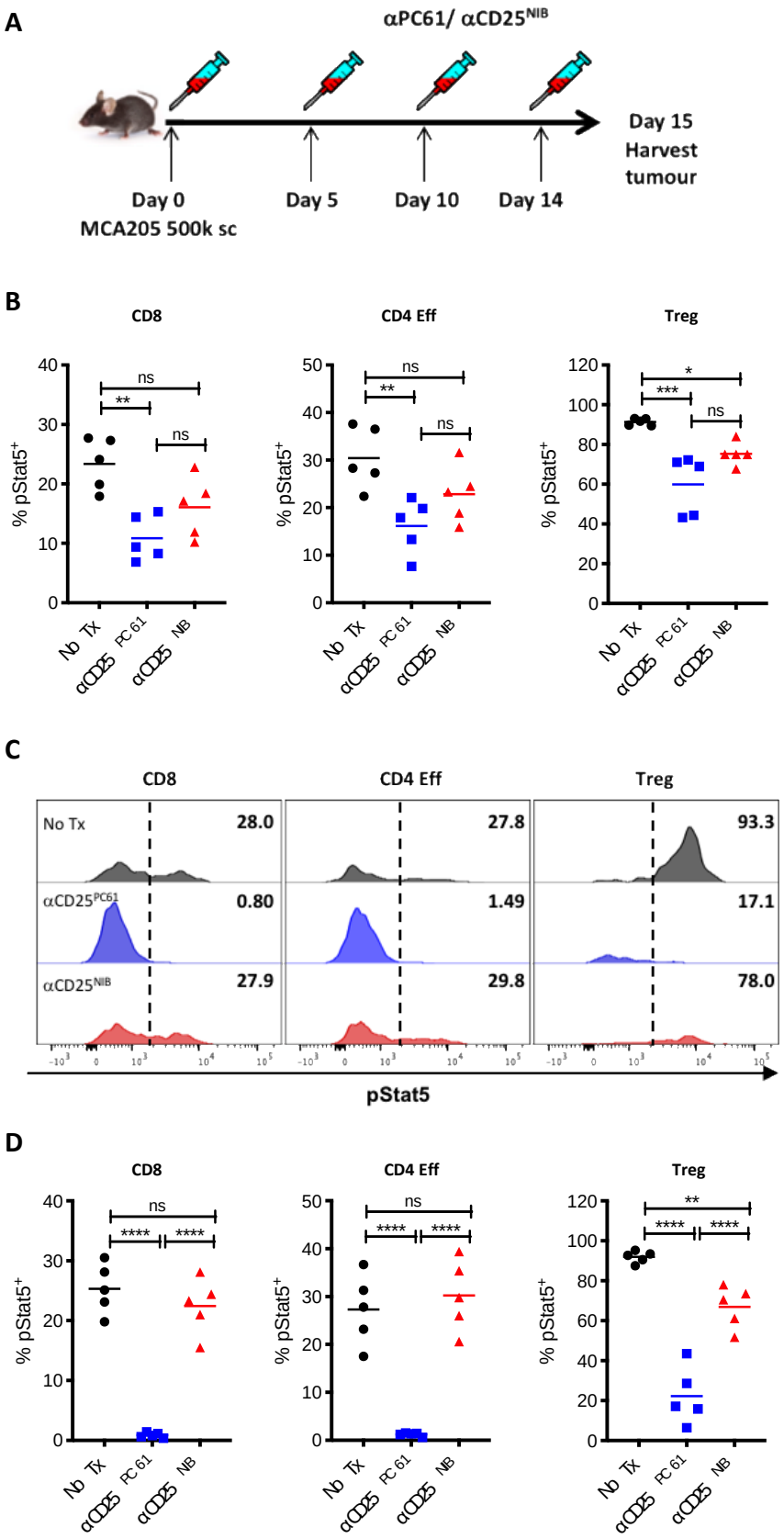

Figure 3.4. *Ex vivo* characterisation of αCD25^{NIB}

C57BL6 mice were injected s.c. with 500,000 MCA205 tumour cells. Once tumours were palpable, mice were injected IP with αCD25^{PC61}/ αCD25^{NIB} antibodies (200μg) on days 5, 10 and 14. Tumours were harvested on day 15 post-tumour inoculation **(A)**. Tumours were processed as described in the materials and methods section. 200,000 cells were plated in a 96-well plate, antibody was either added at 50μg/ml for 30 mins **(D)** or omitted **(B)** followed by IL-2 stimulation (50U/ml) for 10 mins. Cells were fixed and stained for STAT5 as described. **C)** Representative histograms showing percentage of STAT5 phosphorylation by CD8, CD4 eff and Treg cells post-treatments with antibodies shown in **(D)**. **(B and D)** Graphs showing percentage of STAT5 phosphorylation by CD8, CD4 Eff and Treg cells (n=5). All quantification plots: mean ± SEM, 1-way ANOVA (ns=p>0.05, *p<0.05, **p<0.01, ***p<0.001, ****p<0.0001).

3.4.2 Monotherapy αCD25^{NIB} drives rejection of established tumours in different mouse models

We next sought to compare the activity of αCD25^{NIB} and αCD25^{PC61} *in vivo* in different syngeneic tumour models. In all the models tested, a single dose of αCD25^{NIB} monotherapy 6 days after tumour implantation, resulted in complete tumour rejection and long-term survival, with 10/10 and 9/10 mice remaining free of CT26 or MC38 tumours up to 70 days, respectively. In contrast only 1/10 or 6/10 mice rejected CT26 or MC38 tumours when treated with a single dose of the IL-2-blocking αCD25^{PC61} **(Figure 3.5A and B).**

As CD25 is upregulated on cells exposed to IL-2 *in vitro* (Malek and Castro, 2010), we sought to exclude the possibility of potential depletion of CD25^{+} effector cells by treating mice with multiple weekly doses of αCD25^{NIB}. If CD25 were to be significantly upregulated on tumour reactive T cells activated by the first dose of a Treg depleting anti-CD25, we would expect that multiple doses would thwart anti-tumour activity. Mice were challenged with MCA205 tumours and received either 1 dose or 5 doses (1 dose weekly for 5 weeks) of the αCD25^{NIB} antibody. In both groups we achieved significant tumour control with 9/15 and 14/15 complete response. Multiple doses of the αCD25^{NIB} resulted in significant improvement in complete responses compared to a single dose, hence arguing against potential depletion of relevant effector populations (**Figure 3.6A**).

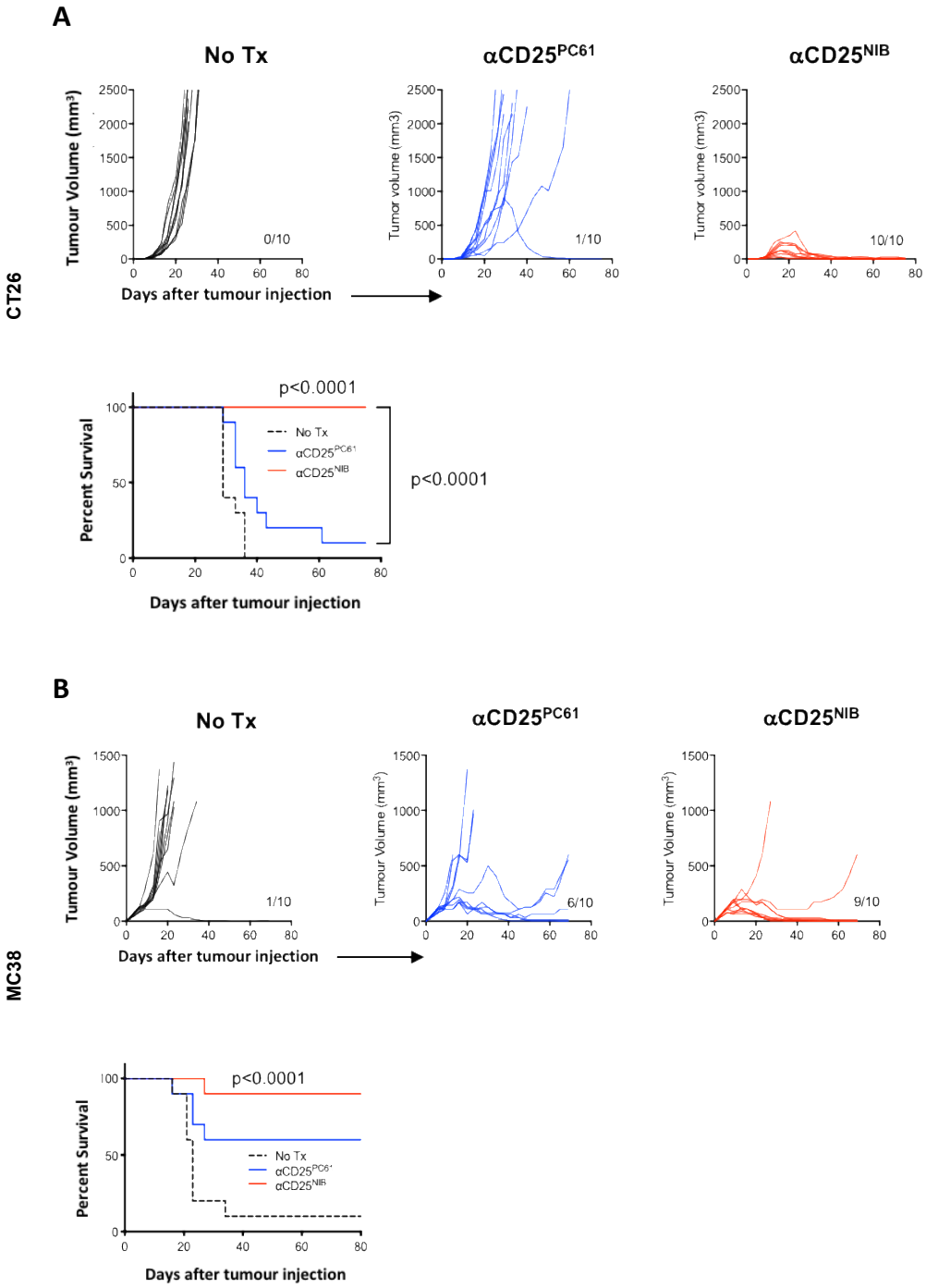

Figure 3.5. Monotherapy αCD25^{NIB} drives rejection of established tumours in different mouse models.

(A) Balb/C mice were injected s.c. with 500,000 CT26 tumour cells. Treatment with αCD25^{PC61}/αCD25^{NIB} (200μg) was started on day 6 post-tumour inoculation. At the top, growth curves showing growth of tumour. On the bottom, survival**. (B)** C57BL6 mice were injected s.c. with 1,000,000 MC38 tumour cells in Matrigel. Treatment started on day 6 post-tumour inoculation. At the top, growth curves showing growth of tumour. At the bottom, survival**.**

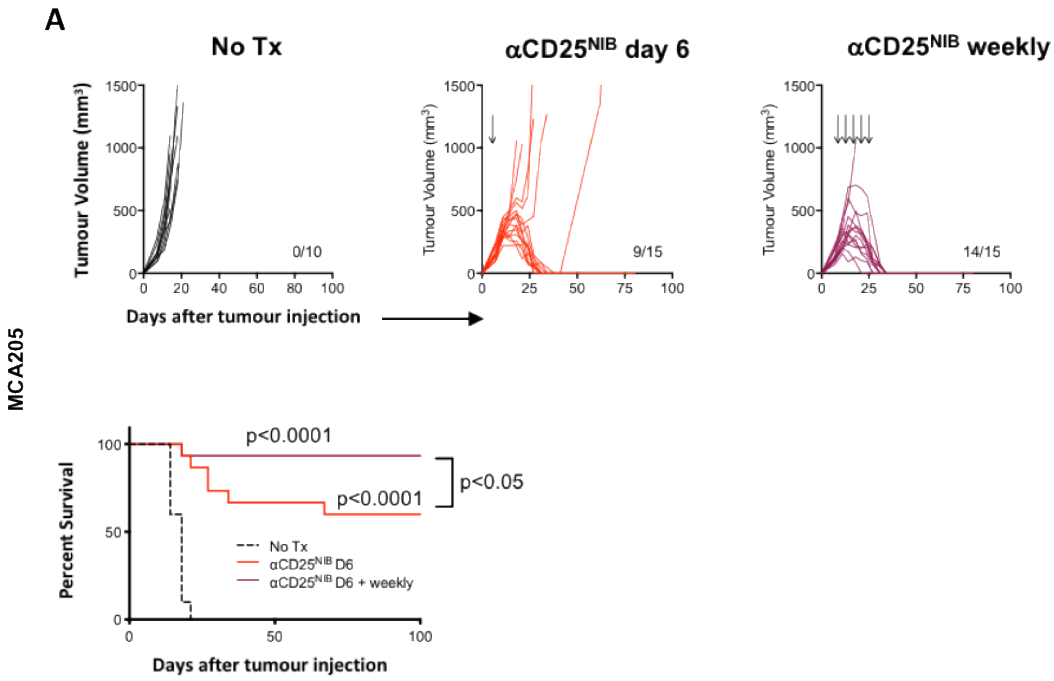

Figure 3.6. Multiple doses of αCD25^{NIB} result in significant improvement in complete responses compared to a single dose.

(A) C57BL6 mice were injected s.c. with 500,000 MCA205 tumour cells. Treatment started on day 6 (200μg) and continued weekly afterwards for 4 consecutive weeks for the αCD25^{NIB} weekly group. At the top, growth curves showing growth of tumour. On the bottom, survival**.**

3.4.3 Non IL-2 blocking feature of CD25^{NIB} is key for its therapeutic activity

Last, to determine whether the difference in the therapeutic activity of αCD25^{PC61} and αCD25^{NIB} was due to the differences in their IL-2 blocking activity *in vivo*, we treated MCA205-bearing mice with αCD25^{NIB} and neutralised IL-2 signalling with either an anti-IL-2 neutralizing mAb or the IL-2-blocking αCD25^{PC61} (**Figure 3.7A**). Impairing IL-2 signalling either by neutralising IL-2 or by blocking the high affinity IL-2 receptor interaction with IL-2 through αCD25^{PC61} ablated the therapeutic activity of αCD25^{NIB}. This confirms the critical role of IL-2 in tumour control and suggests that lack of single agent activity of αCD25^{PC61} (and potentially Daclizumab and Basilixumab) could be associated to their IL-2 blocking activity (**Figure 3.7A**). Similar results were observed in the CT26 model of colorectal carcinoma, with tumour control only achieved in mice treated with αCD25^{NIB}, and loss of control observed upon IL-2 neutralisation or signalling blockade in the αCD25^{PC61}-treated group (**Figure 3.7B**). The data supports αCD25^{NIB} antibodies as a powerful new approach to target regulatory T cells and boost anti-tumour immunity by taking advantage of endogenous IL-2 availability and signalling.

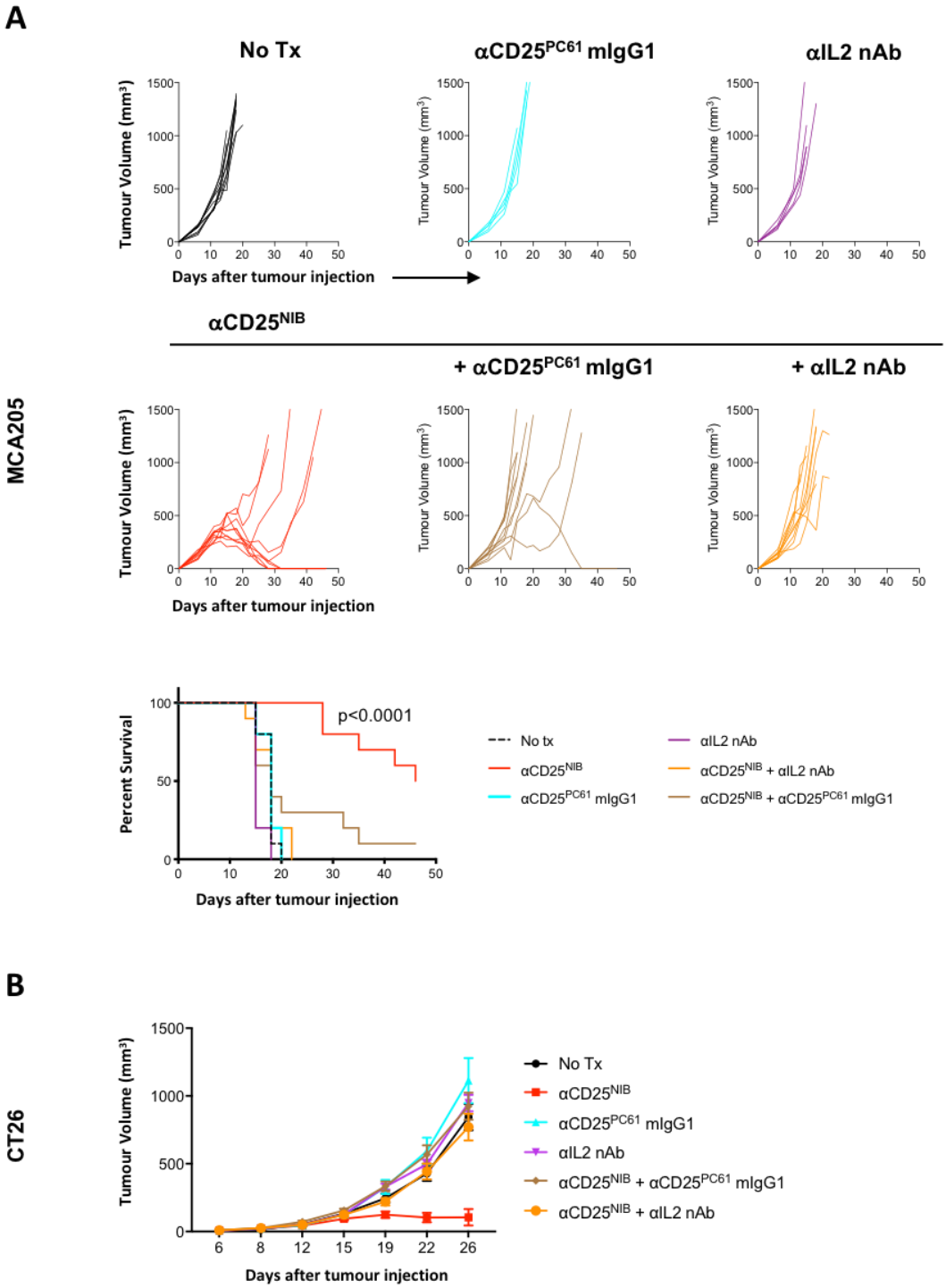

Figure 3.7. Non IL-2 blocking activity of αCD25^{NIB} is key for its therapeutic activity.

(A) C57BL6 mice were injected s.c. with 500,000 MCA205 tumour cells. Treatment (200μg IP) started on day 6 post tumour inoculation. Survival of these mice shown on the bottom. **(B)** Balb/C mice were injected s.c. with 500,000 CT26 tumour cells. Treatment was started on day 6 post-tumour inoculation. Mean tumour volume of the tumour-bearing mice, n=10.

3.4.4 αCD25^{NIB} and αCD25^{PC61} promote equivalent Treg depletion

We next sought to determine the mechanisms underpinning the superior *in vivo* activity of αCD25^{NIB}. Mice were challenged with MCA205 tumours, treated on day 5 and sacrificed at day 12 for analysis. Both αCD25^{PC61} and αCD25^{NIB} induced similar levels of intra-tumoural Treg depletion measured as percentage and absolute number of Foxp3+ T cells (**Figure 3.8A, 3.8B and 3.8C)**. Interestingly, whilst both antibodies significantly increased the CD8^{+}/Treg, CD4^{+}eff/Treg and NK/Treg cell ratios, αCD25^{PC61} had a stronger (although not significant) impact in the balance of effector and regulatory immune cells within tumours (**Figure 3.8D**) potentially due to the slightly higher reduction in Treg frequency induced by αCD25^{PC61} **(Figure 3.8B and C).**

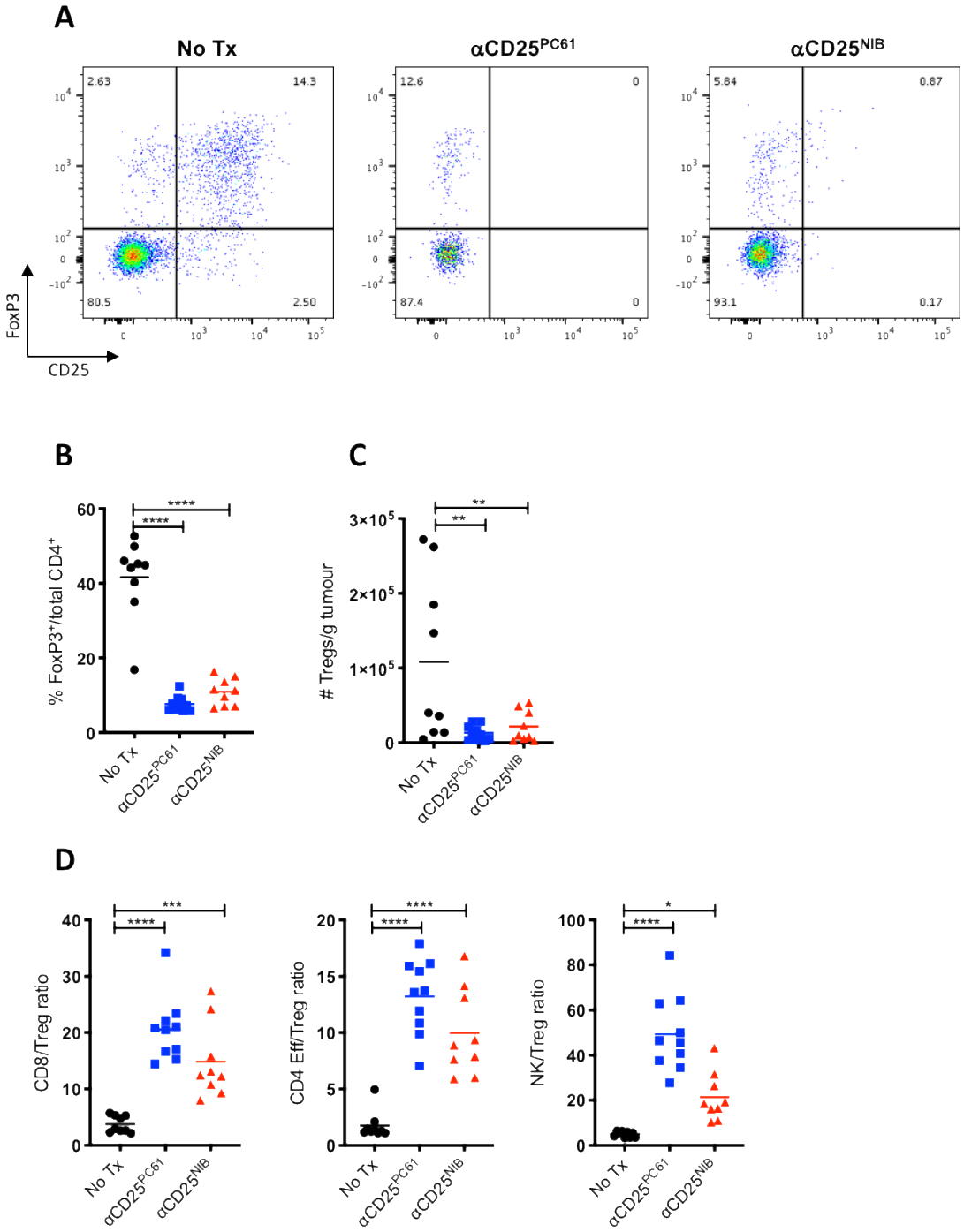

Figure 3.8. αCD25^{NIB} and αCD25^{PC61} promote equivalent Treg depletion.

C57BL6 mice were injected s.c. with 500,000 MCA205 tumour cells. Once tumours were palpable, on day 5, mice were injected IP with αCD25^{PC61}/αCD25^{NIB}/αCD25^{NIB} + αIL-2 (200μg). Tumours and LN were harvested on day 12 post-tumour inoculation and processed as described in materials and methods section. **(A)** Representative FACS plots showing expression of Foxp3 versus CD25 in CD4$^+$ T cells. **(B)** Graph showing % Foxp3$^+$ cells of total CD4$^+$ cells. **(C)** Absolute number of Tregs shown as number of Tregs/g of tumour. **(D)** Ratio of effector T cells over Tregs.

3.4.5 αCD25^{NIB} and αCD25^{PC61} lead to different effector T cell activation *in vivo*

Research has shown that IL-2 regulates granzyme gene expression independently of its effects on survival and proliferation (Janas *et al.*, 2005) and IL-2 activated nuclear factor kB (NF-κB) signalling and NF-κB binding sites have been identified in both mouse and human Granzyme B promoters (Zhou and Meadows, 2003; Huang *et al.*, 2006). Data from our lab has shown that upon depletion of regulatory T cells, an excess of IL-2 in the tumour microenvironment supports the acquisition of cytotoxic activity by T helper cells, and that this is orchestrated by the transcription factor Blimp-1 (Śledzińska *et al.*, 2020). Taking this into account, we next investigated the effects of the anti-CD25 antibodies on granzyme B production by CD8, NK and CD4 effector T cells.

Whilst having a slightly lower impact on the Teff/Treg balance within tumours, αCD25^{NIB} induced the highest levels of T cell activation with approximately 80% of CD8 TILs expressing high levels of Granzyme B in the αCD25^{NIB} group compared to 50% in αCD25^{PC61} treated mice and 65% in untreated mice. A similar trend was observed in the CD4 Teff and NK compartment. Strikingly, αCD25^{PC61} had a negative impact on the levels of Granzyme B expression by tumour infiltrating CD8^{+} T cells (**Figure 3.9A and C**) potentially due to its IL-2 blocking activity. Last, IL-2 neutralisation ablated the impact of αCD25^{NIB} on granzyme B within tumour infiltrating lymphocytes (**Figure 3.9A, 3.9B and 3.9C**). Levels of Granzyme B expression by CD8+ and CD4+ T cells were equivalent in mice treated with αCD25^{PC61} and those treated with αCD25^{NIB} and the neutralising anti-IL-2 mAb (**Figure 3.9A and 3.9C**) underscoring the relevance of endogenous IL-2 and detrimental impact of αCD25^{PC61} and IL-2 blockade on T cells within tumours.

Other markers that were evaluated for changes include: CTLA4, LAG3, TIM3, TIGIT, PD-1, GITR, OX40, ICOS and 4-1BB. No differences were observed for any of these markers in response to the antibody therapies that were used.

Similar patterns of Treg depletion, frequency of Granzyme B producing effector cells and levels of expression were observed in the MC38 mouse model of colorectal cancer confirming these findings are not specific to the MCA205 model (**Figures 3.10 and 3.11**). These findings suggest that IL-2 availability post Treg depletion is critical to the superior anti-tumour activity of $\alpha CD25^{NIB}$.

Both the tumour types tested, MCA205 and MC38 are chemically induced tumours which are very immunogenic (Lewis and Goldrosen, 1983) and capable of activating $CD4^+$ T cells. Even though these tumours do not express MHC class II molecules, tumours are not good antigen presenting cells and this signal would be provided by professional antigen presenting cells, such as macrophages, expressing MHC class II on their surface.

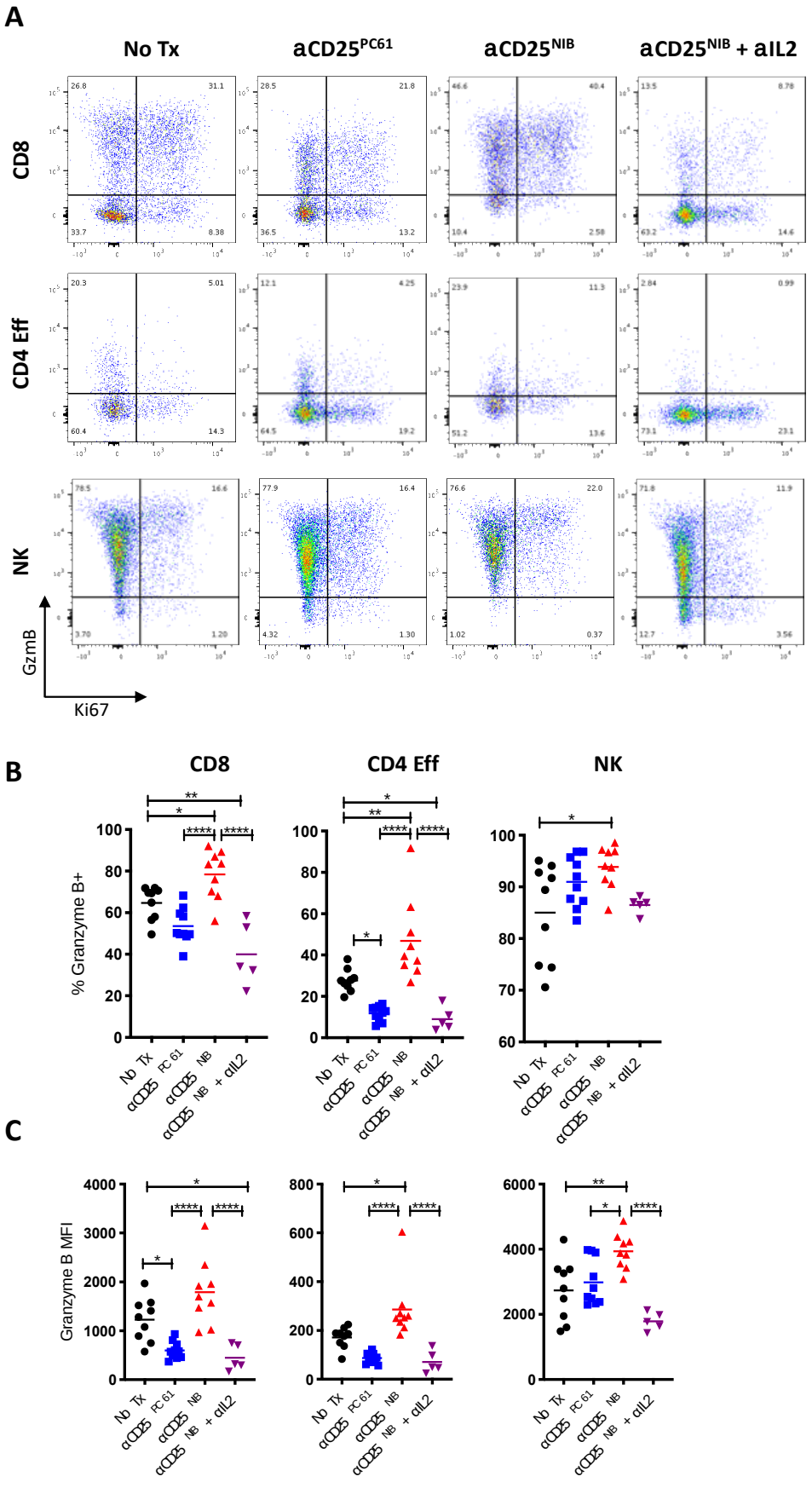

Figure 3.9. αCD25^{NIB} and αCD25^{PC61} lead to different effector T cell activation *in vivo.*

(continued from previous page).

C57BL6 mice were injected s.c. with 500,000 MCA205 tumour cells. Mice were injected IP on day 5 with $\alpha CD25^{PC61}$/$\alpha CD25^{NIB}$/$\alpha CD25^{NIB}$ + αIL-2 (200µg). Tumours and LN were harvested on day 12 post-tumour inoculation and processed as described in materials and methods section. **(A)** Representative FACS plots showing Granzyme B expression versus Ki67 expression in CD8, CD4 effectors and NK cells. **(B)** Graph showing percentage of Granzyme B+ cells in different effector subsets. **(C)** Graph showing the Mean Fluorescence Intensity of Granzyme of the effector cells plotted in **(B).**

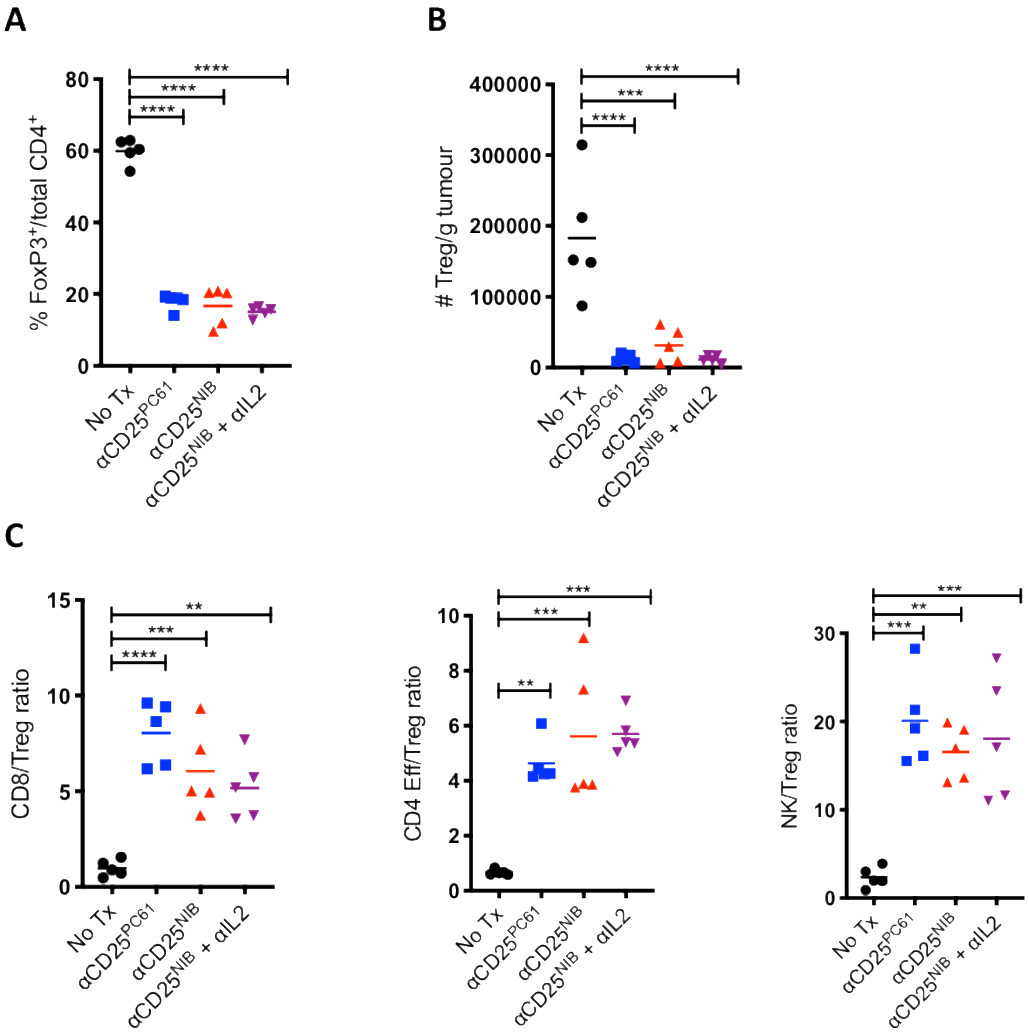

Figure 3.10. αCD25^{NIB} and αCD25^{PC61} promote equivalent Treg depletion (MC38).

C57BL6 mice were injected s.c. with 500,000 MC38 tumour cells. Once tumours were palpable, on day 7, mice were injected IP with αPC61/αCD25^{NIB}/αCD25^{NIB} + αIL-2 (200µg). Tumours and LN were harvested on day 15 post-tumour inoculation and processed as described in materials and methods section. **(A)** Graph showing % Foxp3^{+} cells of total CD4^{+} cells. **(B)** Absolute number of Tregs shown as number of Tregs/g of tumour. **(C)** Ratio of effector T cells over Tregs.

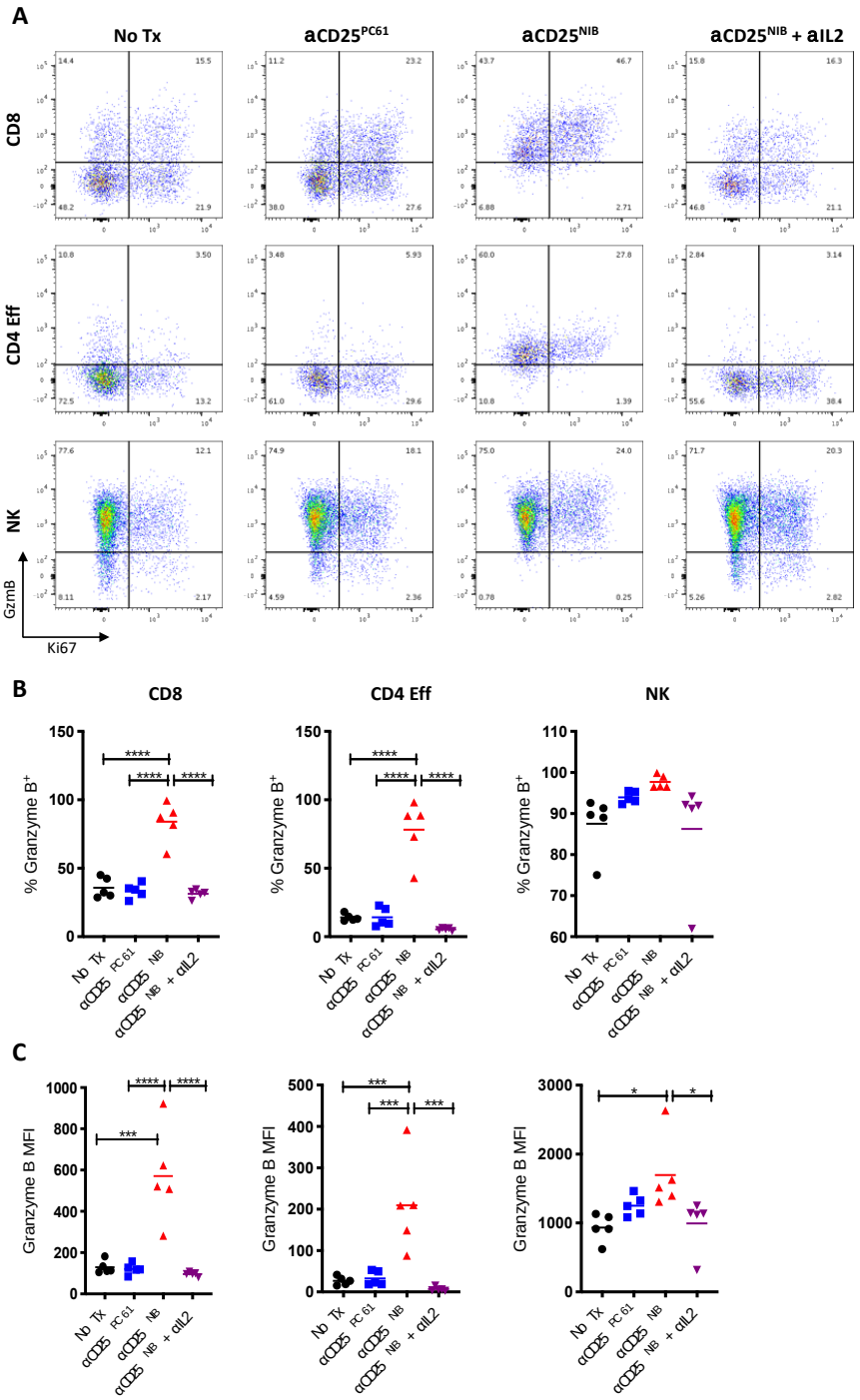

Figure 3.11. αCD25^{NIB} and αCD25^{PC61} promote different effector T cell activation *in vivo* (MC38).

C57BL6 mice were injected s.c. with 500,000 MC38 tumour cells. On day 7, mice were injected IP with αPC61/αCD25^{NIB}/αCD25^{NIB} + αIL-2 (200µg). Tumours and LN were harvested on day 15 post-tumour inoculation **(A)** Representative FACS plots showing Granzyme B expression versus Ki67 expression in CD8, CD4 effectors and NK cells. **(B)** Graph showing percentage of Granzyme B+ cells in different effector subsets. **(C)** Graph showing the Mean Fluorescence Intensity of Granzyme of the effector cells plotted in **(B)**.

3.4.6 αCD25^{NIB} treatment synergises with αPD-L1

We next evaluated the potential value of late αCD25^{NIB} intervention as a means to reduce or prevent resistance to αPD-L1. In this resistance model, mice challenged with MCA205 tumours and treated with αPD-L1 on days 6, 9, 12 and 18 (clone 10F.9G2) exhibit a short period of tumour control (between days 10 and 20) followed by rapid tumour relapse (**Figure 3.12A and 3.12B)**. To determine whether αCD25^{NIB} could reduce resistance post initiation of anti PD-L1 therapy, mice received a single dose of αCD25^{NIB} on day 10 or two doses (day 10 and 15) (**Figure 3.12A**). Whilst monotherapy αPD-L1 resulted in tumour delay and long term survival only in 10% of the mice (**Figure 3.12B and 3.12C**), a single dose of αCD25^{NIB} with αPD-L1 resulted in significantly higher (p-value<0.0001) tumour rejection and survival (52% of mice with complete rejection), which was further enhanced when giving an additional dose of αCD25^{NIB} on day 15 (70% of mice with complete rejection), demonstrating a synergistic activity with these two therapies (**Figure 3.12B and 3.12C**). Of relevance and as a control, monotherapy αCD25^{NIB} at day 10 led to tumour rejection and survival in 35% of the mice (**Figure 3.12C**). This data suggests that αCD25^{NIB} can be used in combination with checkpoint blockade to boost the immune response of tumours resistant to αPD-L1 blockade or other targets.

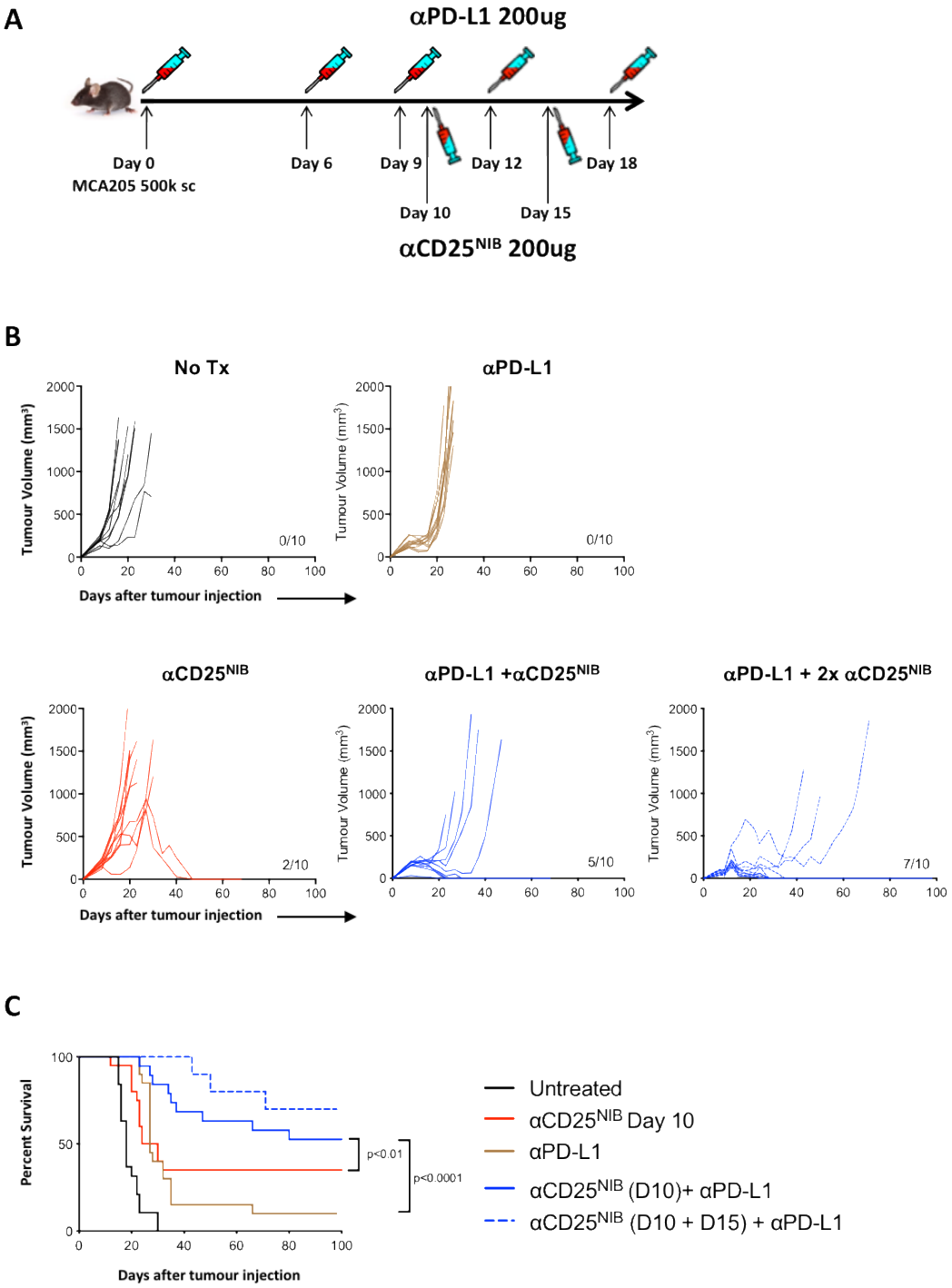

Figure 3.12. αCD25^{NIB} treatment synergises with αPD-L1.

(A) C57BL6 mice were injected with 500,000 MCA205 tumour cells. Treatment with αPD-L1 (200µg) was started day 6 and continued on days 9, 12 and 18. Groups receiving αCD25^{NIB} (200µg) received either 1 dose at day 10 or an additional dose at day 15. **(B)** Representative growth curves. **(C)** Cumulative survival from 2 independent experiments of those mice shown in **(B)**.

3.4.7 Development of a non-IL-2-blocking anti-human CD25 antibody

To test this hypothesis for human cancer immunotherapy, TUSK Therapeutics and Roche developed a non-IL-2-blocking anti-human CD25 antibody along the strategy illustrated in **Figure 3.13**. Briefly, CD25 binding antibodies were identified through phage display selections on recombinant human and cynomolgus CD25 protein starting from the Adimab antibody library. 43 derived hits were converted in human CD25 antibodies and were tested for their ability to bind to human Tregs, to not block IL-2 signalling in a STAT5 phosphorylation assay and to deplete *in vitro*-derived human Tregs in ADCC and ADCP assays (depicted in **Figure 3.13**). RG6292 was selected from the 31 qualifying clones as the lead preclinical candidate.

The data acquired by Roche using the RG6292 antibody are shown in the annex, supplementary **Figure 7.1 and Figure 7.2**. Their data confirms that the anti-human CD25 antibody produced, RG6292, does not block IL-2 signalling, is capable of performing ADCC and ADCP and preferentially depletes regulatory T cells in vitro and in patient tumour samples. In addition, their data showed that a single dose of RG6292 (anti-CD25^{NIB} GlyMAXX) depletes Treg cells in tumour-bearing humanised mice whilst allowing accumulation of activated CD8+ cells.

Figure 3.13. Strategy used for the development of the anti-human CD25 antibody (RG6292).

From the 43 human CD25 antibodies generated by Adimab, 31 were shown to not compete with IL-2 binding to CD25. All the antibodies that were binding to CD25 expressed on Treg cells were assessed for their ability not to block IL-2 signalling in a STAT5 assay. Killing of these non-IL-2 blocking antibodies was then assessed in classical ADCC and ADCP assays resulting in the selection of the lead candidates.

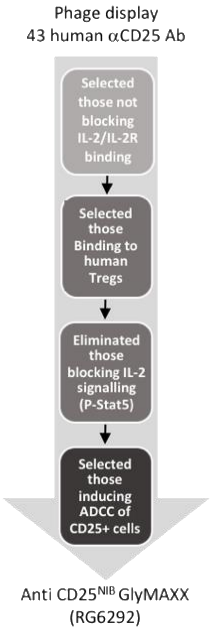

3.5 DISCUSSION

Effective Treg depleting strategies have been extensively investigated as an approach to enhance anti-tumour immune responses, with the primary limitation being the identification of targets expressed primarily on Treg whilst absent on activated Teff cells. Whilst several agents have moved from pre-clinical to the clinical setting, success remains limited. More recently, it has been shown that ADCC enabled antibodies directed to immune modulatory receptors such as CTLA-4, OX40 and GITR, can also deplete Treg in mouse tumour models, supporting the development of “dual activity antibodies”. These would kill Treg expressing high levels of the target receptor whilst blocking a co-inhibitory signal (CTLA-4) or delivering an activating signal (OX-40, GITR) to Teff cells expressing lower levels of the same receptor (Tyler R Simpson *et al.*, 2013; Wolchok *et al.*, 2013; Bulliard *et al.*, 2014; Furness *et al.*, 2014; Vargas *et al.*, 2018). However, upregulation of CTLA-4, OX-40 or GITR on activated effector T cells *in vivo*, could also result in their partial depletion, especially in the context of the new generation of ADCC-enhanced antibodies (i.e afucosylated CTLA-4), highlighting the need for more specific targets.

Our lab recently demonstrated that CD25 is expressed at high levels on Treg in mice and humans but at lower levels on $Foxp3^{-}CD4^{+}$ cells, and almost undetectable levels on tumour infiltrating $CD8^{+}$ T cells (Vargas *et al.*, 2017). In humans this expression pattern is retained even in the context of anti-PD-1 therapy (Vargas *et al.*, 2017)underscoring the potential value of this target for Treg depletion. This selective expression pattern, however, has not been leveraged to deliver significant clinical responses with currently available anti-human CD25 mAb Daclizumab and Basilixumab. Daclizumab and Basilixumab were designed to block IL-2 signalling rather than deplete Treg and are employed as immune suppressants in the context of autoimmune diseases and transplant rejection (Guo *et al.*, 2009; Baldassari and Rose, 2017). In addition, whilst both antibodies have an IgG1 isotype, they were not selected on ADCC capacity but for IL-2 blockade instead. In early phase clinical trials in cancer patients, Daclizumab caused some degree of circulating

Treg depletion but had limited anti-tumour activity (Jacobs *et al.*, 2010; Rech *et al.*, 2012). We hypothesized this might be due to its IL-2-blocking activity. IL-2 is critical for T cell responses and was the first immunotherapy tested in humans (Rosenberg *et al.*, 1989), leading to durable, complete responses in patients with metastatic melanoma and renal cancer (Rosenberg, 2014). Blockade might therefore be detrimental to anti-tumour activity. In keeping with this hypothesis, the mouse CD25-targeting antibody PC61 also blocks IL-2R signalling, potentially explaining its suboptimal in vivo activity as a single agent.

Our data demonstrate the critical importance of endogenous IL-2 to the function of the CD4 and CD8 effector compartments in the context of Treg depletion. Despite the very low levels of surface CD25 expression by tumour infiltrating CD8+ T cells (Vargas *et al.*, 2017), anti-CD25^{PC61} completely ablated pSTAT5 in these cells, highlighting the relevance of CD25 to IL-2R complex signalling in response to endogenous IL-2. In addition to depleting Treg, blockade of IL-2 signalling on tumour infiltrating effector T cells by anti-CD25^{PC61} resulted in reduced T cell cytotoxicity and tumour control. *In vitro* and *in vivo* evaluation of an ADCC enabled anti-CD25 mAb lacking IL-2 blocking activity (anti-CD25^{NIB}) demonstrated superior T cell activation and tumour control as a single agent against established mouse tumours. The data therefore support therapeutic attempts directed at Treg depletion over those directed at Treg inactivation, as depletion will increase availability of IL-2 and enhance Teff function, as long as IL-2 signalling is not concurrently blocked. Based on these data, Roche have developed a novel non-IL-2-blocking anti-human CD25^{NIB} (RG6292). This was generated in an enhanced ADCC format to enable maximal depleting activity in the tumour where high levels of the inhibitory FcγRIIB (CD32B) are usually found (Vargas *et al.*, 2017). Consistent with the mouse data, RG6292 effectively depleted human Treg whilst preserving IL-2R signalling on effector T cells, whereas Daclizumab, reduced both IL-2R signalling, and T cell activation. Evaluation of their clinical lead in humanised mouse models also showed reduction in Treg compared to control, and, equally importantly, increased CD8 T cell activation in tumours. In the

same experiments anti CTLA-4 (Ipilimumab) showed Treg depleting activity, but failed to significantly increase CD8 T cell activation.

The potent single agent activity of anti-CD25^{NIB} in immunogenic mouse tumour models characterised by Treg infiltration, suggests potential targets for future evaluation of RG6292 i.e. human malignancies that are known to be immunogenic in which Treg infiltration appears to correlate adversely with clinical outcomes (melanoma, lung cancer, head and neck and Microsatellite Instability-Hi (MSI-H) tumours). Our data also support evaluation in combination studies, since late intervention with anti-CD25^{NIB} in MCA205 bearing mice undergoing anti-PD-L1 treatment prevented tumour relapse in almost 50% of the cases. Clinical evaluation of concomitant versus sequential delivery of RG6292 with PD-1/PD-L1 blocking agents will be needed to optimise scheduling. The data thus far suggest that anti-CD25^{NIB} can be administered repeatedly as a single-agent, or alternated with anti PD-L1 yielding significantly better tumour control.

A further consideration relates to toxicities associated with manipulation of Treg number or function. Whereas Treg depleting agents can boost anti-tumour immunity, sustained systemic depletion promotes severe toxicities in mouse models such as the Foxp3-DTR model (Kim, Rasmussen and Rudensky, 2007). CD25^{NIB} fails to completely deplete Treg, with a maximum of 60% depletion observed. This incomplete depletion may be important with respect to the lack of toxicity seen in mice repeatedly treated with ADCC enabled anti-CD25 mAbs (Arce Vargas *et al*, 2017b).The toxicity profile of RG6292 will have to be assessed in the clinic. If toxicities are observed, future pre-clinical work with anti CD25^{NIB} antibodies should aim to target their activity to the tumour site either by local intra-tumour administration or by antibody engineering approaches such as bispecific mAbs targeting CD25 and a tumour target, or masked pro-antibody approaches with activation within the tumour microenvironment.

In conclusion, our data demonstrate that targeting CD25 with ADCC-enabled antibodies preserving IL-2 signalling is a novel and powerful strategy to

promote rejection of established tumours, delivering both depletion of Treg and enhanced, cell intrinsic IL-2-driven effector T cell activation. RG6292 is the first anti-human CD25 antibody developed to specifically deplete human Treg while preserving IL-2 signalling and effector T-cell activity and provides a novel therapeutic substrate for combination in cancer immunotherapy.

4 PRODUCTION OF A NOVEL BISPECIFIC ANTIBODY CO-TARGETING CD25 AND PD-L1

4.1 OVERVIEW

In this chapter, the production of a novel bispecific antibody, targeting both CD25 and PD-L1 is discussed. The “duobody technology”, developed by Genmab, was chosen as the most feasible strategy to produce this BsAb in the lab, with the work leading to the production and testing of the BsAb being presented and discussed below.

4.2 INTRODUCTION

4.2.1 Antibody production

Whole mAbs are large molecules (140-160kDa) and consist of 4 polypeptide chains; 2 heavy and 2 light, bound together by disulphide bonds and interchain non-covalent interactions. Antibodies are glycosylated at position N297 (location in heavy chain), which is critical for its stability as well as downstream immune effector functions (Thomson, 2016). Due to these features, in order for the antibody to be produced properly and to be functional, an expression system for the production of an antibody needs to be capable of many features. This includes production of protein and cell machinery capable of glycosylating, folding, orienting and covalently binding the peptide chain. This is not possible in lower organism expression platforms such as bacteria, yeast, insect and plant cells, which lack the machinery to glycosylate the antibody properly as well as generating the tertiary structure needed. Nonetheless, these platforms are commonly used for the production of smaller antibody fragments as these systems are much cheaper, quicker and easier to use than mammalian expression systems (Frenzel, Hust and Schirrmann, 2013; Vazquez-Lombardi *et al.*, 2018; Sifniotis *et al.*, 2019).

Various mammalian expression systems have now been developed with the aim of making antibody production more efficient in terms of yield, quality, scalability and reproducibility. Commercially, the most common cell lines used for whole therapeutic antibody expression are Chinese hamster (CHO), mouse myeloma (NS0), and mouse hybridoma (Sp2/0) cell lines (Elgundi *et al.*, 2017). However, for smaller amounts needed for the purpose of research and development, transient expression in human cell lines such as human embryonic kidney (HEK 293) are preferred over CHO cells as these allow for an easier and quicker production of needed quantities for smaller experiments (20-200mg/L versus 3g/L with CHO cells) (Frenzel, Hust and Schirrmann, 2013; Lalonde and Durocher, 2017).

The process of antibody production consists of the three main stages outlined below (Vazquez-Lombardi *et al.*, 2018)

1. **Cloning of antibody sequences into an appropriate expression vector**
    - Sequences are codon optimised according to the expression system of choice
    - Sequences are added to enable efficient transcription, secretion and selection (such as addition of a Kozak sequence, N terminal signal peptide (to allow secretion into media) and a C terminal stop codon) (You *et al.*, 2018).

2. **Transfection** into mammalian cell lines optimised for antibody expression and secretion

3. **Purification** from supernatant via affinity chromatography

4.2.1.1 Transfection

Cloning of antibody sequences is discussed in detail in the materials and methods section. Once the sequences are cloned, the constructs are transfected into the cell line of choice. The ultimate goal of transfection is to

get a high expression of the gene of interest, while maintaining the health of the cell. Transfection is therefore performed on cell cultures with high viability and high cell density. The most common transfection reagents used to enhance transgene delivery into the mammalian cell lines are cationic polymers. These tightly condense DNA and form endosomes which are absorbed by the cell (Geisse, 2009). PEI is the most commonly used transfection reagent as it's cheap and pretty efficient (Huh *et al.*, 2007). More effective, but also more expensive reagents have been developed since then, such as Freestyle MAX and FuGENE6 (Geisse, 2009; Jain *et al.*, 2017).

Each antibody needs to have the ratio of light: heavy chain adjusted for optimal antibody expression and having the chains on separate plasmids makes this easier (Wijesuriya *et al.*, 2018). This is based on the fact that free antibody heavy chains are not exported unless assembled into an IgG molecule. Therefore, the ratio of heavy chain to light chain in the endoplasmic reticulum of the cell is crucial as it determines the rate of folding and assembly. An excess of light chain is preferred in most cases as it is thought to facilitate the production of the antibody and minimise accumulation of the unfolded heavy chain peptide (Kaloff and Haas, 1995).

4.2.1.2 Antibody purification

Antibodies are harvested from the supernatant of the cells and purified using affinity chromatography, by using columns containing protein A or protein G. These are proteins derived from bacteria, which have a high affinity for the Fc portion of antibodies. They bind to different sites between the CH2 and CH3 domains, with protein A binding to 5 sites, and protein G to 1-2 sites. Protein G and protein A have developed different strategies for binding to the Fc region. The protein G: Fc complex involves mainly charged and polar contacts, whereas protein A and Fc are held together through nonspecific hydrophobic interactions and a few polar interactions (Choe, Durgannavar and Chung, 2016). The choice of protein depends on the antibody to be purified, with binding affinity of antibody backbones from different species to protein A and G shown in **Table 4.1** below.

Table 4.1. Binding affinity of different immunoglobulins to protein G and protein A.

++++= *strong binding.++ = medium binding.— = weak or no binding.*
(GE Life Sciences, 2016)

SPECIES	SUBCLASS	PROTEIN G BINDING	PROTEIN A BINDING
Human	IgG_1	++++	++++
	IgG_2	++++	++++
	IgG_3	++++	–
	IgG_4	++++	++++
Mouse	IgG_1	++++	+
	IgG_{2a}	++++	++++
	IgG_2	+++	+++
	IgG_3	+++	++

The purification process is shown below in **Figure 4.1**. Briefly, the supernatant is mixed with binding buffer (antibody-antigen binding is usually most efficient in aqueous buffers at physiological pH and ionic strength such as PBS), added to the column, allowing the target molecule to bind to the column. The non-bound components are then washed away. Buffer conditions are then used to disrupt the affinity interaction and elution is achieved by lowering the pH. The most widely used elution buffer is glycine (at pH 2.5-3), as it effectively dissociates the interaction between the antibody and protein, without permanently affecting protein structure (GE Life Sciences, 2016).

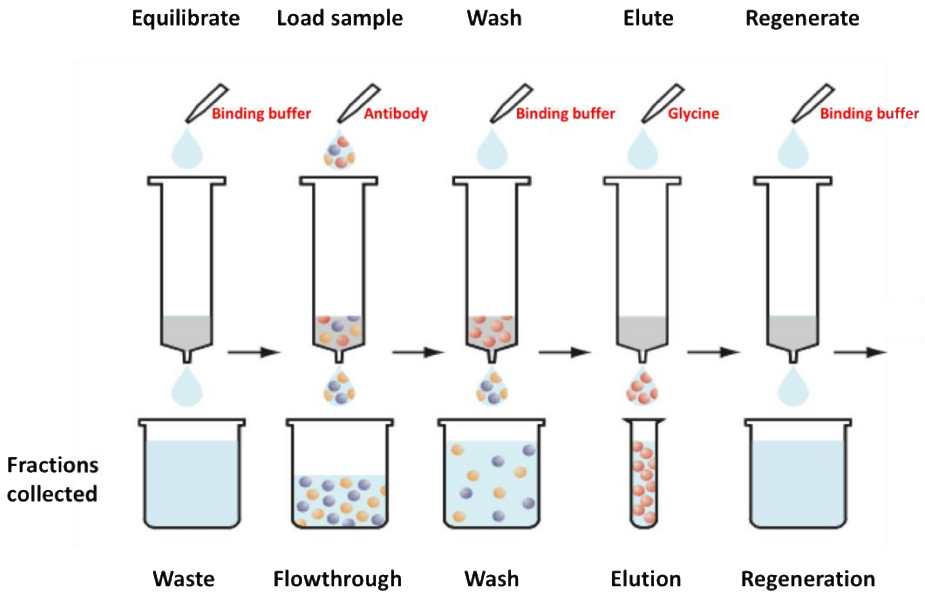

Figure 4.1. Schematic of antibody purification using protein A/protein G columns.

Modified from (GE Life Sciences, 2016)

4.2.2 BISPECIFIC ANTIBODIES

4.2.2.1 What are bispecific antibodies?

A bispecific antibody is an antibody that combines the specificities of two antibodies. It can simultaneously bind to two different antigens or epitopes. These include receptors or ligands associated with cancer, proliferation or inflammation. They can also place targets into close proximity and thus trigger contacts between cells leading to the recruitment of immune cells to tumours (Labrijn *et al.*, 2014; Spiess, Zhai and Carter, 2015).

Cancer is a multifactorial heterogeneous disease, and depends on multiple targets of survival and proliferation, with a lot of crosstalk between signalling cascades. Therefore, targeting one target is often not enough to destroy cancer cells. Many patients do not adequately respond to monospecific therapy and acquire resistance to treatment. Hence, targeting several aspects at the same time increases the chance of the treatment being successful and reduces the risk of tumour escape. In addition, bispecific antibodies have the potential to display a novel function that's not observed in any combination of the parental antibodies. Moreover, from a development point of view, obtaining regulatory approval for one molecule is often faster as well as more cost-effective. However, the use of a bispecific antibody as opposed to a combination of two monospecific antibodies also has some drawbacks. Dosing is difficult as individual doses cannot be properly optimised, whereas by using a combination of monospecific antibodies, this is possible. In addition, production of these is not as simple as production of monospecific antibodies, and is discussed in more detail below (Labrijn *et al.*, 2019).

Bispecific antibodies were first described more than 50 years ago (Labrijn *et al.*, 2019), yet only two bispecific antibodies are currently approved for therapy; Blinatumomab, a T cell engaging BITE (αCD19 x αCD3) for relapsed/refractory (r/r) ALL (Gökbuget *et al.*, 2018) and Emicizumab (coagulation factor IXa (FIXa) x FX) for haemophilia A (Oldenburg *et al.*, 2017). The reason it took so long for these antibodies to be used for therapy, is because production of these

bispecific antibodies has proven to be very challenging, mainly due to the natural physiology of antibodies. Co-expression of 2 heavy and 2 light chains of different specificities in a host cell leads to a very low yield of BsAb production. This is because mispairing of heavy and light chains occurs; termed the “heavy chain problem” and “light chain problem”.

The “heavy chain problem” occurs when heavy chains form both homo- and heterodimers. The “light chain problem” occurs when light chains mispair with non-cognate heavy chains. This mispairing results in up to 9 unwanted antibodies in addition to the desired BsAb (Milstein and Cuello, 1983). However, in the last 20 years, many more efficient methods have been developed, which has allowed for easier production of bispecific antibodies. Breakthrough in the development of these arose when a technology called “knobs into holes” developed. This method relies on forced heavy chain heterodimerisation by the introduction of various mutations into both CH3 domains. In one of these chains, a smaller amino acid is replaced with a larger one, forming a sort of knob, whereas in the other chain, a larger amino acid is replaced with a smaller one, creating a sort of hole (Labrijn *et al.*, 2014). Nowadays, multiple strategies have been developed with the aim of promoting heterodimerisation of the two different heavy chains, all leading to the efficient pairing of these heavy chains and are discussed in detail in “Alternative molecular formats and therapeutic applications for bispecific antibodies” (Spiess et. Al., 2015). However, using these methods, the light chain problem still exists. Therefore, nowadays, the most common method to produce these BsAbs is by expression of the parental antibodies separately and their subsequent re-assembly *in vitro*.

With antibody engineering becoming more and more advanced, there is now a variety of bispecific formats available, with over 100 existing BsAb formats (illustrated in **Figure 4.2**) ranging from small proteins, to large IgG-like molecules with additional domains attached. Of those, more than 85 are in clinical development, with the majority of these being evaluated in patients with cancer. Around half of these are based on T cell redirection to the tumour site (Labrijn *et al.*, 2019). The various formats vary in terms of molecular weight,

number of antigen binding sites, geometry of these sites, half-life and engagement of effector functions. Therefore, the choice of format depends on the outcome required by the user. Importantly, these antibodies can be divided into two major types; those which contain an Fc region and those that do not. The Fc region serves several purposes to the BsAb. Firstly, it allows for easier purification of the BsAb post-production. Secondly, it bestows the antibody with an increased stability and solubility. Finally, it allows for Fc mediated effector functions such as ADCC and CDC as well as FcR-mediated recycling via the neonatal Fc receptor (FcRn) (which confers a longer half-life onto the antibody) (Kontermann and Brinkmann, 2015).

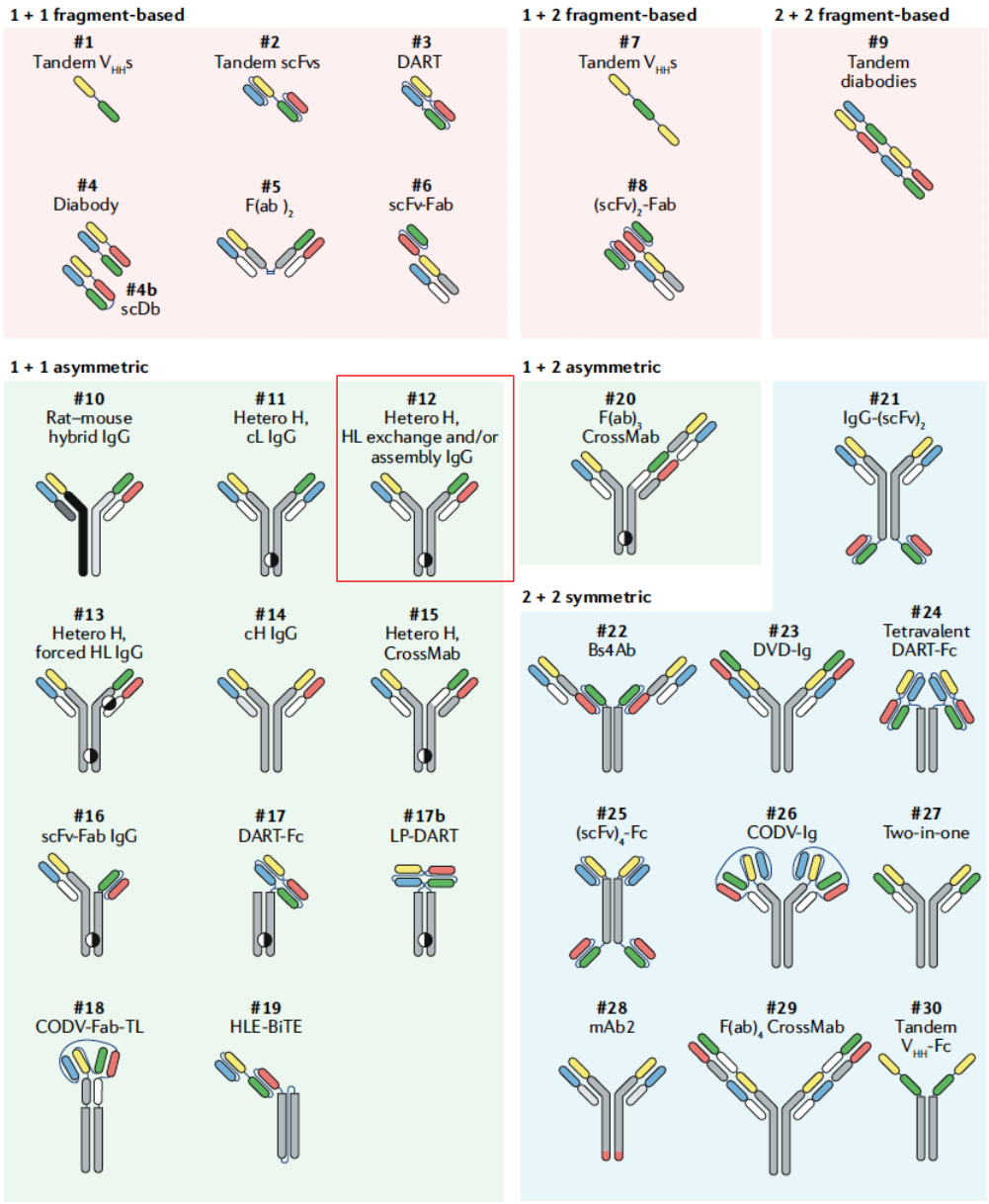

Figure 4.2. Selection of BsAb formats.

Bispecific antibodies (BsAbs) are categorized by increasing valency for each of the two target specificities from left to right and their format class. Formats are classified as fragment-based (without an Fc domain) and asymmetric or symmetric Fc-bearing molecules. Antibody domains are coloured according to their architecture: orange, variable heavy (H) chain specificity 1; green, variable H chain specificity 2; blue, variable light (L) chain specificity 1; red, variable L chain specificity 2; grey , H chain constant region; white, L chain constant region; light grey , alternative L chain constant region; format #10: dark grey and black , rat L chain and immunoglobulin G2b (IgG2b) H chain; and white and light grey , mouse L chain and IgG2a H chain. cH common heavy ; cL , common light; HLE, half-life extended; scDb, single-chain diabody ; scFv, single-chain variable fragment; VHH, heavy chain-only variable domain **Format chosen for this thesis is highlighted by a red square - #12** (Labrijn *et al.*, 2019).

4.2.3 Rationale for αCD25 x αPD-L1 BsAb

As mentioned in depth in Chapter 3, CD25 is a good target for Treg depletion. The rationale behind this BsAb was to target Treg depletion to the tumour, with the aim of limiting toxicity effects by systemic depletion of Tregs. The αPD-L1 arm was selected for a number of reasons. Firstly, PD-L1 is known to be upregulated on a wide range of tumour cells and is often used by cancer cells as a mechanism to avoid immune surveillance (Sznol and Chen, 2013). This overexpression can result from a number of different factors, including activation of important oncogenic pathways (such as the PI3K and MAPK pathway). In addition, IFNγ in the TME increases levels of PD-L1 expression (Parsa *et al.*, 2007; Pardoll, 2012). Therefore, PD-L1 upregulation in the TME could favour accumulation of the bispecific in the tumour, which would lead to

1. Blockade of PD-L1/PD1 interaction
2. ADCC/ADCP of Tregs
3. ADCC of PD-L1 high tumours

As a caveat for this approach, it is important to mention that PD-L1 is not expressed exclusively by tumour cells. It's also expressed on T and B cells, myeloid and dendritic cells as well as non-haematopoietic tissues (such as lung and heart) although at lower levels (Śledzińska *et al.*, 2015). The impact of this compound on these cell subsets will be evaluated *in vivo*.

4.2.4 Duobody technology

Considering the characteristics desired for the BsAb αCD25 x αPD-L1, a full-length bispecific antibody structure was chosen, with production based on the duobody technology developed by Genmab (Labrijn *et al.*, 2014). This technology is based on a process called "fab-arm exchange", which is a physiological process that occurs naturally *in vivo* in human IgG4 half-molecules, where antigen-binding sites are naturally exchanged *in vivo* between antibody molecules leading to novel binding combinations in the new BsAb (Kolfschoten *et al.*, 2007). This protocol is based on the separate expression of two parental hIgG1s containing matching point mutations in the

CH3 domain – K409R and F405L (EU numbering (Johnson, 2001). Separate expression of these antibodies followed by their equimolar combination in reducing conditions allows fab-arm exchange and the generation of a stable bispecific antibody. This process removes the heavy and light chain problem discussed above and allows for the easy exploration of several combinations of bispecific antibodies. The exact protocol is outlined in (Labrijn *et al.*, 2014).

4.3 AIMS

The aim of the work presented below was to produce and test the activity of a novel bispecific antibody targeting both CD25 and PD-L1. To do this, the main objectives were to:

- Optimise antibody production in the lab
- Produce the parental antibodies required for the subsequent production of the BsAb
- Produce the BsAb using the “duobody technology”
- Test functionality of the BsAb *in vitro* in terms of binding to its targets
- Test activity of the BsAb *in vivo* in mouse tumour models

4.4 RESULTS

4.4.1 Cloning of constructs into vectors suitable for the production of antibodies in the Freestyle 293 expression system

The first step required for the production of antibodies, is the cloning of the constructs into an appropriate vector. Prior antibody production in the lab involved using K562 cells (human cell line from the bone marrow). However, the maximum yield obtained using these cells in our lab was 1mg/L, and involved handling litres of supernatant, expensive reagents and extensive purification techniques. Taking all of this into account, an alternative expression system was chosen, the Freestyle MAX 293 expression system with the aim of increasing the yield of antibody produced. This system makes use of suspension HEK 293 cells that are adapted to high density growth. For this expression system to work, a mammalian expression vector is needed with a strong CMV promoter. The UCOE vector (Merck) was chosen as it has this feature. In addition, this vector has sequences which alter chromatin organisation and therefore promote the transcription of genes and lead to increased expression of the genes.

Having already cloned the sequences into the SFG vector (retroviral vector kindly donated by Martin Pule), the new vector, UCOE, had to be re-engineered, due to the site available for cloning, Bmt1, cutting inside the human IgG sequence and there not being any other appropriate restriction enzymes available for more practical, subsequent use of the vector. Using the Q5 mutagenesis kit (NEB), a PacI restriction site was inserted, along with two other restriction sites (AsiSI and NgoMIV) in case more sites were needed for future cloning. The primers were designed using Q5 NEBuilder (**Figure 4.3A**). The UCOE vector prior to the addition of the new restriction sites is shown in **Figure 4.3B**.

The cloning steps undertaken to produce the final vector containing the αPD-L1 hIgG1.F405L sequence are outlined in **Figure 4.3 C-E**. Briefly, the variable

region of the anti-PD-L1 sequence (S70 clone – cross-reactive to mouse and human PD-L1) was PCRd from a construct that had been previously made in the lab, αPD-L1 mIgG2a. A PacI restriction site was added to the 5' end of the sequence and a Bmt1 to the 3'end and cloned into the UCOE vector containing the sequence of αCD25 hIgG1 (cloning of which is described in the materials and methods section). The next step was to introduce the F405L mutation into the hIgG1 backbone of the sequence. This was attempted using the Q5 site-directed mutagenesis protocol from NEB, but was not successful and the mutation was then introduced using primers designed to introduce that mutation into hIgG1, and then using an overlap PCR to overlap the two fragments together, as is outlined in **Figure 4.3D** and described in detail in the materials and methods section. The final step, outlined in **Figure 4.3E**, involved the digestion of the UCOE vector using PacI and MluI restriction sites and the insertion and ligation of the new αPD-L1 hIgG1 sequence containing the F405L mutation. The sequence was verified by sequencing services provided by GATC. Exact details of how all these cloning steps were undertaken are outlined in the materials and methods section.

A

IS173_UCOE_mut_FW	GGCGCGATCGCGCTAGCATGGAGACCGAC	insertion of restriction sites into UCOE - PacI, AsiSI, NgoMIV	Tm=63 Ta(annealing temp)=66
IS174_UCOE_mut_RV	GGCTTAATTAAGGCCGGCCGTTAACTTAA		Tm=64 Ta(anneal temp)=66

B

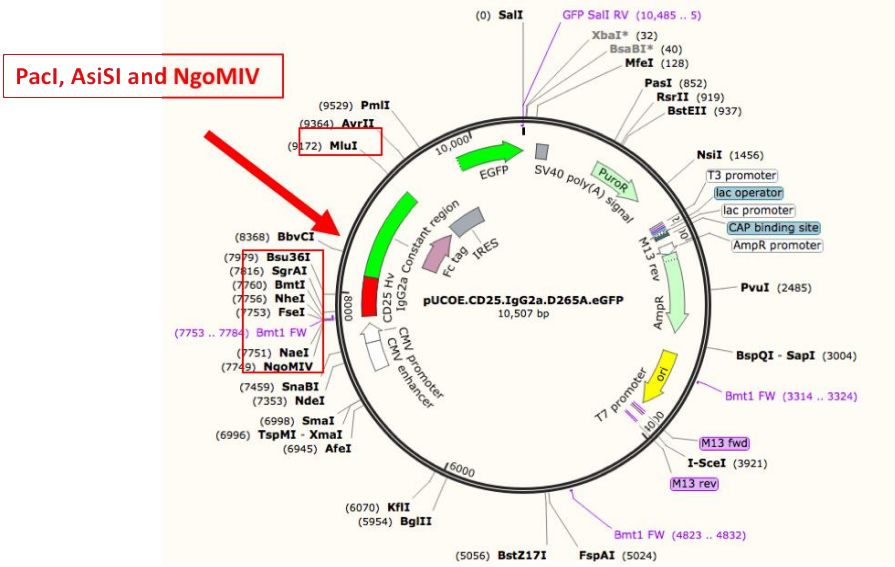

C

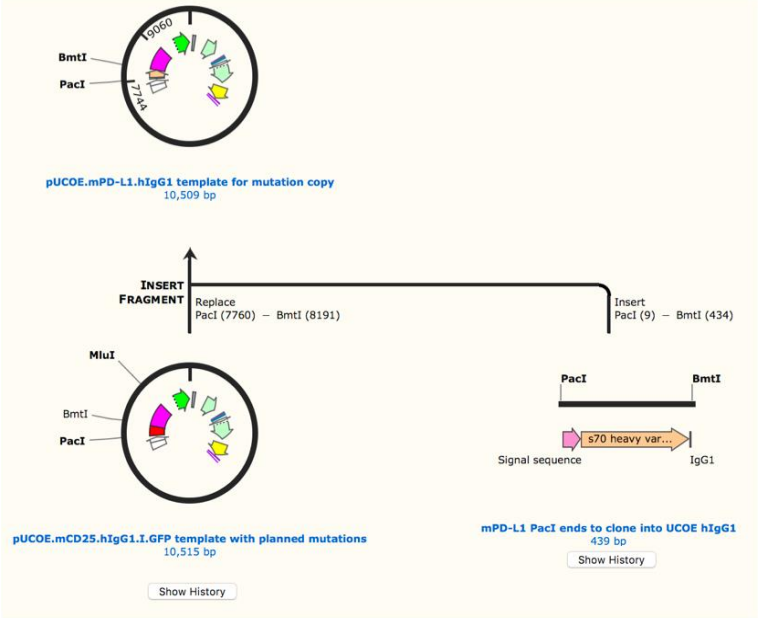

Figure 4.3. Cloning of constructs into vectors suitable for the production of antibodies in the Freestyle 293 expression system.

(A) Primers used for the introduction of the restriction sites into the UCOE vector. **(B)** Map of UCOE vector prior to introduction of the restriction sites, shown in red. **(C)** Cloning of the variable region of the anti-PD-L1 sequence onto a human IgG1 backbone. *(Figure continued on next page)*

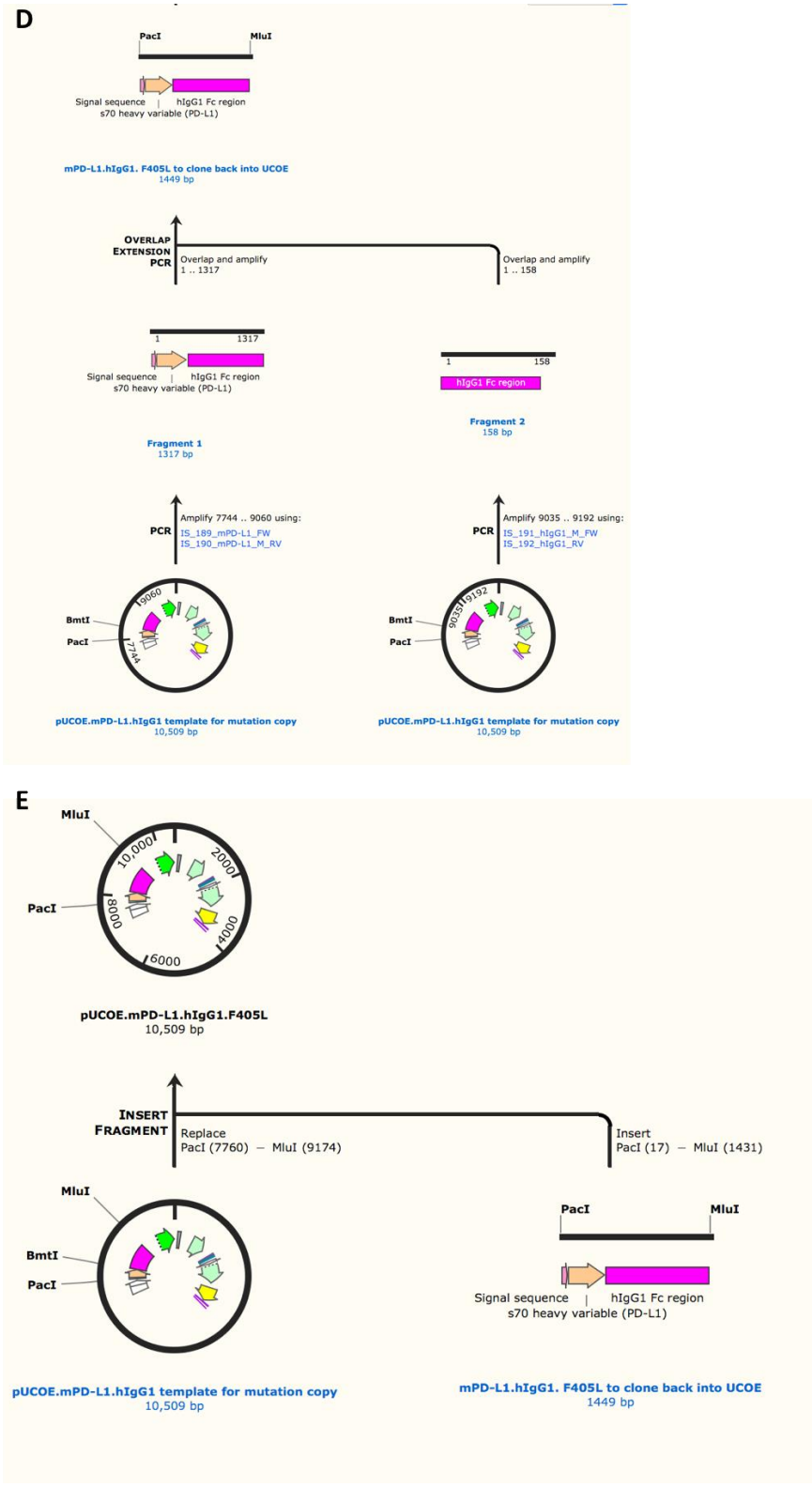

Figure 4.3. Cloning of constructs into vectors suitable for the production of antibodies in the Freestyle 293 expression system *(continued from previous page).*

(D) Mutation of the hIgG1 backbone and overlap PCR. **(E)** Insertion and ligation of the new αPD-L1 hIgG1 sequence containing the F405L mutation into the UCOE vector.

4.4.2 Optimisation of the Freestyle MAX 293 expression system – using Freestyle Max reagent as a transfection reagent

For the first transfection, Invitrogen's protocol for transfection was followed (as described in the materials and methods section), using 293F cells and Freestyle Max reagent as a transfection reagent. A 1:1 ratio of light: heavy vector was used as a starting point, and a time-course experiment was performed, whereby 50 µl of supernatant was collected on days 1-9 post-transfection, and used for

- Western blot to compare antibody levels (**Figure 4.4A**)
- FACS to monitor transfection efficiencies (**Figure 4.4C**)
- Viability post-transfection (**Figure 4.4D**)

The western blot performed on the supernatant at different days post-transfection (**Figure 4.4A**) shows that antibody was being produced, with faint bands starting to appear on day 2 post-transfection, and the strongest signal being observed on day 6. As the blots were done separately, they could not be compared to one another, and so they were compared to the positive control (rat antibody) on the same plot. The signal of the heavy and light chains was quantified, using ImageJ, normalised to the signal of the control bands and plotted in **Figure 4.4B**. Transfection efficiency was assessed by flow cytometry, with the percentage of double positive cells (cells transfected with both heavy and light chain vectors; heavy vector contains GFP and light vector contains BFP) being plotted on different days versus the antibody production assessed in **Figure 4.4B**. Percentage of transfected cells peaked at day 2, with levels steadily declining, and antibody production starting day 2 and peaking at day 6. Viability and cell density were assessed using MUSE cell counter, with numbers plotted in **Figure 4.4D**. Viability decreased from 98% on day 0, to around 60% on day 6, and 50% on day 9. Transfection did not stop cell growth, with cell numbers increasing from 1 million cells/ml to about 2.3 million/ml on day 6, peaking on day 8 at 3 million/ml. Taking all this data into account, day 6 was chosen as the optimal day to collect supernatant post-transfection of the 293F cells. The remaining supernatant of the first transfection, 25ml, was concentrated 50 times to a total volume of 500ul,

loaded onto a protein G column for purification of the antibody and aliquots taken at each step for visualisation on a Western Blot (**Figure 4.4E**). No antibody was recovered in the elution step, with antibody being lost in the flow-through, as well as the wash (**Figure 4.4E**). Having failed twice to produce antibody using Invitrogen's protocol and Freestyle Max Reagent, we then went on to try a different method which was being used for antibody production in Professor Kerry Chester's lab at the UCL Cancer Institute.

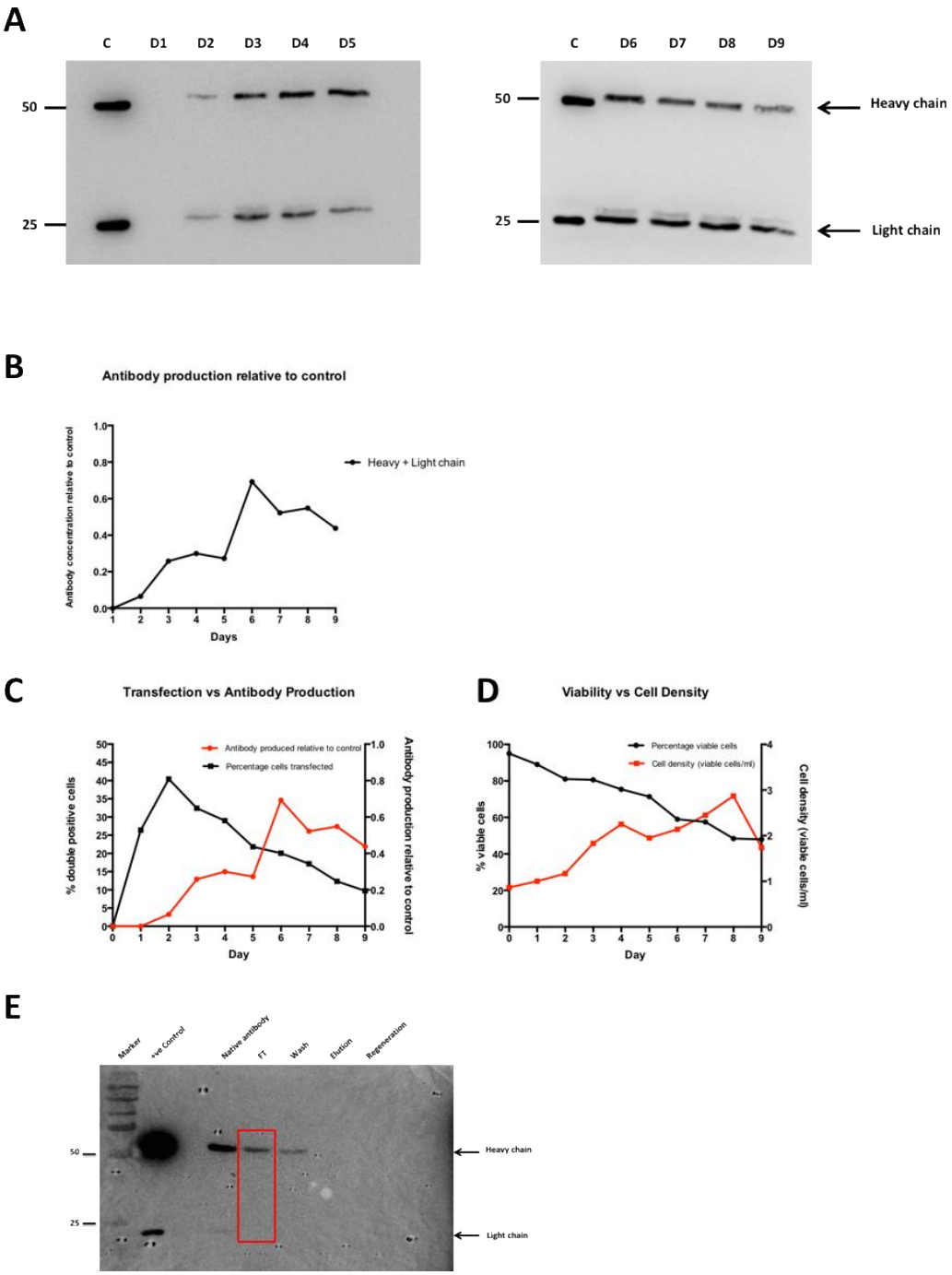

Figure 4.4. Optimisation of the Freestyle MAX 293 expression system

293F cells were transfected using Freestyle Max reagent as outlined in the materials and methods section. 50μl of supernatant was collected on days 1-9 post-transfection and used for a Western blot **(A)**, FACS **(C)** and viability post-transfection **(D)**. Remaining supernatant from the transfection was concentrated and loaded onto a protein G column for purification of the antibody **(E)**. **(A)** Western blot of supernatant collected days 1-9 post-transfection. **(B)** Quantification of antibody production relative to control. **(C)** Transfection efficiency versus antibody production. **(D)** Viability versus cell density. **(E)** Protein G column purification – western blot showing the intermediate steps.

4.4.3 Optimisation of the Freestyle MAX 293 expression system – using PEI as a transfection reagent

We next tried to produce the antibody in 293F cells, using the PEI transfection reagent and protocol used in the Chester lab, and using a positive control construct given by their lab, which is known to express well in these cells. As with the MAX reagent, a test transfection was set up, collecting supernatant every day until day 7 post-transfection. Different ratios of light : heavy vector ratios were tested which are shown in (**Figure 4.5A**) and quantified in (**Figure 4.5B**), using signal density as explained above. The lowest band signal was observed for the 2:1 ratio, with 1:1 and 3:1 reaching similar densities around day 6.

The positive control given to us, a modified human IgG1 antibody, showed high levels of production, which is shown in (**Figure 4.5C**) with the highest signal density being observed on day 6 post-transfection and a saturation threshold being reached. These densities were quantified and plotted in (**Figure 4.5D**) as a fold change in density compared to the control antibody, with the highest level reached on day 6 post-transfection, with a 25-fold greater density of the bands than those in the control lane. The viability of these cells was measured post-PEI transfection (**Figure 4.5E**) with all transfections leading to a similar small decrease in viability post-transfection, as expected and confirming that PEI is not too toxic to use, with around 50% of the cells remaining viable 7 days post-transfection. As with the Freestyle Max Reagent, the percentage of transfection of the cells was recorded (data not shown) and the percentage of cells transfected with both vectors was higher and the signal stronger, than that using PEI as a transfection reagent. The antibody from the 3:1 ratio was collected and purified using a new protein G column, with aliquots at different steps of the purification being run on a Western blot, shown in (**Figure 4.6A**). This once again showed that even though the antibody is being produced, it does not bind to the column, and all of it is lost in the flow-through, with none being eluted. The positive control that was used was also purified using a protein G column, but as opposed to our antibody, bound to the

column, was not lost in the flow-through and was eluted from the column properly (**Figure 4.6B**) with 5 mg of protein being recovered post-elution from the column.

Taking all of the data into account, as well as published data, we proceeded with efforts to optimise production and purification, with the 3:1 and 1:1 transfection ratios of light : heavy chain and returned to Invitrogen's protocol of transfection using Freestyle Max Reagent, with the aim of optimising the purification step of the antibody post-production.

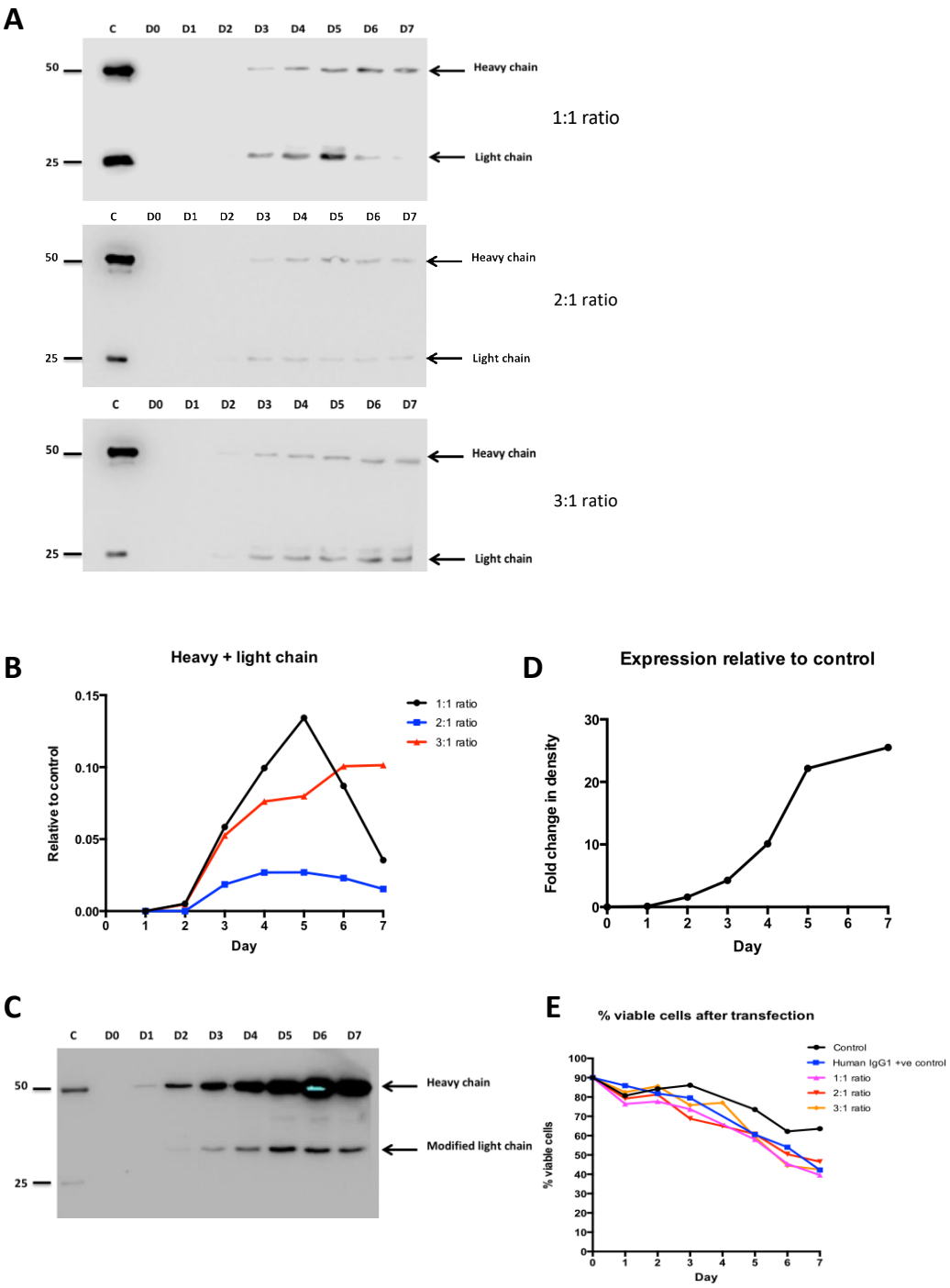

Figure 4.5. Optimisation of the Freestyle MAX 293 expression system (PEI transfection)

293F cells were transfected using PEI as a transfection reagent as outlined in the materials and methods section. Supernatant was collected days 1-7 post-transfection of the cells **(A)** Western blot of the supernatant collected days 1-7 post-transfection with PEI at different ratios of L:H chain transfection. **(B)** Quantification of the bands in A, signal density relative to the control **(C)** Western blot of the supernatant collected days 1-7 post-transfection with PEI of the human IgG positive control antibody. **(D)** Quantification of the bands in C, signal density relative to the control. **(E)** Viability of cells post-transfection with PEI.

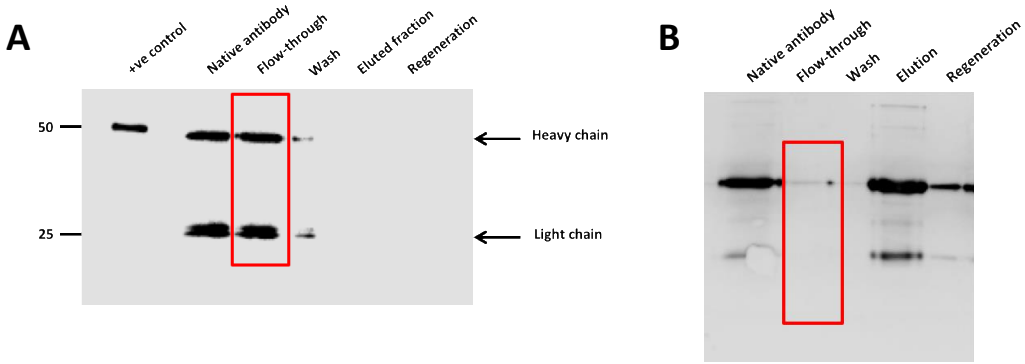

Figure 4.6. Purification of the antibody using a protein G column.

The supernatant of the transfected cells in Figure 4.5 (3:1 ratio as well as the positive control) was concentrated and run through a protein G column. Fractions were collected at every step and visualised using a western blot of the different fractions. **(A)** Antibody purification using protein G column – western blot showing different steps. **(B)** Antibody purification of the positive control, using a protein G column – western blot showing different steps.

4.4.4 Optimisation of the antibody purification steps

A different construct was chosen for the transfection of the 293F cells to test whether it was expressed differently to the one used before, which was on a mIgG1 backbone. In addition, the pH at which the antibody was loaded onto a protein G column was also altered, with pHs 7.2 and 7.5 being tested. 100 µg was recovered from the 3:1 ratio transfection and purification using a pH of 7.5 (**Figure 4.7B**). No antibody was recovered post-purification for any of the other conditions tested (**Figure 4.7A**).

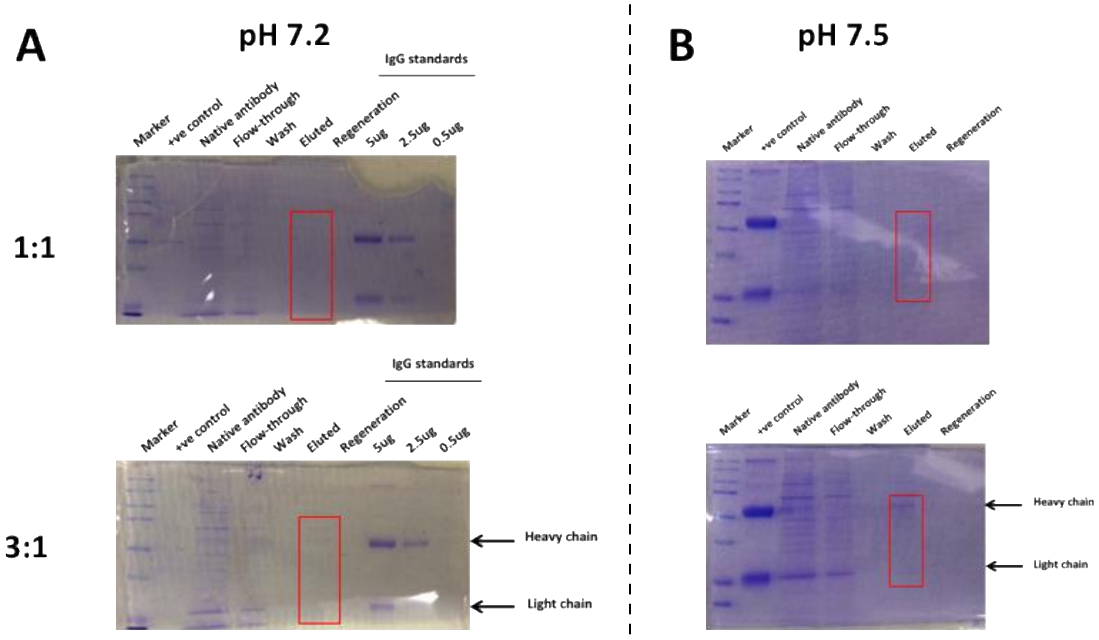

Figure 4.7. Optimisation of the antibody purification steps – pH change.

293F cells were transfected at different ratios of the heavy and light chains of the antibody. Supernatant was collected on day 7 post-transfection of the cells, concentrated and run through a protein G column using 2 different pHs for the loading of the antibody onto the column. **(A)** and **(B)** Coomassies showing the different steps of antibody purification, using 1:1 and 3:1 ratio with purification at pH 7.2 **(A)** versus purification at pH 7.5 **(B)**.

In parallel, production and purification of a hIgG2 construct was tested, with a small amount of antibody seemingly being produced and lost in the flow-through and none being present post-elution (**Figure 4.8A**). The flow-through was taken, concentrated using 15ml spin columns and run on a new column, adding 1ml at a time, in order to increase retention time on the column, as was advised by GE Healthcare technical support, but once again was all lost in the flow-through and did not bind to the column (**Figure 4.8B**).

As a 100µg of the αCD25 hIgG1 antibody was recovered from a 30ml transfection, a 250ml transfection was set-up, to try and increase the amount of antibody produced and test whether that would bind to the column. This was set-up and purified on a protein G column (**Figure 4.8C**), with antibody still being lost in the flow-through, but some being present at the elution step, with 500µg being recovered post-elution. Once again the flow-through was concentrated using 15ml spin-columns, and run on a new column (**Figure 4.8D**) with the aim of recovering some more antibody. Some more antibody was recovered, 150µg, but a large amount was still being lost in the flow-through.

With none of the production yielding promising amounts of antibody, all the constructs were verified once again using sequencing to verify the sequence was correct, binding tests to verify binding of the constructs and diagnostic digestions using multiple different combinations of restriction enzymes to verify the backbone was intact (data not shown). All of these confirmed that the constructs used to produce antibody were correct and functional, but for an unknown reason, were not being produced at high levels nor being eluted properly from the purification columns.

A final effort was made, using a vector containing a different variable region sequence, that specific for mouse/human PD-L1 (cross-reactive S70 clone), on a hIgG1 backbone, containing the F405L mutation, produced in **Figure 4.3**. Using a small culture volume to start with, 30ml, the antibody was produced and properly eluted (**Figure 4.9A**). This was then scaled up to a culture volume of 250ml, yielding 9.25mg of antibody post-elution (**Figure 4.9B**). This was

also repeated using PEI, following the protocol used in Professor Kerry Chester's lab, yielding a similar amount of antibody, indicating that both transfection reagents can be used for production and it was most likely the clone we were using, the αCD25^{PC61} clone, which was problematic and was not being produced or eluted properly. Taking this into account, production of the αCD25^{PC61} hIgG1.K409R antibody was outsourced to an antibody production company, Evitrea, while the αPD-L1 hIgG1.F405L was produced in house, dialysed against PBS and used for the "fab-arm exchange" needed for the production of the bispecific antibody, αPD-L1 x αCD25^{PC61} BsAb.

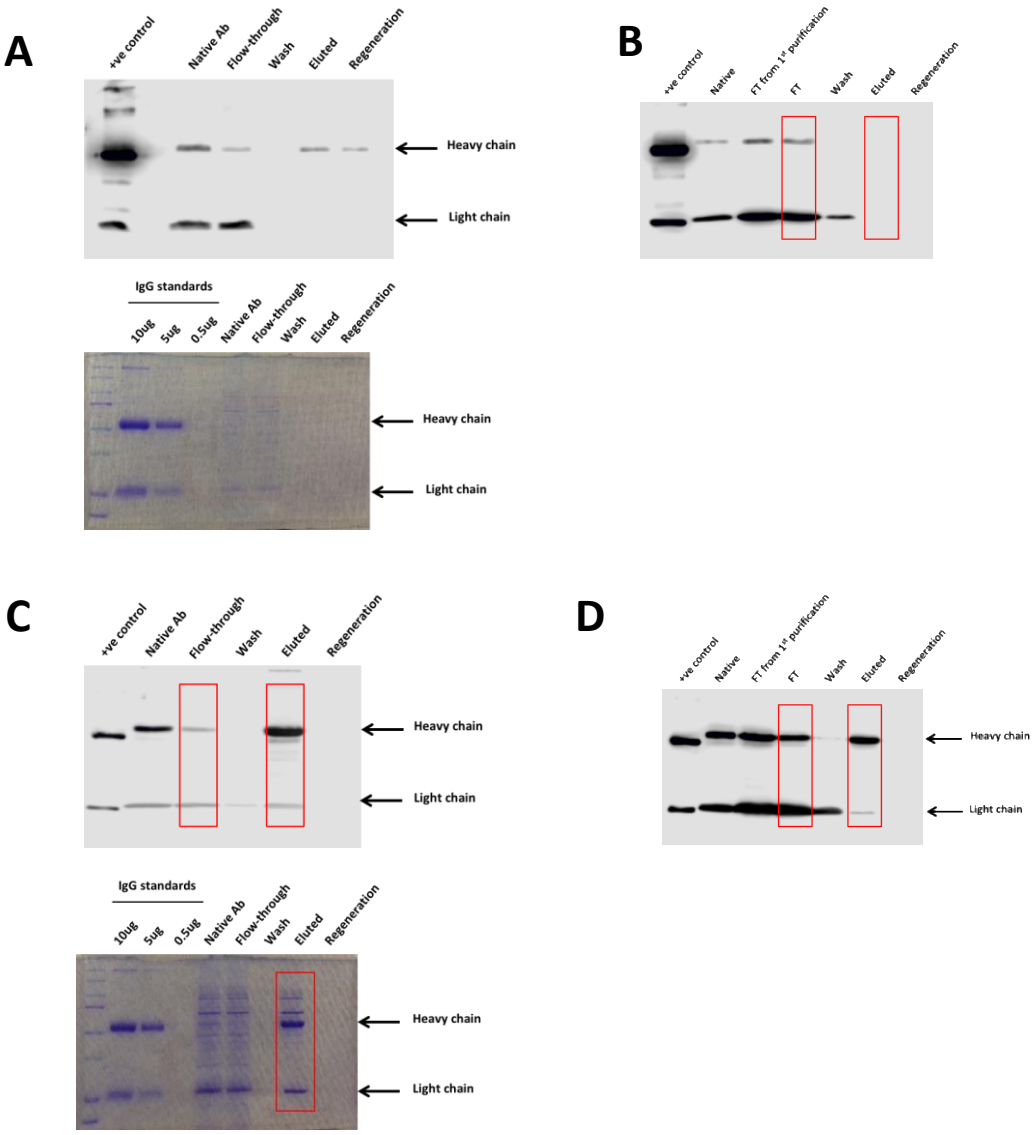

Figure 4.8. Optimisation of the antibody purification steps – new constructs.

293F cells were transfected with different constructs; αCD25 hIgG1 and αCD25 hIgG2. Antibody was collected on day 7, concentrated using spin columns run through a protein G column and the fractions collected were visualized on Coomassies and Western blots. **(A)** Western blot (top) and Coomassie (bottom) showing purification of hIgG2 construct. **(B)** Western blot showing purification of flow through from **(A). (C)** Western blot (top) and Coomassie (bottom) showing purification of hIgG1 construct. **(D)** Western blot showing purification of flow through from **(C).**

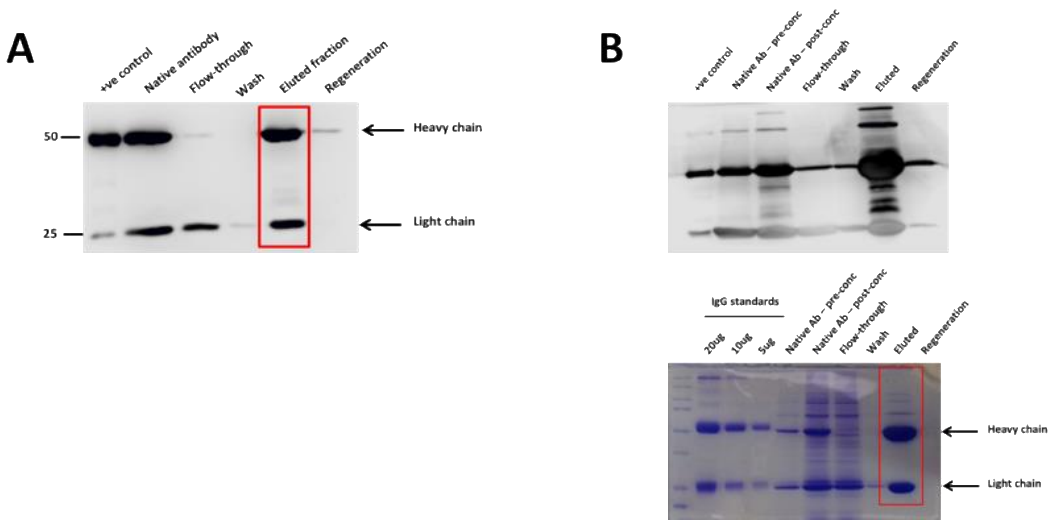

Figure 4.9. Purification of a construct with a different variable region.

293F cells were transfected with a new construct – αPD-L1 hIgG1 F405L. Antibody was collected on day 7, concentrated using spin columns, run through a protein G column and the fractions collected were visualized on Coomassies and Western blots. **(A)** Purification using a protein G column of the antibody collected from a 30ml transfection; western blot showing fractions collected at different steps of purification. **(B)** Purification using a protein G column of the antibody collected from a 250ml transfection; western blot showing fractions collected at different steps of purification (top) and Coomassie on the bottom.

4.4.5 Production of BsAb – αPD-L1 x αCD25^{PC61} BsAb

The bispecific antibody – αPD-L1 x αCD25^{PC61} was produced from the two separate monoclonal antibodies, αPD-L1 hIgG1 (containing the F405L mutation) which was produced using 293F cells in the lab, as described previously, and αCD25^{PC61} hIgG1 (containing the K409R mutation), which was produced by Evitrea. The duobody technology, developed by Genmab was used for the fab arm exchange between the two antibodies, following the step by step protocol published in Nature (Labrijn *et al.*, 2014) outlined in (**Figure 4.10A**). Briefly, the antibodies were mixed in equimolar amounts (5mg/ml each, calculated using exact extinction coefficients), 2-MEA was added and topped up with PBS. The mixture was incubated at 31C for 5 hours, with no shaking. Following this, the antibody was dialysed using dialysis cassettes with 10 MWCO (during which the buffer was changed three times), filtered using 0.22 μm filter and stored in the fridge overnight. The formation of the BsAb was confirmed using Matrix Assisted Laser Desorption/Ionization (MALDI) at UCL School of Pharmacy (Mass Spectrometry Facility), and shown in (**Figure 4.10B**), with the BsAb mass lying exactly in the middle of the individual masses of the parental monospecific antibodies. This confirmed the production of the BsAb but not the actual efficiency of BsAb formation, which was determined using Hydrophobic Interaction Chromatography (HIC) analysis (performed by anaRIC Biologics), shown in **Figure 4.10C**, and showed that the BsAb produced is 85% pure BsAb, with 15% monospecific αCD25 antibody contamination present in the mixture.

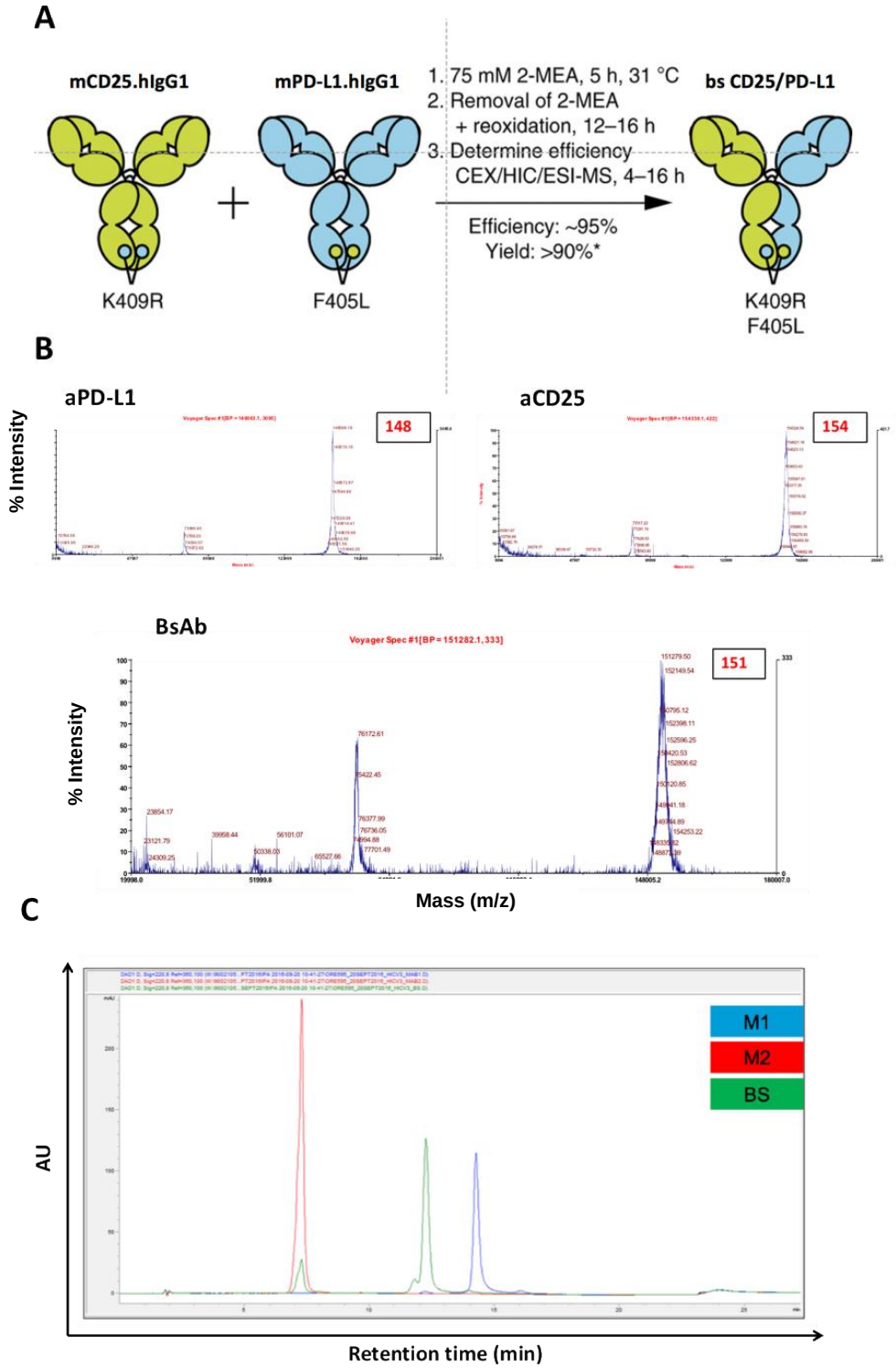

Figure 4.10. Production of BsAb – αPD-L1 x αCD25^{PC61} BsAb.

(A) Schematic of the use of ”duobody technology” for the production of the BsAb. **(B)** Mass of the individual monospecific antibodies (top) and bispecific antibody (bottom), with percentage intensity of the peak on y axis and mass on the x-axis. Plots produced by MALDI. **(C)** HIC analysis of the individual monospecific antibodies and bispecific antibody.

4.4.6 Binding of the BsAb to its targets – CD25 and PD-L1

The binding of the BsAb to its targets, CD25 and PD-L1 was tested using a Supt1 cell line expressing mCD25 on the surface and a second cell line expressing mPD-L1 on its surface. These cell lines were produced by transduction of Supt1 cells as described in the materials and methods section. The binding of the antibody to the cell lines was detected using an anti-human secondary antibody, conjugated to AF647, which binds to the human Fc region of the bound antibody. A control cell line, SupT1 not expressing PD-L1 nor CD25 was used to verify that the antibodies do not bind non-specifically, and bind to their target only. The monospecific parental antibodies were shown to bind well to their targets, with nearly 100% of the cells being bound by the antibody, when added to the respective cell line (**Figure 4.11A**). The BsAb was shown to bind the CD25+ cell line as well as the monospecific, with 99.1% of the cells bound, with a comparable fluorescence intensity recorded as with the monospecific antibody (**Figure 4.11A**). The BsAb also bound to the PD-L1-expressing cell line, but with a slightly lower fluorescence intensity than the monospecific antibody (**Figure 4.11A**).

The bispecific antibody was then tested for its ability to bind to both targets simultaneously. To do this, the SupT1 cell line expressing mCD25 was labelled with FITC, and the SupT1 cell line expressing mPD-L1 with V450 (as described in the materials and methods section). The cells were mixed in a 1:1 ratio, incubated with either no antibody, the parental antibodies, or the bispecific antibody for 30 mins, washed once and run on the FACS machine to evaluate simultaneous binding of the BsAb to both targets. Simultaneous binding was evaluated by plotting FITC versus V450, with double positive cells indicating simultaneous binding of the antibody to both of the cell lines. Representative FACS plots are shown in (**Figure 4.11B**), with the BsAb generating double positive cells ($FITC^+V450^+$), only when incubated with both of its targets, and not when incubated with only one of its targets. This was quantified in (**Figure 4.11C**), where it's shown that none of the other conditions led to double positive cells ($FITC^+V450^+$ cells). An additional assay was used to confirm binding simultaneously to both targets, and is illustrated in (**Figure**

4.12A). Briefly, $CD25^+$ cells were incubated with the BsAb/MsAb for 30 mins. A His-tagged PD-L1 ligand was added to the mix, incubated for another 30 mins, followed by incubation with an anti-His antibody for 30 mins and finally, an anti-rabbit labelled AF647 antibody (**Figure 4.12A**). Due to the number of different antibodies added, the results were only used as a guideline. The only combination that led to a positive APC signal was the BsAb which was added to the CD25+ cells, followed by the PD-L1 ligand, anti-his and anti-rabbit antibody (**Figure 4.12B**). No signal was seen when either of the monospecific antibodies were used, nor when a CD25-negative cell line was incubated with the BsAb (**Figure 4.12B**).

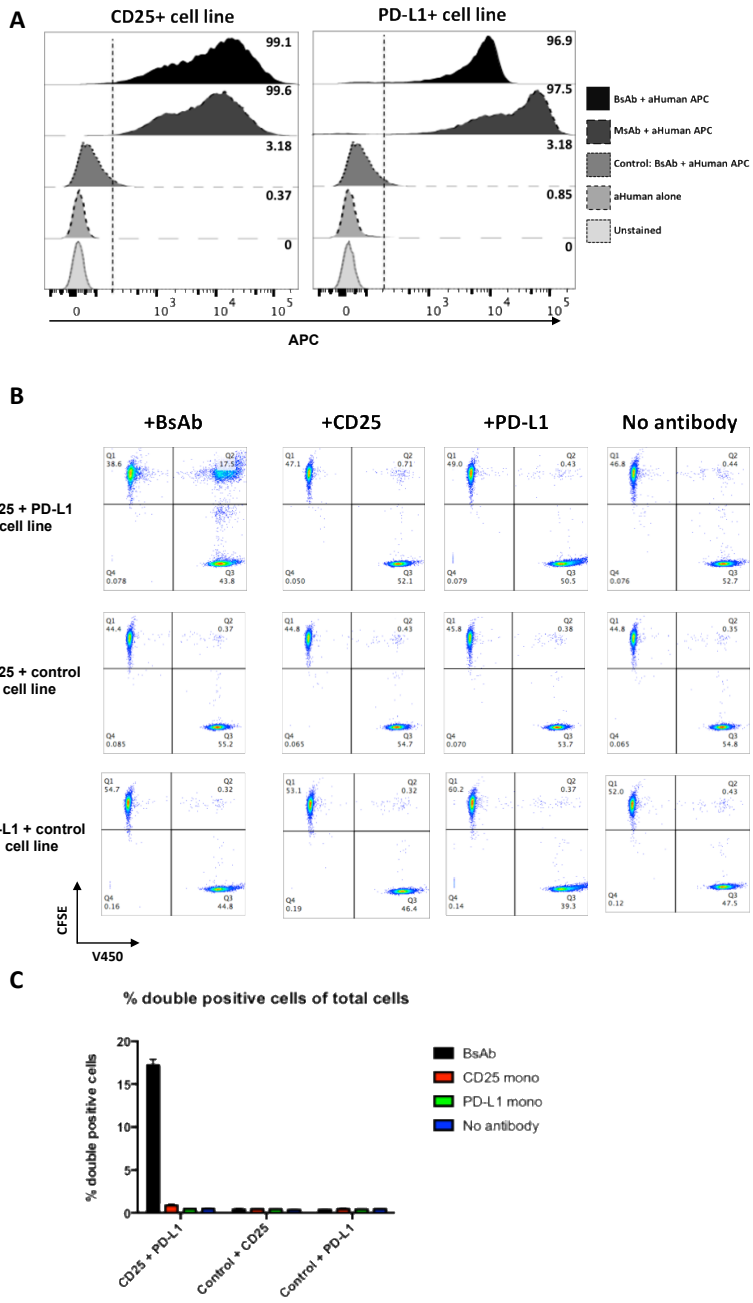

Figure 4.11. Binding of the BsAb to its targets – CD25 and PD-L1.

SupT1 cells were labelled with either CFSE or V450 (as described in materials and methods section). Cells were mixed in a 1:1 ratio, incubated with either no antibody, the parental antibodies, or the bispecific antibody (all at 10μg/ml) for 30 mins, washed once and run on the FACS machine to evaluate simultaneous binding of the BsAb to both targets. Simultaneous binding was evaluated by plotting FITC versus V450, with double positive cells indicating simultaneous binding of the antibody to both of the cell lines. **(A)** Binding of monospecific and bispecific antibodies to a cell line expressing either CD25 or PD-L1 on its surface. **(B)** Flow plots showing percentage of double positive cells formed post-incubation with the monospecific/bispecific antibodies using a mixture of labelled cell lines, expressing, or not expressing the targets of interest. **(C)** quantification of plots in B.

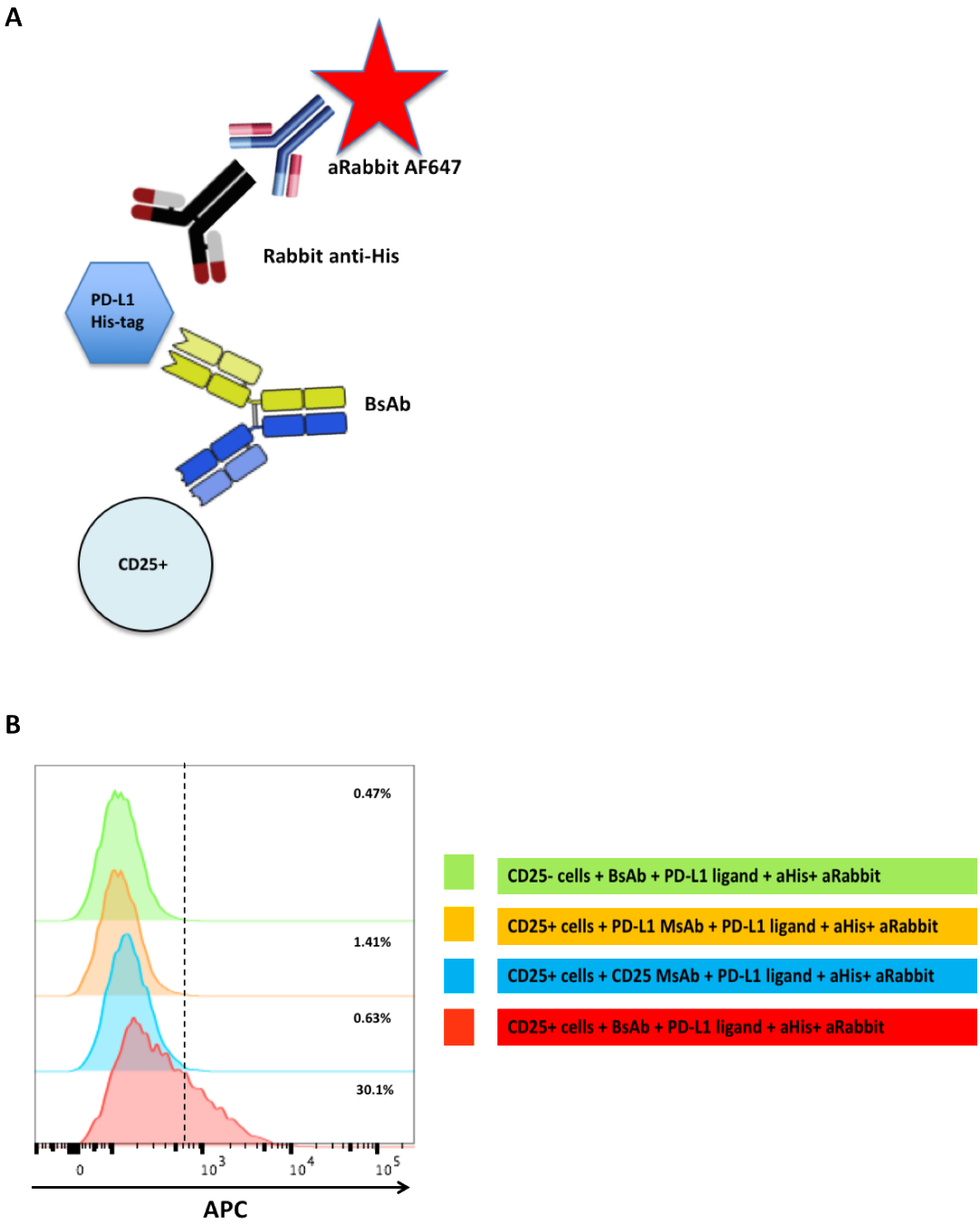

Figure 4.12. Binding of the BsAb to its targets – CD25 and PD-L1 – alternative method.

SupT1 cells expressing CD25 on their surface were incubated with the BsAb/MsAb (at 10μg/ml) for 30 mins. A His-tagged PD-L1 ligand was added to the mix (3μg), incubated for another 30 mins and finally, an anti-rabbit labelled AF647 antibody. The samples were run on the FACS and APC signal was recorded. **(A)** Schematic of the assay used to detect simultaneous binding of the BsAb to its targets. **(B)** Histograms showing percentage of cells generating a positive APC signal post-incubation with the combination of antibodies and cells shown on the right.

4.4.7 Effect of BsAb on Treg depletion *in vivo*

The functional activity of the first BsAb that was produced was evaluated *in vivo*, in MCA205 tumour-bearing mice, where we compared its activity to that of the parental monospecific antibodies, either separately or in combination. Mice received either 1 dose on day 5, or 2 doses of BsAb on days 5 and 7. The rest of the antibodies were administered on day 7 and tumours and draining lymph nodes were harvested on day 10 (**Figure 4.13A**) and processed as described in the materials and methods section. The BsAb was shown to deplete $CD4^{+}Foxp3^{+}$ regulatory T cells in the tumours with equivalent efficacy to the monospecific anti-$CD25^{PC61}$ (**Figure 4.13B**). Similar results were observed in the draining lymph nodes, with Tregs being depleted as well with the BsAb as with the monospecific anti-CD25, or the combination of the anti-CD25 and anti-PD-L1 (**Figure 4.13B**). In turn, the BsAb increased the ratio of CD8/Treg cells in the tumour and the lymph nodes significantly when compared to the control group and to similar low levels as was achieved in the anti-CD25 treated group (**Figure 4.13C**). The CD4 effector/Treg ratio also increased in the tumour for both 1 and 2 doses of the BsAb, as well as the anti-CD25 monotherapy, although the 1 dose was not statistically significant. However, in the lymph nodes, the ratio increased significantly for all groups containing CD25, with the greatest increase observed with 2 doses of the BsAb (**Figure 4.13D**).

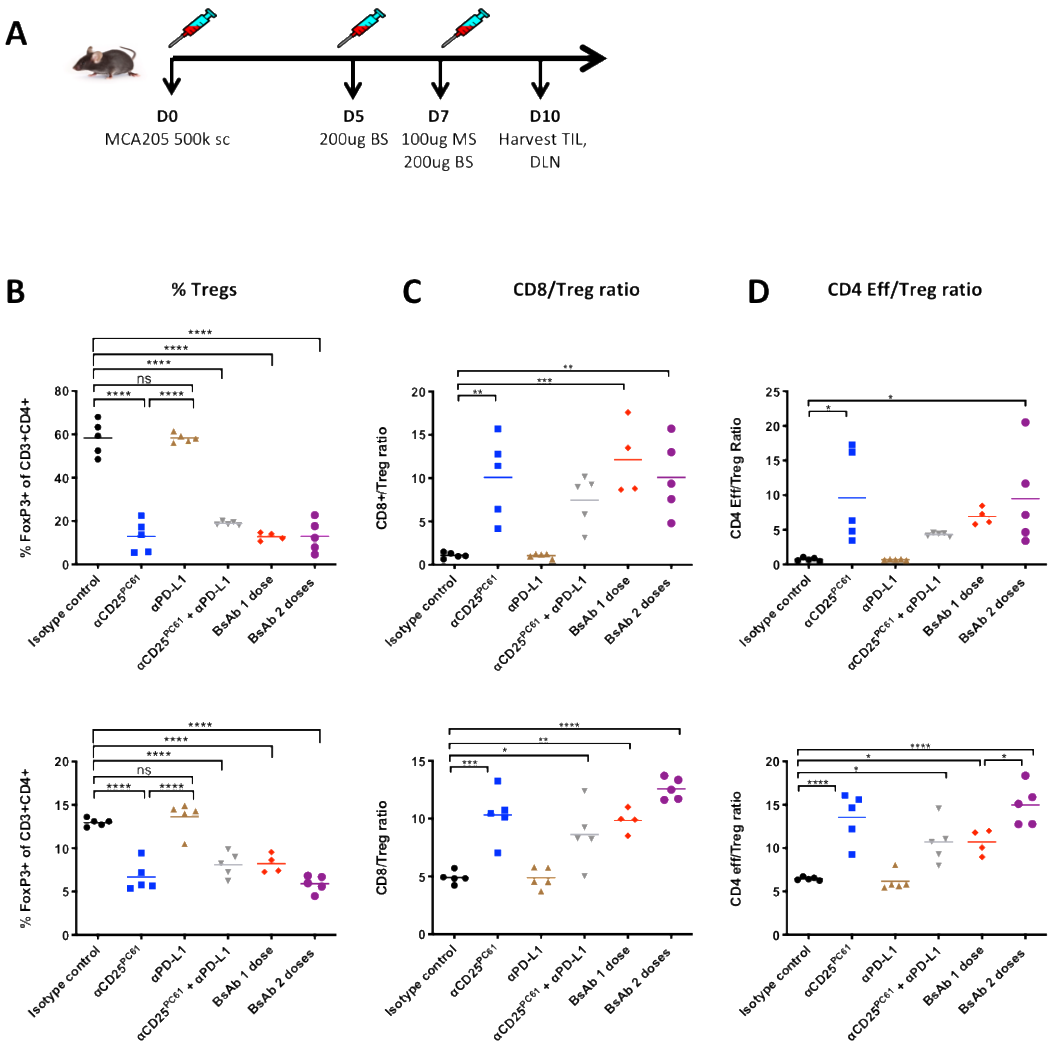

Figure 4.13. Effect of BsAb on Treg depletion *in vivo*.

C57BL6 mice were injected s.c. with 500,000 MCA205 tumour cells. Mice were injected IP with 100μg of either the monospecific antibodies (Day 7) or 200μg of the bispecific antibodies (days 5 and 7). Tumours were harvested on day 10 post-tumour inoculation. Tumours were processed as described in the materials and methods section and stained for flow cytometry. **(A)** Schematic of the treatment schedule. **(B)** Graph showing % Tregs in TILS (top) and LN (bottom). **(C)** Graph showing CD8/Treg ratio in TILS (top) and LN (bottom). **(D)** Graph showing CD4 eff/Treg ratio in TILS (top) and LN (bottom).

4.4.8 Effect of BsAb on functional activation of effector cells *in vivo*

In the same experiment, we then evaluated the effects of the BsAb on the functional activation of effector cells, by looking at changes in Granzyme B, Ki67 and cytokines. The percentage of CD8 cells producing granzyme B was significantly higher for both 1 and 2 doses of the BsAb, when compared to the CD25-treated group as well as the control group, with approximately 90% of $CD8^+$ cells expressing Granzyme B **(Figure 4.14A and B).** A similar trend was seen for CD4 effector cells producing Granzyme B, with 2 doses of BsAb increasing the percentage of CD4 effector cells producing granzyme B to approximately 50%, significantly higher than the control group, CD25-treated group and combination group, where only around 20% of CD4 effector T cells were shown to be Granzyme B^+ **(Figure 4.14A and B**). Cytokine expression by $CD4^+$ and $CD8^+$ T cells was also evaluated (Figure 4.11C) with levels of IFNγ produced by CD8+ T cells remaining similar between the different treatment groups. However, the levels of IFNγ produced by CD4 Effector T cells increased significantly in the combo-treated group and BsAb group compared to the αPD-L1 monotherapy group and the control group, with approximately 12% of the cells expressing IFNγ including the BsAb 2 doses group, albeit not significant statistically **(Figure 4.14C)**.

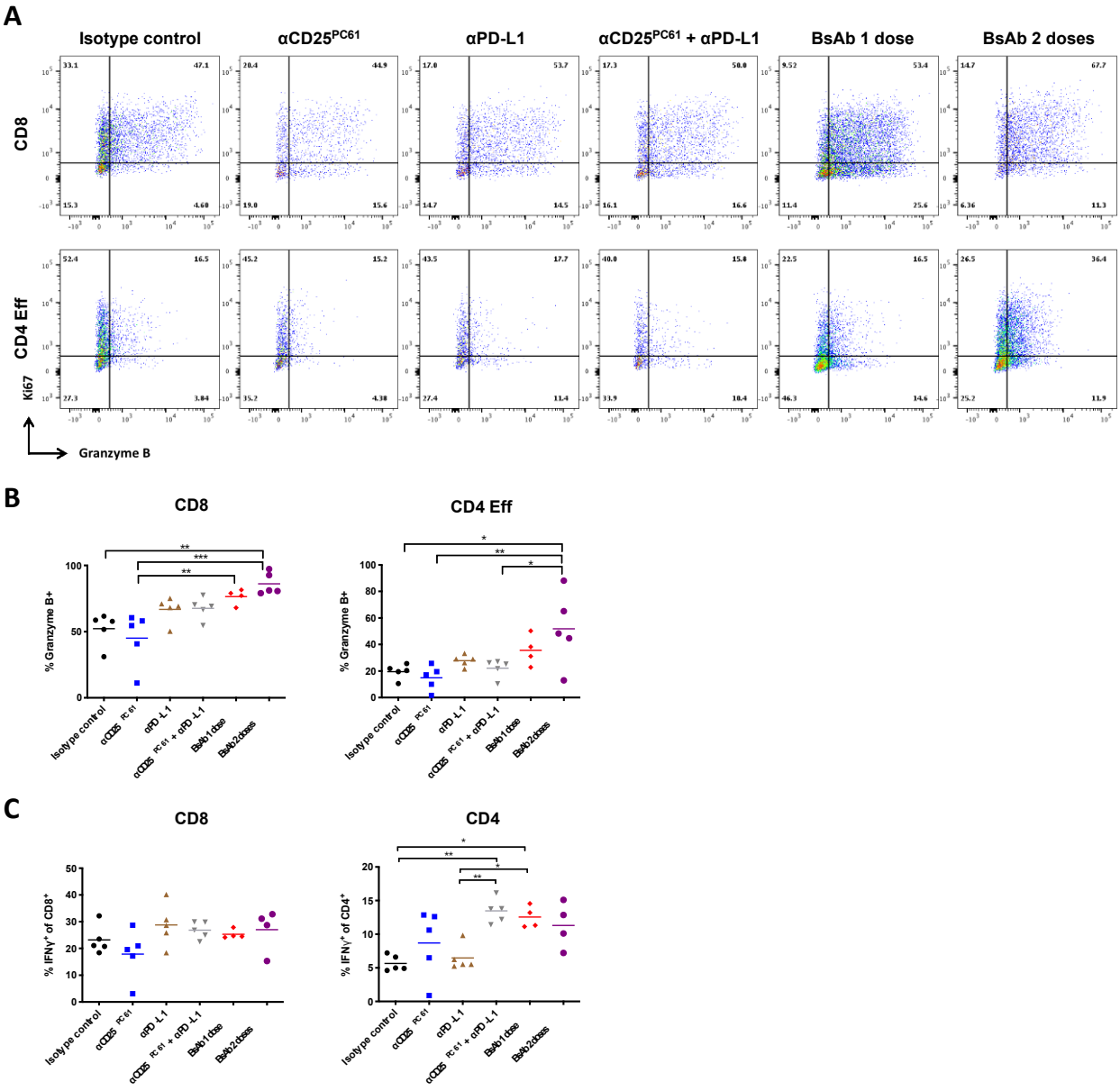

Figure 4.14. Effect of BsAb on functional activation of effector cells *in vivo*.

C57BL6 mice were injected s.c. with 500,000 MCA205 tumour cells (same experiment as in figure 4.13). Mice were injected IP with 100μg of either the monospecific antibodies (Day 7) or 200μg of the bispecific antibodies (days 5 and 7). Tumours were harvested on day 10 post-tumour inoculation. Tumours were processed as described in the materials and methods section and stained for flow cytometry. **(A)** Representative flow plots of Ki67 expression versus Granzyme B expression in CD8 and CD4 effector T cells in TILS. **(B)** Quantification of Granzyme B% CD8 T cells on the left, and CD4 eff cells on the right. **(C)** Quantification of IFNγ production by CD8 T cells on the left, and CD4 on the right.

4.4.9 Testing the activity of the contaminating monospecific antibody present in the bispecific antibody mix – on Treg depletion

A second batch of BsAb was produced, shown to be 93% pure, by HIC, with 3.5% contamination by each of the monospecific antibodies. In order to evaluate the potential effect that this contamination could have on the activity of the BsAb, a control group of 7μg anti-CD25PC61 was included in the next set of experiments, mainly to evaluate whether this contamination interfered with the interpretation of the results from the previous experiment, as that had not been taken into account. Using the same regimen as in Figure 4.13A, the 7μg dose significantly decreased the percentage of Tregs inside the tumour and lymph nodes, to similar levels observed in the 100μg group, combo group and BsAb group **(Figure 4.15A)**. The absolute number of Tregs/g of tumour **(Figure 4.15C)** and in the lymph nodes (data not shown) was also decreased significantly. Additionally, the 7μg dose led to a large increase in the ratio of CD8/Treg cells, comparable to those observed in the CD25 and BsAb - treated groups (**Figure 4.15D)**. As for the CD4 Eff/Treg ratio, treatment with the BsAb was the only group that led to a significant increase in the ratio inside the tumour **(Figure 4.15E)**, with the rest of the antibodies exerting a strong effect on the ratio in the lymph nodes (data for LN not shown).

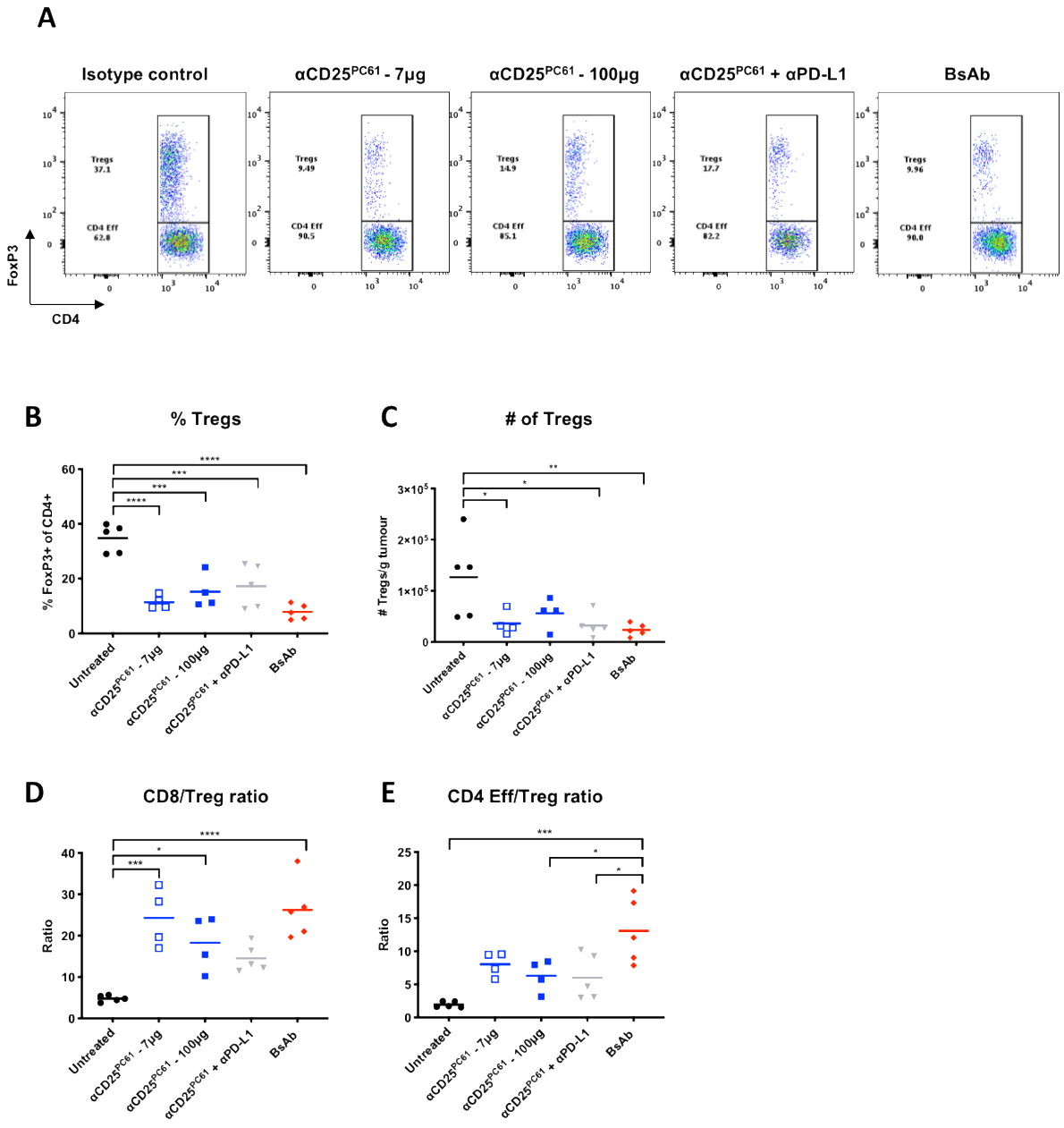

Figure 4.15. Testing the activity of the contaminating monospecific antibody present in the bispecific antibody mix – on Treg depletion.

C57BL6 mice were injected s.c. with 500,000 MCA205 tumour cells. Mice were injected IP on day 5 post-tumour inoculation with either 7μg or 100μg of the monospecific antibodies or 200μg of the bispecific antibodies. Tumours were harvested on day 12 post-tumour inoculation. Tumours were processed as described in the materials and methods section and stained for flow cytometry. **(A)** Representative flow plots of FoxP3 expression versus CD4 expression in TILS. **(B)** Quantification of % Tregs in TILS. **(C)** Graph showing number of Tregs/g of tumour. **(D)** Graph showing CD8/Treg ratio. **(E)** Graph showing CD4 Eff/Treg ratio.

4.4.10 Testing the activity of the contaminating monospecific antibody present in the bispecific antibody mix – on activation of effector cells

In the same experiment, we explored changes in the activation of effector cells, as in Figure 4.14. In terms of function, granzyme B expression by $CD8^+$ T cells was increased by the 7μg dose, combo and BsAb group, albeit not statistically significant (**Figure 4.16A**). Significant changes in granzyme B expression by CD4 effector cells were observed in the combination-treated group compared to the 100μg dose of CD25 monotherapy (**Figure 4.16A**). Finally, all the groups led to an increase in granzyme B expression by NK cells when compared to the control group, even though NK cells in this model express a lot of Granzyme B even in the untreated cohort (**Figure 4.16A**). Proliferation of the effector cells, as assessed by $Ki67^+$ staining, was significantly increased for CD8+, CD4 Eff and NK cells in the combination and BsAb-treated groups (**Figure 4.16B**). Interestingly, the 7μg group increased IFNγ secretion by both $CD4^+$ and $CD8^+$ T cells, with approximately 50% of $CD8^+$ T cells secreting IFNγ, compared to a mere 20% observed for the control and 100μg-treated groups (**Figure 4.16C and D**). This effect was replicated in CD4+ T cells with over 50% of $CD4^+$ T cells secreting IFNγ in the 7μg group, versus a mere 10-15% observed for the control and 100μg-treated groups (**Figure 4.16C and E**).

Taking into account the large effects that the contaminating CD25 dose had on the depletion of Tregs and the activation of effector cells, the experiment was repeated in order to verify the results, but also to explore the effect that this dose had systemically. To this end, non-draining lymph nodes were harvested from the opposite side of the tumour and compared to the tumour draining lymph nodes. Results once again showed that the contaminating dose of 7μg was capable of depleting Tregs both inside the tumour and the draining lymph nodes, as efficiently as the 100μg dose, with this effect being replicated in the non-draining lymph nodes (**Figure 4.16F**). As the effect of the contamination observed was systemic, it was decided that the next set of

experiments would require adequate purification of the BsAb to remove the contaminant.

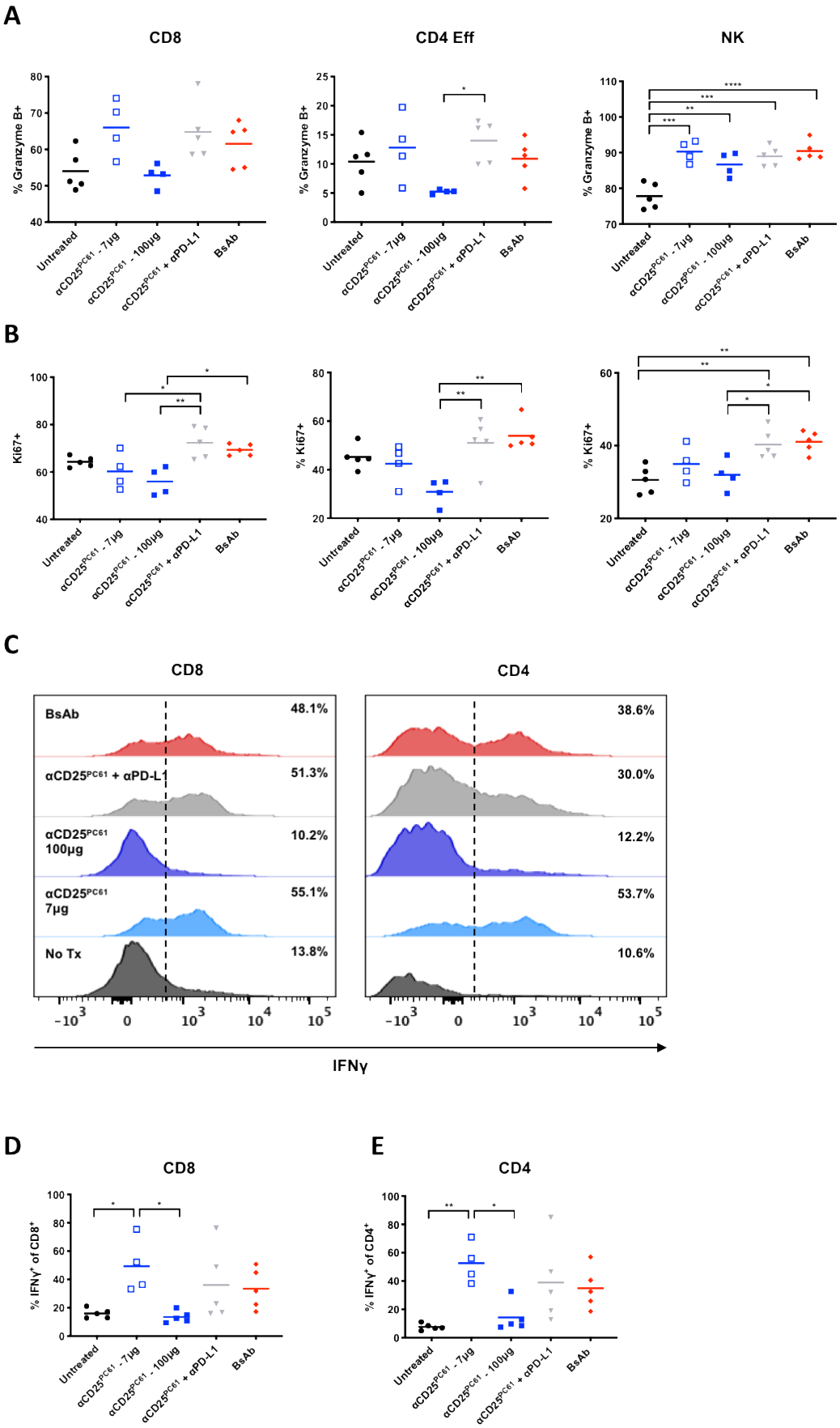

Figure 4.16. Testing the activity of the contaminating monospecific antibody present in the bispecific antibody mix – on activation of effector cells *(continued on next page)*.

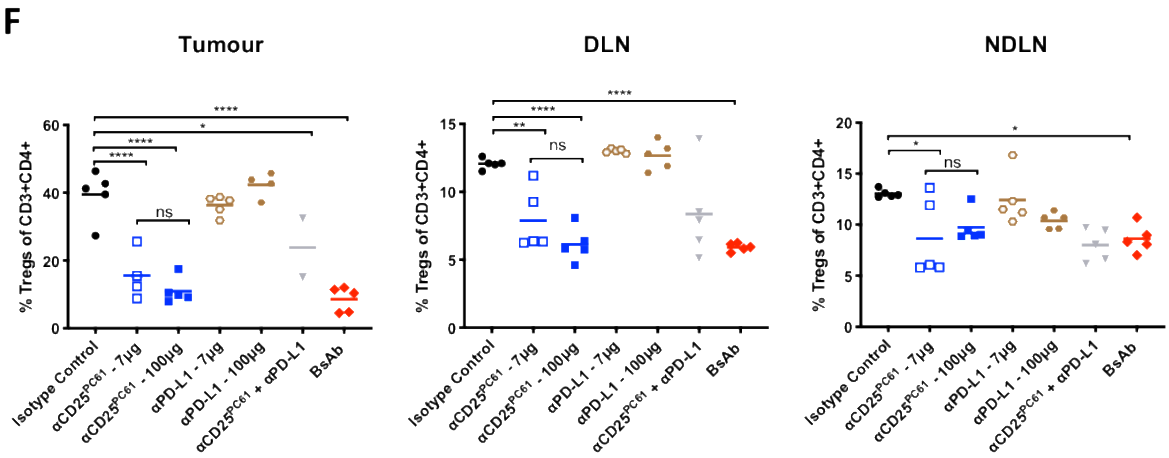

Figure 4.16. Testing the activity of the contaminating monospecific antibody present in the bispecific antibody mix – on activation of effector cells *(continued from previous page).*

C57BL6 mice were injected s.c. with 500,000 MCA205 tumour cells. Mice were injected IP on day 5 post-tumour inoculation with either 7μg or 100μg of the monospecific antibodies or 200μg of the bispecific antibodies. Tumours were harvested on day 12 post-tumour inoculation. Tumours were processed as described in the materials and methods section and stained for flow cytometry. **(A)** Granzyme B expression by CD8, CD4 Eff and NK cells in tumour. **(B)** Ki67 expression by CD8, CD4 eff and NK cells in tumour. **(C)** Quantification of IFNγ production by CD8 T cells on the left, and CD4 on the right. **(D)** Graph showing IFNγ expression by $CD8^+$ T cells. **(E)** Graph showing IFNγ expression by $CD4^+$ T cells. **(F)** Graph showing % Tregs in the tumour (left), draining lymph nodes (DLN) (middle) and non-draining lymph nodes (NDLN) (right).

4.5 DISCUSSION

In this chapter, the production of the BsAb αCD25^{PC61} x αPD-L1 that co-targets CD25 and PD-L1 was outlined. Using the GenMab protocol for "fab arm exchange", the BsAb αCD25^{PC61} x αPD-L1 was produced successfully twice, with the efficiency of production reaching 93% upon second attempt, as measured by HIC analysis.

Prior to testing the antibody *in vivo*, the binding of the antibody to its targets was tested using cells expressing its cognate targets, CD25 and PD-L1. The BsAb was shown to bind to each antigen alone, with a similar efficiency compared to the αCD25 monoclonal antibody but with a slightly compromised efficiency to PD-L1 relative to the αPD-L1 monoclonal antibody (as was shown by the reduced binding intensity in Figure 4.9). Simultaneous binding to both targets was demonstrated using two different assays. Firstly, the "flow cytometric assay for simultaneous binding on cells" was used, as was presented by (Labrijn *et al.*, 2013) and showed that the BsAb was capable of simultaneous binding to the targets on either cell type. The second assay was based on a protocol used in (Piccione *et al.*, 2015) and confirmed the antibody bound both targets simultaneously. However, this assay had several inherent flaws, due to the lack of proper reagents available for the assay and could be improved significantly by the use of a biotinylated PD-L1 ligand and a directly conjugated anti-His secondary antibody.

The bispecific antibody's function was tested in MCA205 tumour-bearing mice and compared to the monospecific antibodies, as well as a combination of both monospecific antibodies. The first batch produced had 15% contamination with the monospecific αCD25 antibody and thus proper conclusions could not be drawn from the specific effect of the BsAb itself in that experiment. Nonetheless, the BsAb did lead to an increase in granzyme B expression by CD8^{+} (significant) and CD4+ effector T cells (not significant) inside the tumour, compared to the monospecific CD25 antibody. In addition, even though IFNγ expression by CD8+ T cells remained relatively unchanged between the treatment groups, a significant increase in expression was observed for both

the combination of the monospecific antibodies as well as the BsAb compared to both αPD-L1 monotherapy alone, and the isotype control.

The second batch of antibody produced was higher in purity, consisting of 93% pure BsAb and 3.5% of each of the monospecific antibodies. Interestingly, the BsAb, but not the combination of both monospecific antibodies led to a significant increase in the ratio of CD8/Treg cells, as well as the CD4 Eff/Treg ratio. The major differences observed in this experiment were the proliferation of the effector cells inside the tumour – $CD8^+$, CD4 Eff and NK cells, which increased significantly in both the combination-treated group and the BsAb groups. IFNγ expression by CD4 and CD8 T cells showed an increase in these groups too, albeit not being statistically significant.

Inclusion of the 7μg αCD25 dose as a treatment arm in this experiment allowed not only the effects of this contamination to be evaluated, but also shed some light on the suppressive activities of the PC61 clone, as was demonstrated in Chapter 3. Firstly, the 7μg dose alone of the αCD25 antibody was capable of depleting T regs inside the tumour and LN significantly and led to a significant increase in the CD8/Treg ratio in the tumour. More importantly, this low dose led to a major, statistically significant increase in IFNγ produced by both CD8 and CD4 T cells, both compared to the isotype control and the higher 100μg dose of $αCD25^{PC61}$. Taking together the data obtained from the previous chapter and this one, this is likely due to more IL-2 availability in the presence of the 7μg dose versus the 100μg dose, prompting us to develop the same bispecific antibody, but using the 7D4 clone instead of the PC61 clone used here.

These strong effects induced by the contaminating amount of αCD25 present in the BsAb mix prompted us to repeat the experiment, not only to validate the results, but also to test whether this dose was capable of depleting Tregs systemically, with the non-draining lymph nodes used as a readout of systemic depletion. As the BsAb managed to deplete Tregs systemically, to the same extent as the higher, 100μg dose of CD25, it was decided that the antibody needed to be 100% pure (or as close to 100% as possible) for use in

downstream experiments. To address the above issues we outsourced the purification of the bispecific by HIC, however not enough pure bispecific was recovered for use in subsequent *in vivo* experiments.

The *in vivo* experiments planned using the pure BsAb included survival experiments, comparing the effect of the BsAb on tumour growth and survival of mice, versus a combination of the monospecific antibodies and dissection of the main differences between these treatments. In addition, by including a non-binding form of the BsAb (by introduction of the N297A mutation into the hIgG1 backbone) (Wang, Mathieu and Brezski, 2018) the differences in the efficiencies of the antibodies with and without depleting activity could be compared. Ideally, mice expressing human FcγRs instead of mouse FcγRs would be used (P. Smith *et al.*, 2012) as this would allow for the interaction between the hIgG1 backbone of the antibody and the hFcγRs to be studied more carefully and effectively than in mice containing mouse FcγRs. However, these mouse models also have their limitations as the FcγR-expression levels and expression patterns are not exactly the same as in humans (P. Smith *et al.*, 2012). Nonetheless, data from several labs show that hIgG1 can bind to all activating mFcγRs and is able to induce ADCC/ADCP with mNK cells and mouse macrophages. hIgG1 is also able to induce ADCC with mPMNs, although this is target dependent (Bruhns *et al.*, 2009; Overdijk *et al.*, 2012; Dekkers *et al.*, 2017). Even though hIgG1 resembles the mIgG2a isotype in terms of its binding to FcγRs, data suggests that it is less efficient than the mouse isotype (Dekkers *et al.*, 2017). Therefore, activation of cellular immune effector functions by hIgG1 could be underestimated in mouse models compared with humans and data acquired needs to be managed with great care.

As mentioned previously, the rationale underpinning the generation of this particular BsAb was to test whether it was able to localise (or at least enrich) Treg depletion to the tumour site due to the high levels of PD-L1 expressed by tumours and the large number of Tregs (expressing high levels of CD25) present in the TME. With more than 85 BsAbs currently in clinical development, 15 of those are antibodies which target immune checkpoint

molecules, with PD1/PD-L1 commonly being used on one arm (9 in early clinical development), and other checkpoint molecules such as CTLA4 or TIM3 on the other arm (Labrijn *et al.*, 2019). These BsAbs targeting two checkpoints simultaneously gained popularity after the success seen with nivolumab and ipilimumab in melanoma patients (Wolchok *et al.*, 2017).

Common mechanisms of resistance to bispecific antibodies, as well as monospecific antibodies include immune suppression by regulatory T cells, and/or immune checkpoints. The BsAb produced and described in this chapter could target both of these aspects and testing this *in vivo*, as a pure BsAb, would allow us to determine not only whether this antibody is capable of targeting Treg depletion to the tumour, but also whether other novel activities are unlocked by using the BsAb as opposed to a combination of the two monospecific antibodies.

Based on the previous chapter, we are now aware of the issues involved with using the PC61 clone and thus the data obtained support the generation of a αCD25^{NIB} x αPD-L1, which will be developed in the lab. Other possible combinations of bispecific antibodies to develop include using a different tumour specific antigen to the one used here, such as B7-H3, an immune checkpoint molecule which is overexpressed in many types of cancer, and associated with a poor clinical prognosis (Dong *et al.*, 2018). In addition, another combination to develop includes targeting FcγRIV, with the aim of enhancing ADCC, as well as enriching the antibody in the TME, potentially minimising the CD32b inhibitory activity within the TME.

5 CONCLUDING REMARKS

The work presented in this thesis focused on CD25 as a target for Treg depletion. CD25 was explored in two different ways; in combination with PD-L1 blockade; as part of a bispecific antibody, and on its own; targeting a different epitope to the traditionally used PC61.

The rationale underpinning the generation of the BsAb was to test whether it was able to localise (or at least enrich) Treg depletion to the tumour site due to the high levels of PD-L1 expressed by tumours and the large number of Tregs cells (expressing high levels of CD25) present in the TME. The bispecific produced was 93% pure, which was thought to be high enough when the project was initiated. However, by including the low dose of the contaminating CD25 monospecific antibody in the experiments, the importance of this contamination was re-considered because of two main findings; the 7μg dose managed to deplete Tregs systemically and also led to a significant increase in IFNγ production by both CD8 and CD4 T cells (both compared to the isotype control and the higher 100μg dose of $\alpha CD25^{PC61}$). Due to these findings, it was decided that in order to evaluate the effects of the bispecific antibody it needed to be 100% pure (or as close to 100% as possible). In addition, as the $CD25^{NIB}$ project was initiated in parallel, the results emphasised the issues involved with using the PC61 clone and the project was no longer continued using this clone. Instead, the data obtained from this project now support the generation of $\alpha CD25^{NIB}$ x αPD-L1 BsAb, which will be developed in the lab, now that the duobody technology has been set up in the lab.

The $CD25^{NIB}$ project initiated as a hypothesis that the *in vivo* activity of available anti-CD25 mAbs targeting human and mouse Treg cells, is likely limited by their IL-2 blocking activity. By developing a CD25 antibody which doesn't block IL-2 signalling, this hypothesis was tested *in vivo* in various mouse tumour models. The work presented in this thesis demonstrates the critical importance of endogenous IL-2 to the function of the CD4 and CD8 effector compartments in the context of Treg depletion and that this is key for

the superior anti-tumour activity of αCD25^{NIB}. The data obtained supports αCD25^{NIB} antibodies as a powerful new approach to target regulatory T cells and boost anti-tumour immunity by taking advantage of endogenous IL-2 availability and signalling. In addition, results suggest that αCD25^{NIB} can be used in combination with checkpoint blockade to boost the immune response of tumours resistant to αPD-L1 blockade or other targets. With Roche's involvement in this project, the first anti-human CD25 antibody (RG6292) was developed to specifically deplete human Treg while preserving IL-2 signalling and effector T-cell activity. Our data provides a novel therapeutic substrate for combination in cancer immunotherapy.

6 REFERENCES

Abbas, A., Lichtman, A. H. and Pillay, S. (2015) *Basic Immunology: Functions and Disorders of the Immune System*. 5th edn. Elsevier.

Akinleye, A. and Rasool, Z. (2019) 'Immune checkpoint inhibitors of PD-L1 as cancer therapeutics', *Journal of Hematology & Oncology*. Journal of Hematology & Oncology, 12(1), pp. 1–13. doi: 10.1186/s13045-019-0779-5.

Ali, K. *et al.* (2014) 'Inactivation of PI(3)K p110δ breaks regulatory T-cell-mediated immune tolerance to cancer', *Nature*. doi: 10.1038/nature13444.

Anthony, R. M., Wermeling, F. and Ravetch, J. V. (2012) 'Novel roles for the IgG Fc glycan', *Annals of the New York Academy of Sciences*. doi: 10.1111/j.1749-6632.2011.06305.x.

Antonia, S. J., Extermann, M. and Flavell, R. A. (1998) 'Immunologic nonresponsiveness to tumors', *Crit Rev Oncog*.

Arenas-ramirez, N. and Woytschak, J. (2015) 'Interleukin-2 : Biology , Design and Application', *Trends in Immunology*, 36, pp. 763–777.

Arenas-ramirez, N., Woytschak, J. and Boyman, O. (2015) 'Trends Immunol. 2015 Arenas-Ramirez'. Elsevier Ltd, 36(12), pp. 763–777.

Atkins, D. *et al.* (2004) 'MHC class I antigen processing pathway defects, ras mutations and disease stage in colorectal carcinoma', *International Journal of Cancer*. doi: 10.1002/ijc.11681.

Atkins, M. B. *et al.* (1999) 'High-dose recombinant interleukin 2 therapy for patients with metastatic melanoma: Analysis of 270 patients treated between 1985 and 1993', *Journal of Clinical Oncology*. doi: 10.1200/jco.1999.17.7.2105.

Azizi, E. *et al.* (2018) 'Single-Cell Map of Diverse Immune Phenotypes in the Breast Tumor Microenvironment Resource Single-Cell Map of Diverse Immune Phenotypes in the Breast Tumor Microenvironment', *Cell*. Elsevier Inc., pp. 1293–1308. doi: 10.1016/j.cell.2018.05.060.

Baldassari, L. E. and Rose, J. W. (2017) 'Daclizumab: Development, Clinical Trials, and Practical Aspects of Use in Multiple Sclerosis', *Neurotherapeutics*. doi: 10.1007/s13311-017-0553-8.

Ballesteros-Tato, A. *et al.* (2012) 'Interleukin-2 Inhibits Germinal Center Formation by Limiting T Follicular Helper Cell Differentiation', *Immunity*. doi:

10.1016/j.immuni.2012.02.012.

Barnhart, B. C. and Quigley, M. (2017) 'Role of Fc-FcγR interactions in the antitumor activity of therapeutic antibodies', *Immunology and Cell Biology*. doi: 10.1038/icb.2016.121.

Barry, M. and Bleackley, R. C. (2002) 'Cytotoxic T lymphocytes: All roads lead to death', *Nature Reviews Immunology*. doi: 10.1038/nri819.

Barthlott, T. *et al.* (2005) 'CD25+CD4+ T cells compete with naive CD4+ T cells for IL-2 and exploit it for the induction of IL-10 production', *International Immunology*. doi: 10.1093/intimm/dxh207.

Bastholt, L. *et al.* (2015) 'Combined Nivolumab and Ipilimumab or Monotherapy in Untreated Melanoma', *New England Journal of Medicine*. doi: 10.1056/nejmoa1504030.

Bauer, S. *et al.* (2018) 'Activation of NK cells and T cells by NKG2D, a receptor for stress-Inducible MICA', *Journal of Immunology*. doi: 10.1126/science.285.5428.727.

Bayer, A. L., Yu, A. and Malek, T. R. (2007) ' Function of the IL-2R for Thymic and Peripheral CD4 + CD25 + Foxp3 + T Regulatory Cells ', *The Journal of Immunology*. doi: 10.4049/jimmunol.178.7.4062.

Beck, C., Schreiber, H. and Rowley, D. A. (2001) 'Role of TGF-β in immune-evasion of cancer', *Microscopy Research and Technique*. doi: 10.1002/1097-0029(20010215)52:4<387::AID-JEMT1023>3.0.CO;2-W.

Berraondo, P. *et al.* (2018) 'Cytokines in clinical cancer immunotherapy', *British Journal of Cancer*. Springer US, (June 2018). doi: 10.1038/s41416-018-0328-y.

Besser, M. J. *et al.* (2013) 'Adoptive transfer of tumor-infiltrating lymphocytes in patients with metastatic melanoma: Intent-to-treat analysis and efficacy after failure to prior immunotherapies', *Clinical Cancer Research*. doi: 10.1158/1078-0432.CCR-13-0380.

Boruchov, A. M. *et al.* (2005) 'Activating and inhibitory IgG Fc receptors on human DCs mediate opposing functions', *Journal of Clinical Investigation*. doi: 10.1172/JCI24772.

Bournazos, S. and Ravetch, J. V. (2017) 'Diversification of IgG effector functions', *International Immunology*, 29(7), pp. 303–310. doi: 10.1093/intimm/dxx025.

Brandenburg, S. *et al.* (2008) 'IL-2 induces in vivo suppression by CD4+CD25+Foxp3+ regulatory T cells', *European Journal of Immunology*. doi: 10.1002/eji.200737791.

Bronte, V. and Zanovello, P. (2005) 'Regulation of immune responses by L-arginine metabolism', *Nature Reviews Immunology*. doi: 10.1038/nri1668.

Brudno, J. N. and Kochenderfer, J. N. (2016) 'Toxicities of chimeric antigen receptor T cells: Recognition and management', *Blood*. doi: 10.1182/blood-2016-04-703751.

Bruhns, P. *et al.* (2009) 'Specificity and affinity of human Fcγ receptors and their polymorphic variants for human IgG subclasses', *Blood*. doi: 10.1182/blood-2008-09-179754.

Bulliard, Y. *et al.* (2014) 'OX40 engagement depletes intratumoral Tregs via activating FcγRs, leading to antitumor efficacy', *Immunology and Cell Biology*. doi: 10.1038/icb.2014.26.

Burnet, M. (1957) 'Cancer-A Biological Approach* Iii. Viruses Associated With Neoplastic Conditions', *British Medical Journal*. doi: 10.1136/bmj.1.5023.841.

Capece, D. *et al.* (2012) 'Targeting costimulatory molecules to improve antitumor immunity', *Journal of Biomedicine and Biotechnology*. doi: 10.1155/2012/926321.

Carreno, B. M. *et al.* (2015) 'A dendritic cell vaccine increases the breadth and diversity of melanoma neoantigen-specific T cells', *Science*. doi: 10.1126/science.aaa3828.

Cartron, G. *et al.* (2002) 'Therapeutic activity of humanized anti-CD20 monoclonal antibody and polymorphism in IgG Fc receptor FcγrIIIa gene', *Blood*. doi: 10.1182/blood.V99.3.754.

Charych, D. *et al.* (2017) 'Modeling the receptor pharmacology, pharmacokinetics, and pharmacodynamics of NKTR-214, a kinetically-controlled interleukin-2 (IL2) receptor agonist for cancer immunotherapy', *PLoS ONE*. doi: 10.1371/journal.pone.0179431.

Cheng, G., Yu, A. and Malek, T. R. (2011) 'T-cell tolerance and the multi-functional role of IL-2R signaling in T-regulatory cells', *Immunological Reviews*. doi: 10.1111/j.1600-065X.2011.01004.x.

Chevrier, S. *et al.* (2017) 'An Immune Atlas of Clear Cell Renal Cell Carcinoma', *Cell*, 169(4), pp. 736-749.e18. doi: 10.1016/j.cell.2017.04.016.

Choe, W., Durgannavar, T. A. and Chung, S. J. (2016) ‘Fc-binding ligands of immunoglobulin G: An overview of high affinity proteins and peptides’, *Materials*. doi: 10.3390/ma9120994.

Coe, D. *et al.* (2010) ‘Depletion of regulatory T cells by anti-GITR mAb as a novel mechanism for cancer immunotherapy’, *Cancer Immunology, Immunotherapy*. doi: 10.1007/s00262-010-0866-5.

Colombo, M. P. and Trinchieri, G. (2002) ‘Interleukin-12 in anti-tumor immunity and immunotherapy’, *Cytokine and Growth Factor Reviews*. doi: 10.1016/S1359-6101(01)00032-6.

Cote-Sierra, J. *et al.* (2004) ‘Interleukin 2 plays a central role in Th2 differentiation’, *Proceedings of the National Academy of Sciences of the United States of America*. doi: 10.1073/pnas.0400339101.

Deaglio, S. *et al.* (2007) ‘Adenosine generation catalyzed by CD39 and CD73 expressed on regulatory T cells mediates immune suppression’, *Journal of Experimental Medicine*. doi: 10.1084/jem.20062512.

Dekkers, G. *et al.* (2017) ‘Affinity of human IgG subclasses to mouse Fc gamma receptors’, *mAbs*. doi: 10.1080/19420862.2017.1323159.

Dhodapkar, K. M. *et al.* (2007) ‘Selective blockade of the inhibitory Fcγ receptor (FcγRIIB) in human dendritic cells and monocytes induces a type I interferon response program’, *Journal of Experimental Medicine*. doi: 10.1084/jem.20062545.

Dijstelbloem, H. M., Kallenberg, C. G. M. and Van De Winkel, J. G. J. (2001) ‘Inflammation in autoimmunity: Receptors for IgG revisited’, *Trends in Immunology*. doi: 10.1016/S1471-4906(01)02014-2.

DiLillo, D. J. and Ravetch, J. V. (2015) ‘Fc-Receptor Interactions Regulate Both Cytotoxic and Immunomodulatory Therapeutic Antibody Effector Functions’, *Cancer Immunology Research*, 3(7), pp. 704–713. doi: 10.1158/2326-6066.cir-15-0120.

Dong, P. *et al.* (2018) ‘B7H3 As a promoter of metastasis and promising therapeutic target’, *Frontiers in Oncology*. doi: 10.3389/fonc.2018.00264.

Dudley, M. E. *et al.* (2002) ‘Cancer regression and autoimmunity in patients after clonal repopulation with antitumor lymphocytes’, *Science*. doi: 10.1126/science.1076514.

Dunn, G. P. *et al.* (2002) ‘Cancer immunoediting: From immunosurveillance to

tumor escape', *Nature Immunology*. doi: 10.1038/ni1102-991.

Dunn, G. P., Old, L. J. and Schreiber, R. D. (2004a) 'The immunobiology of cancer immunosurveillance and immunoediting', *Immunity*. doi: 10.1016/j.immuni.2004.07.017.

Dunn, G. P., Old, L. J. and Schreiber, R. D. (2004b) 'The Three Es of Cancer Immunoediting', *Annual Review of Immunology*. doi: 10.1146/annurev.immunol.22.012703.104803.

Elgundi, Z. *et al.* (2017) 'The state-of-play and future of antibody therapeutics', *Advanced Drug Delivery Reviews*. doi: 10.1016/j.addr.2016.11.004.

Elpek, K. G. *et al.* (2007) ' CD4 + CD25 + T Regulatory Cells Dominate Multiple Immune Evasion Mechanisms in Early but Not Late Phases of Tumor Development in a B Cell Lymphoma Model ', *The Journal of Immunology*, 178(11), pp. 6840–6848. doi: 10.4049/jimmunol.178.11.6840.

Esensten, J. H. *et al.* (2016) 'CD28 Costimulation: From Mechanism to Therapy', *Immunity*. doi: 10.1016/j.immuni.2016.04.020.

Fontenot, J. D. *et al.* (2005) 'A function for interleukin 2 in Foxp3-expressing regulatory T cells', *Nature Immunology*. doi: 10.1038/ni1263.

Frenzel, A., Hust, M. and Schirrmann, T. (2013) 'Expression of recombinant antibodies', *Frontiers in Immunology*. doi: 10.3389/fimmu.2013.00217.

Furness, A. J. S. *et al.* (2014) 'Impact of tumour microenvironment and Fc receptors on the activity of immunomodulatory antibodies', *Trends in Immunology*. doi: 10.1016/j.it.2014.05.002.

Furtado, G. C. *et al.* (2002) 'Interleukin 2 signaling is required for CD4+ regulatory T cell function', *Journal of Experimental Medicine*. doi: 10.1084/jem.20020190.

Gabrilovich, D. I. and Nagaraj, S. (2009) 'Myeloid-derived suppressor cells as regulators of the immune system', *Nature Reviews Immunology*. doi: 10.1038/nri2506.

GE Life Sciences (2016) *Affinity Chromatography Vol. 1: Antibodies*. Available at: https://cdn.gelifesciences.com/dmm3bwsv3/AssetStream.aspx?mediaformatid=10061&destinationid=10016&assetid=11660 (Accessed: 20 September 2019).

Geisse, S. (2009) 'Reflections on more than 10 years of TGE approaches',

Protein Expression and Purification. doi: 10.1016/j.pep.2008.10.017.

Genmab (2019) *Fab Arm Exchange*. Available at: http://www.genmab.com/duobody/biology (Accessed: 5 September 2019).

Gökbuget, N. *et al.* (2018) 'Blinatumomab for minimal residual disease in adults with B-cell precursor acute lymphoblastic leukemia', *Blood*. doi: 10.1182/blood-2017-08-798322.

Golgher, D. *et al.* (2002) 'Depletion of CD25+ regulatory cells uncovers immune responses to shared murine tumor rejection antigens', *European Journal of Immunology*, 32(11), pp. 3267–3275. doi: 10.1002/1521-4141(200211)32:11<3267::AID-IMMU3267>3.0.CO;2-1.

Gregersen, P. K. and Olsson, L. M. (2009) 'Recent Advances in the Genetics of Autoimmune Disease', *Annual Review of Immunology*. doi: 10.1146/annurev.immunol.021908.132653.

Griseri, T. *et al.* (2010) 'OX40 is required for regulatory T cell-mediated control of colitis', *Journal of Experimental Medicine*. doi: 10.1084/jem.20091618.

Grossman, W. J. *et al.* (2004) 'Human T regulatory cells can use the perforin pathway to cause autologous target cell death', *Immunity*. doi: 10.1016/j.immuni.2004.09.002.

Guo, H. *et al.* (2009) 'Structural Basis for the Blockage of IL-2 Signaling by Therapeutic Antibody Basiliximab', *The Journal of Immunology*. doi: 10.4049/jimmunol.0903178.

Ha, D. *et al.* (2019) 'Differential control of human Treg and effector T cells in tumor immunity by Fc-engineered anti–CTLA-4 antibody', *Proceedings of the National Academy of Sciences of the United States of America*, 116(2), pp. 609–618. doi: 10.1073/pnas.1812186116.

Henning, A. N., Roychoudhuri, R. and Restifo, N. P. (2018) 'Epigenetic control of CD8+ T'cell differentiation', *Nature Reviews Immunology*. doi: 10.1038/nri.2017.146.

Holmgaard, R. B. *et al.* (2015) 'Tumor-Expressed IDO Recruits and Activates MDSCs in a Treg-Dependent Manner', *Cell Reports*. doi: 10.1016/j.celrep.2015.08.077.

Huang, C. *et al.* (2006) 'A Novel NF-κB Binding Site Controls Human Granzyme B Gene Transcription', *The Journal of Immunology*. doi: 10.4049/jimmunol.176.7.4173.

Huh, S. H. *et al.* (2007) 'Optimization of 25 kDa linear polyethylenimine for efficient gene delivery', *Biologicals*. doi: 10.1016/j.biologicals.2006.08.004.

Ibrahim, N. *et al.* (2015) 'Pembrolizumab versus Ipilimumab in Advanced Melanoma', *New England Journal of Medicine*. doi: 10.1056/nejmoa1503093.

Ikeda, H., Old, L. J. and Schreiber, R. D. (2002) 'The roles of IFNγ in protection against tumor development and cancer immunoediting', *Cytokine and Growth Factor Reviews*. doi: 10.1016/S1359-6101(01)00038-7.

Jacobs, J. F. M. *et al.* (2010) 'Dendritic cell vaccination in combination with anti-CD25 monoclonal antibody treatment: A phase I/II study in metastatic melanoma patients', *Clinical Cancer Research*. doi: 10.1158/1078-0432.CCR-10-1757.

Jain, N. K. *et al.* (2017) 'A high density CHO-S transient transfection system: Comparison of ExpiCHO and Expi293', *Protein Expression and Purification*. doi: 10.1016/j.pep.2017.03.018.

Janas, M. L. *et al.* (2005) ' IL-2 Regulates Perforin and Granzyme Gene Expression in CD8 + T Cells Independently of Its Effects on Survival and Proliferation ', *The Journal of Immunology*. doi: 10.4049/jimmunol.175.12.8003.

Jarnicki, A. G. *et al.* (2006) ' Suppression of Antitumor Immunity by IL-10 and TGF-β-Producing T Cells Infiltrating the Growing Tumor: Influence of Tumor Environment on the Induction of CD4 + and CD8 + Regulatory T Cells ', *The Journal of Immunology*. doi: 10.4049/jimmunol.177.2.896.

Johnson, G. (2001) 'Kabat Database and its applications: future directions', *Nucleic Acids Research*. doi: 10.1093/nar/29.1.205.

Jones, E. *et al.* (2002) 'Depletion of CD25+ regulatory cells results in suppression of melanomagrowth and induction of autoreactivity in mice', *Cancer Immunity*.

Jonuleit, H. *et al.* (2001) 'Dendritic cells as a tool to induce anergic and regulatory T cells', *Trends in Immunology*. doi: 10.1016/S1471-4906(01)01952-4.

Kalia, V. *et al.* (2010) 'Prolonged Interleukin-2Rα Expression on Virus-Specific CD8+ T Cells Favors Terminal-Effector Differentiation In Vivo', *Immunity*. doi: 10.1016/j.immuni.2009.11.010.

Kaloff, C. R. and Haas, I. G. (1995) 'Coordination of immunoglobulin chain

folding and immunoglobulin chain assembly is essential for the formation of functional IgG', *Immunity*, 2(6), pp. 629–637. doi: 10.1016/1074-7613(95)90007-1.

Kantoff, P. W. *et al.* (2010) 'Sipuleucel-T immunotherapy for castration-resistant prostate cancer', *New England Journal of Medicine*. doi: 10.1056/NEJMoa1001294.

Kapic, E., Becic, F. and Kusturica, J. (2004) 'Basiliximab, mechanism of action and pharmacological properties', *Med Arh*.

Khalil, D. N. *et al.* (2016) 'The future of cancer treatment: Immunomodulation, CARs and combination immunotherapy', *Nature Reviews Clinical Oncology*. doi: 10.1038/nrclinonc.2016.25.

Kim, J. M., Rasmussen, J. P. and Rudensky, A. Y. (2007) 'Regulatory T cells prevent catastrophic autoimmunity throughout the lifespan of mice', *Nature Immunology*. doi: 10.1038/ni1428.

Kirkwood, J. M. (1998) 'Systemic adjuvant treatment of high-risk melanoma: The role of interferon alfa-2b and other immunotherapies', in *European Journal of Cancer*. doi: 10.1016/s0959-8049(97)10159-9.

Klein, C. *et al.* (2017) 'Cergutuzumab amunaleukin (CEA-IL2v), a CEA-targeted IL-2 variant-based immunocytokine for combination cancer immunotherapy: Overcoming limitations of aldesleukin and conventional IL-2-based immunocytokines', *OncoImmunology*. doi: 10.1080/2162402X.2016.1277306.

Kohm, A. P. and Miller, S. D. (2006) ' Response to Comment on "Cutting Edge: Anti-CD25 Monoclonal Antibody Injection Results in the Functional Inactivation, Not Depletion, of CD4 + CD25 + T Regulatory Cells" ', *The Journal of Immunology*, 177(4), pp. 2037–2038. doi: 10.4049/jimmunol.177.4.2037.

Kolfschoten, M. V. D. N. *et al.* (2007) 'Anti-inflammatory activity of human IgG4 antibodies by dynamic Fab arm exchange', *Science*. doi: 10.1126/science.1144603.

Kontermann, R. E. and Brinkmann, U. (2015) 'Bispecific antibodies; different formats', *Drug Discovery Today*. doi: 10.1016/j.drudis.2015.02.008.

de la Rosa, M. *et al.* (2004) 'Interleukin-2 is essential for CD4+CD25+ regulatory T cell function', *European Journal of Immunology*. doi:

10.1002/eji.200425274.
Labrijn, A. F. *et al.* (2013) 'Efficient generation of stable bispecific IgG1 by controlled Fab-arm exchange', *Proceedings of the National Academy of Sciences of the United States of America*. doi: 10.1073/pnas.1220145110.
Labrijn, A. F. *et al.* (2014) 'Controlled Fab-arm exchange for the generation of stable bispecific IgG1', *Nature Protocols*. doi: 10.1038/nprot.2014.169.
Labrijn, A. F. *et al.* (2019) 'Bispecific antibodies: a mechanistic review of the pipeline', *Nature Reviews Drug Discovery*. doi: 10.1038/s41573-019-0028-1.
Lalonde, M. E. and Durocher, Y. (2017) 'Therapeutic glycoprotein production in mammalian cells', *Journal of Biotechnology*. doi: 10.1016/j.jbiotec.2017.04.028.
Latchman, Y. *et al.* (2001) 'PD-L2 is a second ligand for PD-1 and inhibits T cell activation', *Nature Immunology*. doi: 10.1038/85330.
Laurence, A. *et al.* (2007) 'Interleukin-2 Signaling via STAT5 Constrains T Helper 17 Cell Generation', *Immunity*. doi: 10.1016/j.immuni.2007.02.009.
Lenschow, D. J., Walunas, T. L. and Bluestone, J. A. (2002) 'CD28/B7 SYSTEM OF T CELL COSTIMULATION', *Annual Review of Immunology*. doi: 10.1146/annurev.immunol.14.1.233.
Lewis, D. A. and Goldrosen, M. H. (1983) 'Demonstration of immunogenicity with the poorly immunogenic b16 melanoma', *Cancer Research*.
Liao, W. *et al.* (2008) 'Priming for T helper type 2 differentiation by interleukin 2-mediated induction of interleukin 4 receptor α-chain expression', *Nature Immunology*. doi: 10.1038/ni.1656.
Liao, W. *et al.* (2011) 'Modulation of cytokine receptors by IL-2 broadly regulates differentiation into helper T cell lineages', *Nature Immunology*. doi: 10.1038/ni.2030.
Liao, W., Lin, J. X. and Leonard, W. J. (2011) 'IL-2 family cytokines: New insights into the complex roles of IL-2 as a broad regulator of T helper cell differentiation', *Current Opinion in Immunology*. doi: 10.1016/j.coi.2011.08.003.
Liao, W., Lin, J. X. and Leonard, W. J. (2013) 'Interleukin-2 at the Crossroads of Effector Responses, Tolerance, and Immunotherapy', *Immunity*. Elsevier, 38(1), pp. 13–25. doi: 10.1016/j.immuni.2013.01.004.
Lin, J. X. *et al.* (2012) 'Critical Role of STAT5 Transcription Factor

Tetramerization for Cytokine Responses and Normal Immune Function', *Immunity*. doi: 10.1016/j.immuni.2012.02.017.

Liu, S. D. *et al.* (2015) 'Afucosylated Antibodies increase activation of Fcg RIIIa-dependent signaling components to intensify processes promoting ADCC', *Cancer Immunology Research*. doi: 10.1158/2326-6066.CIR-14-0125.

Long, G. V *et al.* (2019) 'Epacadostat plus pembrolizumab versus placebo plus pembrolizumab in patients with unresectable or metastatic melanoma (ECHO-301/KEYNOTE-252): a phase 3, randomised, double-blind study', *The Lancet Oncology*. doi: 10.1016/s1470-2045(19)30274-8.

Lux, A. and Nimmerjahn, F. (2011) 'Impact of differential glycosylation on IgG activity', in *Advances in Experimental Medicine and Biology*. doi: 10.1007/978-1-4419-5632-3_10.

Malek, T. R. *et al.* (2002) 'CD4 regulatory T cells prevent lethal autoimmunity in IL-2Rβ-deficient mice: Implications for the nonredundant function of IL-2', *Immunity*. doi: 10.1016/S1074-7613(02)00367-9.

Malek, T. R. (2003) 'The main function of IL-2 is to promote the development of T regulatory cells', *Journal of Leukocyte Biology*. doi: 10.1189/jlb.0603272.

Malek, T. R. and Castro, I. (2010) 'Interleukin-2 Receptor Signaling: At the Interface between Tolerance and Immunity', *Immunity*. Elsevier Inc., 33(2), pp. 153–165. doi: 10.1016/j.immuni.2010.08.004.

Medema, J. P. *et al.* (2001) 'Blockade of the granzyme B/perforin pathway through overexpression of the serine protease inhibitor PI-9/SPI-6 constitutes a mechanism for immune escape by tumors', *Proc Natl Acad Sci U S A*. doi: 10.1073/pnas.201398198.

Melero, I. *et al.* (2015) 'Evolving synergistic combinations of targeted immunotherapies to combat cancer', *Nature Reviews Cancer*. doi: 10.1038/nrc3973.

Mihm, M. C. *et al.* (2008) 'Immunologic and clinical effects of antibody blockade of cytotoxic T lymphocyte-associated antigen 4 in previously vaccinated cancer patients', *Proceedings of the National Academy of Sciences*. doi: 10.1073/pnas.0712237105.

Milstein, C. and Cuello, A. C. (1983) 'Hybrid hybridomas and their use in immunohistochemistry', *Nature*. doi: 10.1038/305537a0.

Milstein, O. *et al.* (2011) ‘CTLs respond with activation and granule secretion when serving as targets for T-cell recognition’, *Blood*. doi: 10.1182/blood-2010-05-283770.

Moreau, J. -L *et al.* (1987) ‘Monoclonal antibodies identify three epitope clusters on the mouse p55 subunit of the interleukin 2 receptor: relationship to the interleukin 2-binding site’, *European Journal of Immunology*. doi: 10.1002/eji.1830170706.

Morvan, M. G. and Lanier, L. L. (2016) ‘NK cells and cancer: You can teach innate cells new tricks’, *Nature Reviews Cancer*. doi: 10.1038/nrc.2015.5.

Murphy, K. (2017) *Immunobiology 9th Edition*, *Janeway’s Immunobiology*. doi: 10.1007/s13398-014-0173-7.2.

Namuduri, M. and Brentjens, R. J. (2016) ‘Medical management of side effects related to CAR T cell therapy in hematologic malignancies’, *Expert Review of Hematology*. doi: 10.1080/17474086.2016.1183479.

Nimmerjahn, F. and Ravetch, J. V. (2005) ‘Immunology: Divergent immunoglobulin G subclass activity through selective Fc receptor binding’, *Science*. doi: 10.1126/science.1118948.

Nimmerjahn, F. and Ravetch, J. V. (2007a) ‘Antibodies, Fc receptors and cancer’, *Current Opinion in Immunology*, 19(2), pp. 239–245. doi: 10.1016/j.coi.2007.01.005.

Nimmerjahn, F. and Ravetch, J. V. (2007b) ‘Fc-Receptors as Regulators of Immunity’, *Advances in Immunology*, 96(07), pp. 179–204. doi: 10.1016/S0065-2776(07)96005-8.

Nimmerjahn, F. and Ravetch, J. V. (2010) ‘FcyRs in health and disease’, *Current Topics in Microbiology and Immunology*. doi: 10.1007/82-2010-86.

Nobel Media AB (2018) *Press release: The Nobel Prize in Physiology or Medicine 2018*. Available at: https://www.nobelprize.org/prizes/medicine/2018/prize-announcement (Accessed: 5 October 2019).

O’Shea, J. and Paul, W. E. (2010) ‘Mechanisms underlying lineage commitment and plasticity of helper CD4 + T cells’, *Science*. doi: 10.1126/science.1178334.

Ochsenbein, A. F. (2005) ‘Immunological ignorance of solid tumors’, *Springer Seminars in Immunopathology*. doi: 10.1007/s00281-004-0192-0.

Odin, J. A. *et al.* (1991) 'Regulation of phagocytosis and [Ca2+]i flux by distinct regions of an Fc receptor', *Science*. doi: 10.1126/science.1837175.

Oldenburg, J. *et al.* (2017) 'Emicizumab prophylaxis in hemophilia A with inhibitors', *New England Journal of Medicine*. doi: 10.1056/NEJMoa1703068.

Onizuka, S. *et al.* (1999) 'Tumor rejection by in vivo administration of anti-CD25 (interleukin-2 receptor α) monoclonal antibody', *Cancer Research*.

Ono, M. *et al.* (1996) 'Role of the inositol phosphatase SHIP in negative regulation of the immune system by the receptor FcγRIIB', *Nature*. doi: 10.1038/383263a0.

Ott, P. A. *et al.* (2017) 'An immunogenic personal neoantigen vaccine for patients with melanoma', *Nature*. doi: 10.1038/nature22991.

Overdijk, M. B. *et al.* (2012) 'Crosstalk between Human IgG Isotypes and Murine Effector Cells', *The Journal of Immunology*. doi: 10.4049/jimmunol.1200356.

Pandiyan, P. *et al.* (2007) 'CD4+CD25+Foxp3+ regulatory T cells induce cytokine deprivation-mediated apoptosis of effector CD4+ T cells', *Nature Immunology*. doi: 10.1038/ni1536.

Pardoll, D. M. (2012) 'The blockade of immune checkpoints in cancer immunotherapy', *Nature Reviews Cancer*. doi: 10.1038/nrc3239.

Parsa, A. T. *et al.* (2007) 'Loss of tumor suppressor PTEN function increases B7-H1 expression and immunoresistance in glioma', *Nature Medicine*. doi: 10.1038/nm1517.

Pedicord, V. A. *et al.* (2010) 'Single dose of anti-CTLA-4 enhances CD8+ T-cell memory formation, function, and maintenance', *Proceedings of the National Academy of Sciences*. doi: 10.1073/pnas.1016791108.

Peggs, K. S. and Quezada, S. A. (2010) 'Ipilimumab: Attenuation of an inhibitory immune checkpoint improves survival in metastatic melanoma', *Expert Review of Anticancer Therapy*. doi: 10.1586/era.10.144.

Peggs, K. S., Quezada, S. A. and Allison, J. P. (2008) 'Cell intrinsic mechanisms of T-cell inhibition and application to cancer therapy', *Immunological Reviews*. doi: 10.1111/j.1600-065X.2008.00649.x.

Piccione, E. C. *et al.* (2015) 'A bispecific antibody targeting CD47 and CD20 selectively binds and eliminates dual antigen expressing lymphoma cells', *mAbs*. doi: 10.1080/19420862.2015.1062192.

Pipkin, M. E. *et al.* (2010) 'Interleukin-2 and Inflammation Induce Distinct Transcriptional Programs that Promote the Differentiation of Effector Cytolytic T Cells', *Immunity*. doi: 10.1016/j.immuni.2009.11.012.

Plitas, G. and Rudensky, A. Y. (2016) 'HHS Public Access', 4(9), pp. 721–725. doi: 10.1158/2326-6066.CIR-16-0193.Regulatory.

Quezada, S. A. *et al.* (2006) 'CTLA4 blockade and GM-CSF combination immunotherapy alters the intratumor balance of effector and regulatory T cells', *Journal of Clinical Investigation*. doi: 10.1172/JCI27745.

Quezada, S. A. *et al.* (2010) 'Tumor-reactive CD4 $^{+}$ T cells develop cytotoxic activity and eradicate large established melanoma after transfer into lymphopenic hosts', *The Journal of Experimental Medicine*. doi: 10.1084/jem.20091918.

Ray, J. P. *et al.* (2015) 'The Interleukin-2-mTORc1 Kinase Axis Defines the Signaling, Differentiation, and Metabolism of T Helper 1 and Follicular B Helper T Cells', *Immunity*. doi: 10.1016/j.immuni.2015.08.017.

Rech, A. J. *et al.* (2012) 'CD25 blockade depletes and selectively reprograms regulatory T cells in concert with immunotherapy in cancer patients', *Science Translational Medicine*. doi: 10.1126/scitranslmed.3003330.

Reem, G. H. and Yeh, N. H. (1984) 'Interleukin 2 regulates expression of its receptor and synthesis of gamma interferon by human T lymphocytes', *Science*. doi: 10.1126/science.6429853.

Ribas, A. and Wolchok, J. D. (2018) 'Cancer immunotherapy using checkpoint blockade', *Science*. doi: 10.1126/science.aar4060.

Roland, C. L. *et al.* (2009) 'Cytokine levels correlate with immune cell infiltration after anti-VEGF therapy in preclinical mouse models of breast cancer', *PLoS ONE*. doi: 10.1371/journal.pone.0007669.

Rosenberg, S. A. *et al.* (1989) 'Experience with the Use of High-Dose Interleukin-2 in the Treatment of 652 Cancer Patients', *Annals of Surgery*, 210(4), pp. 474–484.

Rosenberg, S. A. *et al.* (2011) 'Durable complete responses in heavily pretreated patients with metastatic melanoma using T-cell transfer immunotherapy', *Clinical Cancer Research*. doi: 10.1158/1078-0432.CCR-11-0116.

Rosenberg, S. A. (2014) 'IL-2: The First Effective Immunotherapy for Human

Cancer', *The Journal of Immunology*. doi: 10.4049/jimmunol.1490019.
Rudensky, A. Y. (2011) 'Regulatory T cells and Foxp3', *Immunological Reviews*. doi: 10.1111/j.1600-065X.2011.01018.x.
Sadlack, B. *et al.* (1993) 'Ulcerative colitis-like disease in mice with a disrupted interleukin-2 gene', *Cell*. doi: 10.1016/0092-8674(93)80067-O.
Sahin, U. *et al.* (2017) 'Personalized RNA mutanome vaccines mobilize poly-specific therapeutic immunity against cancer', *Nature*. doi: 10.1038/nature23003.
Sakaguchi, S. *et al.* (1995) 'Immunologic self-tolerance maintained by activated T cells expressing IL-2 receptor alpha-chains (CD25). Breakdown of a single mechanism of self-tolerance causes various autoimmune diseases.', *Journal of immunology (Baltimore, Md. : 1950)*.
Scheffold, A., Murphy, K. M. and Höfer, T. (2007) 'Competition for cytokines : T reg cells take all', *Nature Immunology*, 8(12), pp. 1285–1287.
Schildberg, F. A. *et al.* (2016) 'Coinhibitory Pathways in the B7-CD28 Ligand-Receptor Family', *Immunity*. doi: 10.1016/j.immuni.2016.05.002.
Schwartz, J. C. D. *et al.* (2002) 'Structural mechanisms of costimulation', *Nature Immunology*. doi: 10.1038/ni0502-427.
Selby, M. J. *et al.* (2013) 'Anti-CTLA-4 Antibodies of IgG2a Isotype Enhance Antitumor Activity through Reduction of Intratumoral Regulatory T Cells', 1(July), pp. 32–43. doi: 10.1158/2326-6066.CIR-13-0013.
Shang, B. *et al.* (2015) 'Prognostic value of tumor-infiltrating FoxP3+ regulatory T cells in cancers: A systematic review and meta-analysis', *Scientific Reports*. doi: 10.1038/srep15179.
Shankaran, V. *et al.* (2001) 'IFNγ, and lymphocytes prevent primary tumour development and shape tumour immunogenicity', *Nature*. doi: 10.1038/35074122.
Sharfe, N. *et al.* (1997) 'Human immune disorder arising from mutation of the α chain of the interleukin-2 receptor', *Proceedings of the National Academy of Sciences of the United States of America*. doi: 10.1073/pnas.94.7.3168.
Sharma, A. *et al.* (2019) 'Anti-CTLA-4 immunotherapy does not deplete Foxp3 þ regulatory T cells (Tregs) in human cancers', *Clinical Cancer Research*, 25(4), pp. 1233–1238. doi: 10.1158/1078-0432.CCR-18-0762.
Sharpe, A. H. and Freeman, G. J. (2002) 'The B7-CD28 superfamily', *Nature*

Reviews Immunology. doi: 10.1038/nri727.

Shimizu, J. *et al.* (2002) 'Stimulation of CD25 + CD4 + regulatory T cells through GITR breaks immunological self-tolerance', *Nature Immunology*, 3(2), pp. 135–142. doi: 10.1038/ni759.

Shimizu, J., Yamazaki, S. and Sakaguchi, S. (1999) 'Induction of tumor immunity by removing CD25+CD4+ T cells: a common basis between tumor immunity and autoimmunity.', *Journal of immunology (Baltimore, Md. : 1950)*, 163(10), pp. 5211–8. Available at: http://www.ncbi.nlm.nih.gov/pubmed/10553041.

Sifniotis, V. *et al.* (2019) 'Current Advancements in Addressing Key Challenges of Therapeutic Antibody Design, Manufacture, and Formulation', *Antibodies*. doi: 10.3390/antib8020036.

Simpson, Tyler R *et al.* (2013) 'Fc-dependent depletion of tumor-infiltrating regulatory T cells co-defines the efficacy of anti-CTLA-4 therapy against melanoma.', *The Journal of experimental medicine*. doi: 10.1084/jem.20130579.

Simpson, Tyler R. *et al.* (2013) 'Fc-dependent depletion of tumor-infiltrating regulatory t cells co-defines the efficacy of anti-CTLA-4 therapy against melanoma', *Journal of Experimental Medicine*. doi: 10.1084/jem.20130579.

Śledzińska, A. *et al.* (2015) 'Review 2015-Negative immune checkpoints on T lymphocytes and cancer immunotherapy', *Molecular oncology*. doi: 10.1016/j.molonc.2015.10.008.

Śledzińska, A. *et al.* (2020) 'Regulatory T Cells Restrain Interleukin-2- and Blimp-1-Dependent Acquisition of Cytotoxic Function by CD4+ T Cells', *Immunity*. doi: 10.1016/j.immuni.2019.12.007.

Smith, C. *et al.* (2012) 'IDO is a nodal pathogenic driver of lung cancer and metastasis development', *Cancer Discovery*. doi: 10.1158/2159-8290.CD-12-0014.

Smith, P. *et al.* (2012) 'Mouse model recapitulating human Fcγ receptor structural and functional diversity', *Proceedings of the National Academy of Sciences of the United States of America*. doi: 10.1073/pnas.1203954109.

So, T. *et al.* (2005) 'Haplotype loss of HLA class I antigen as an escape mechanism from immune attack in lung cancer', *Cancer Research*. doi: 10.1158/0008-5472.CAN-04-3787.

Song, J. *et al.* (2008) 'Intracellular signals of T cell costimulation', *Cellular and Molecular Immunology*. doi: 10.1038/cmi.2008.30.

Spiess, C., Zhai, Q. and Carter, P. J. (2015) 'Alternative molecular formats and therapeutic applications for bispecific antibodies', *Molecular Immunology*. doi: 10.1016/j.molimm.2015.01.003.

Spolski, R., Li, P. and Leonard, W. J. (2018) 'Biology and regulation of IL-2: from molecular mechanisms to human therapy', *Nature Reviews Immunology*. Springer US, 18(10), pp. 648–659. doi: 10.1038/s41577-018-0046-y.

Suzuki, H. *et al.* (1995) 'Deregulated T cell activation and autoimmunity in mice lacking interleukin-2 receptor β', *Science*. doi: 10.1126/science.7770771.

Swanson, J. A. and Hoppe, A. D. (2004) 'The coordination of signaling during Fc receptor-mediated phagocytosis', *Journal of Leukocyte Biology*. doi: 10.1189/jlb.0804439.

Sznol, M. and Chen, L. (2013) 'Antagonist antibodies to PD-1 and B7-H1 (PD-L1) in the treatment of advanced human cancer', *Clinical Cancer Research*. doi: 10.1158/1078-0432.CCR-12-2063.

Takahashi, T. *et al.* (1998) 'Immunologic self-tolerance maintained by CD25 + CD4 + naturally anergic and suppressive T cells: Induction of autoimmune disease by breaking their anergic/suppressive state', *International Immunology*. doi: 10.1093/intimm/10.12.1969.

Terme, M. *et al.* (2013) 'VEGFA-VEGFR pathway blockade inhibits tumor-induced regulatory T-cell proliferation in colorectal cancer', *Cancer Research*. doi: 10.1158/0008-5472.CAN-12-2325.

Thomson, C. A. (2016) 'IgG Structure and Function', in *Encyclopedia of Immunobiology*. doi: 10.1016/B978-0-12-374279-7.05002-5.

Thornton, A. M. and Shevach, E. M. (1998) 'CD4+CD25+ immunoregulatory T cells suppress polyclonal T cell activation in vitro by inhibiting interleukin 2 production', *Journal of Experimental Medicine*, 188(2), pp. 287–296. doi: 10.1084/jem.188.2.287.

Todd, J. A. (2010) 'Etiology of Type 1 Diabetes', *Immunity*. doi: 10.1016/j.immuni.2010.04.001.

Togashi, Y., Shitara, K. and Nishikawa, H. (2019) 'Regulatory T cells in cancer immunosuppression — implications for anticancer therapy', *Nature Reviews Clinical Oncology*. doi: 10.1038/s41571-019-0175-7.

Umansky, V. *et al.* (2016) 'The role of myeloid-derived suppressor cells (MDSC) in cancer progression', *Vaccines*. doi: 10.3390/vaccines4040036.

Valzasina, B. *et al.* (2005) 'Triggering of OX40 (CD134) on CD4+CD25+ T cells blocks their inhibitory activity: A novel regulatory role for OX40 and its comparison with GITR', *Blood*. doi: 10.1182/blood-2004-07-2959.

Vargas, F. A. *et al.* (2017) 'Fc-Optimized Anti-CD25 Depletes Tumor-Infiltrating Regulatory T Cells and Synergizes with PD-1 Blockade to Eradicate Established Tumors', *Immunity*, 46(4), pp. 577–586. doi: 10.1016/j.immuni.2017.03.013.

Vargas, F. A. *et al.* (2018) 'Fc Effector Function Contributes to the Activity of Human Anti-CTLA-4 Antibodies', *Cancer Cell*, 33(4), pp. 649-663.e4. doi: 10.1016/j.ccell.2018.02.010.

Vazquez-Lombardi, R. *et al.* (2018) 'Transient expression of human antibodies in mammalian cells', *Nature Protocols*. doi: 10.1038/nprot.2017.126.

Villadolid, J. and Amin, A. (2015) 'Immune checkpoint inhibitors in clinical practice: Update on management of immune-related toxicities', *Translational Lung Cancer Research*. doi: 10.3978/j.issn.2218-6751.2015.06.06.

Waight, J. D. *et al.* (2018) 'Selective FcγR Co-engagement on APCs Modulates the Activity of Therapeutic Antibodies Targeting T Cell Antigens', *Cancer Cell*, 33(6), pp. 1033-1047.e5. doi: 10.1016/j.ccell.2018.05.005.

Walker, L. S. K. and Sansom, D. M. (2011) 'The emerging role of CTLA4 as a cell-extrinsic regulator of T cell responses', *Nature Reviews Immunology*. doi: 10.1038/nri3108.

Walunas, T. L. *et al.* (1994) 'CTLA-4 can function as a negative regulator of T cell activation', *Immunity*. doi: 10.1016/1074-7613(94)90071-X.

Wang, T. T. *et al.* (2017) 'Signaling by Antibodies: Recent Progress', *Annual Review of Immunology*, 35(1), pp. 285–311. doi: 10.1146/annurev-immunol-051116-052433.

Wang, X., Mathieu, M. and Brezski, R. J. (2018) 'IgG Fc engineering to modulate antibody effector functions', *Protein and Cell*. doi: 10.1007/s13238-017-0473-8.

Ward-Kavanagh, L. K. *et al.* (2016) 'The TNF Receptor Superfamily in Co-stimulating and Co-inhibitory Responses', *Immunity*. doi: 10.1016/j.immuni.2016.04.019.

Weng, W. K. and Levy, R. (2003) 'Two immunoglobulin G fragment C receptor polymorphisms independently predict response to rituximab in patients with follicular lymphoma', *Journal of Clinical Oncology*. doi: 10.1200/JCO.2003.05.013.

Wijesuriya, S. D. *et al.* (2018) 'Antibody engineering to improve manufacturability', *Protein Expression and Purification*. doi: 10.1016/j.pep.2018.04.003.

Willerford, D. M. *et al.* (1995) 'Interleukin-2 receptor α chain regulates the size and content of the peripheral lymphoid compartment', *Immunity*. doi: 10.1016/1074-7613(95)90180-9.

Wilson, N. S. *et al.* (2013) 'Activating Fc γ receptors contribute to the antitumor activities of immunoregulatory receptor-targeting antibodies', *The Journal of Experimental Medicine*, 210(9), pp. 1685–1693. doi: 10.1084/jem.20130573.

Wolchok, J. D. *et al.* (2013) 'Fc-dependent depletion of tumor-infiltrating regulatory T cells co-defines the efficacy of anti–CTLA-4 therapy against melanoma', *The Journal of Experimental Medicine*. doi: 10.1084/jem.20130579.

Wolchok, J. D. *et al.* (2017) 'Overall Survival with Combined Nivolumab and Ipilimumab in Advanced Melanoma', *New England Journal of Medicine*. doi: 10.1056/NEJMoa1709684.

Yang, X. P. *et al.* (2011) 'Opposing regulation of the locus encoding IL-17 through direct, reciprocal actions of STAT3 and STAT5', *Nature Immunology*. doi: 10.1038/ni.1995.

You, M. *et al.* (2018) 'Efficient mAb production in CHO cells with optimized signal peptide, codon, and UTR', *Applied Microbiology and Biotechnology*. doi: 10.1007/s00253-018-8986-5.

Zheng, P. P., Kros, J. M. and Li, J. (2018) 'Approved CAR T cell therapies: ice bucket challenges on glaring safety risks and long-term impacts', *Drug Discovery Today*. doi: 10.1016/j.drudis.2018.02.012.

Zhou, J. and Meadows, G. G. (2003) 'Alcohol consumption decreases IL-2-induced NF-κB activity in enriched NK cells from C57BL/6 mice', *Toxicological Sciences*. doi: 10.1093/toxsci/kfg047.

Zitvogel, L., Tesniere, A. and Kroemer, G. (2006) 'Cancer despite immunosurveillance: Immunoselection and immunosubversion', *Nature*

Reviews Immunology. doi: 10.1038/nri1936.

7 Annex

7.1 Supplementary Figures

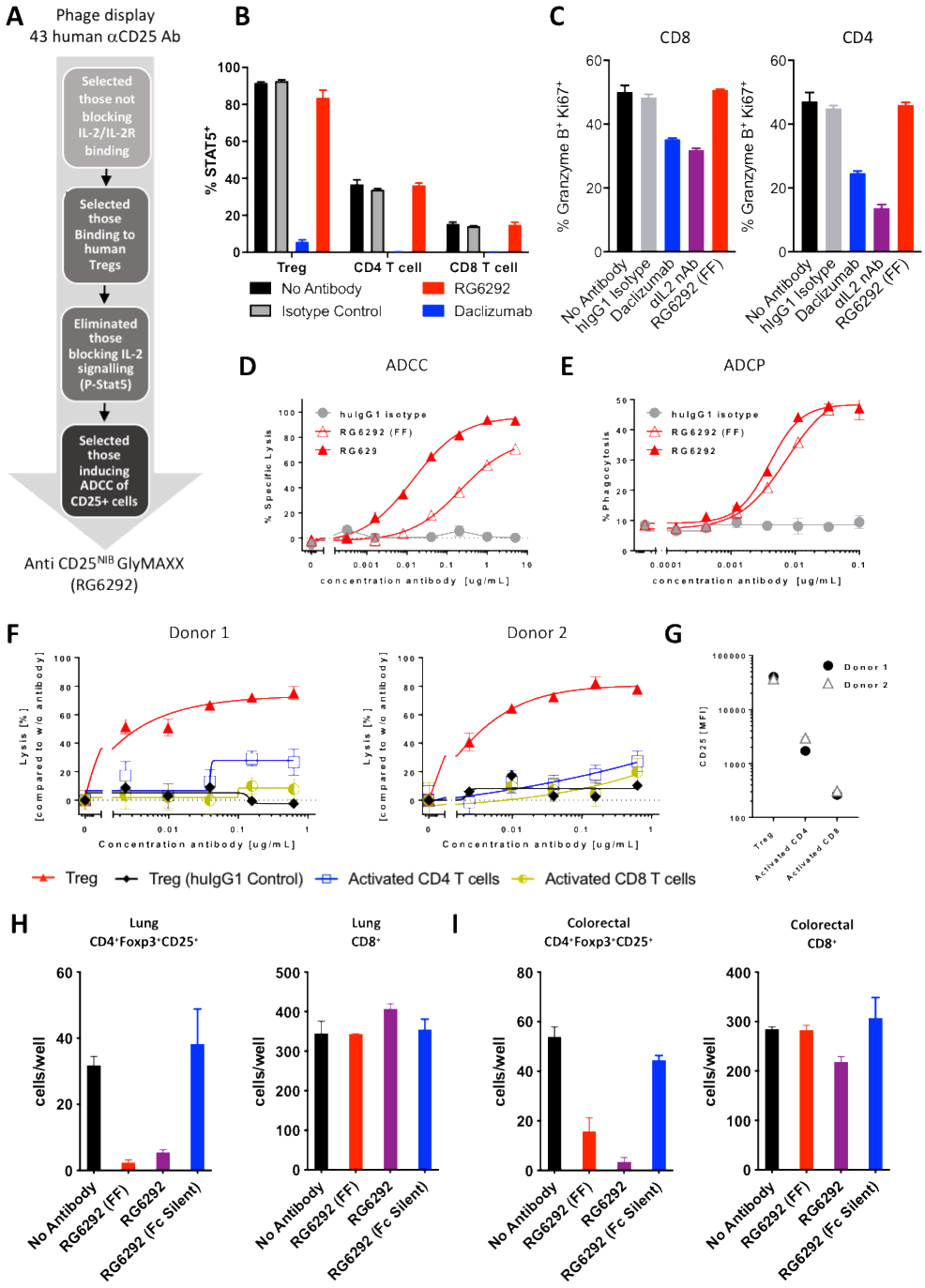

Figure 7.1. the non-IL-2-blocking anti human CD25 antibody RG6292 preferentially depletes Regulatory T cells in vitro and in patient tumour samples.

(A) From the 43 human CD25 antibodies generated by Adimab, 31 were shown to not compete with IL-2 binding to CD25. All the antibodies that were binding to CD25 expressed on Treg cells were assessed for their ability not to block IL-2 signalling in a STAT5 assay. Killing of these non-IL2 blocking antibodies was then assessed in classical ADCC and ADCP assays resulting in the selection of the lead candidates. **(B)** Characterization of CD25 antibodies in respect to blocking IL-2 signalling in a STAT5 phosphorylation assay using PBMCs of human origin. Daclizumab and Basilixumab were used as blocking controls compared to human IgG1 isotype control or in absence of a primary antibody. Cells were incubated with 10µg/ml antibody followed by 10U/ml IL-2. Analysis was restricted to percentage of CD3-positive cells phosphorylating STAT5. **(C)** Impact of IL-2 signalling on Teff responses was characterised in a T cell activation assay, in which intracellular granzyme B upregulation and proliferation were examined. Pan T cells were incubated with 10ug/ml antibody, then activated with CD3/CD28 beads for 72 hours before flow cytometry analysis. **(D)** *in-vitro* differentiated Treg were co-cultured with purified IL-2 activated NK cells and target cell depletion was measured by flow cytometry. **(E)** *in-vitro* differentiated Treg cells were co-cultured with MCSF differentiated Macrophages. Two colour flow cytometric analysis was performed with CD14+ stained Macrophages and eFluor450-dye labelled Tregs to determine percentage of phagocytosis of these cells in the presence of the different aCD25 antibodies. **(F and G)** Resting human PBMC (2 donors) were labelled with CFSE. Cells were cultured on irradiated fibroblast in the presence of CD3 activation beads for three days to induce CD25 expression on T cells. Whilst T cell activation a serial dilution of aCD25^{NIB} GlyMAXX or human IgG control was added for lysis of CD25 positive target cells by PBMC endogenous FcR^{+} cells. CD25 staining was performed to confirm target expression. Flow cytometric analysis was performed to quantify Treg cells (CD4+ FoxP3+ CFSE high) activated CD4 (CD4+ FoxP3- CD69+) and CD8 T cells (CD8+ CD69+) within activated PBMC sample after 72 hrs of cytotoxic reaction. Lysis was calculated for respective fraction and plotted against antibody concentration. For human IgG1 control only Treg cells are shown. Samples were measured in triplicates. **(H and I)** Graphs showing the killing of Foxp3+CD25+ cells within human tumours (frozen dissociated tumour cells obtained from Conversant Bio) supplemented with allogeneic NK cells.

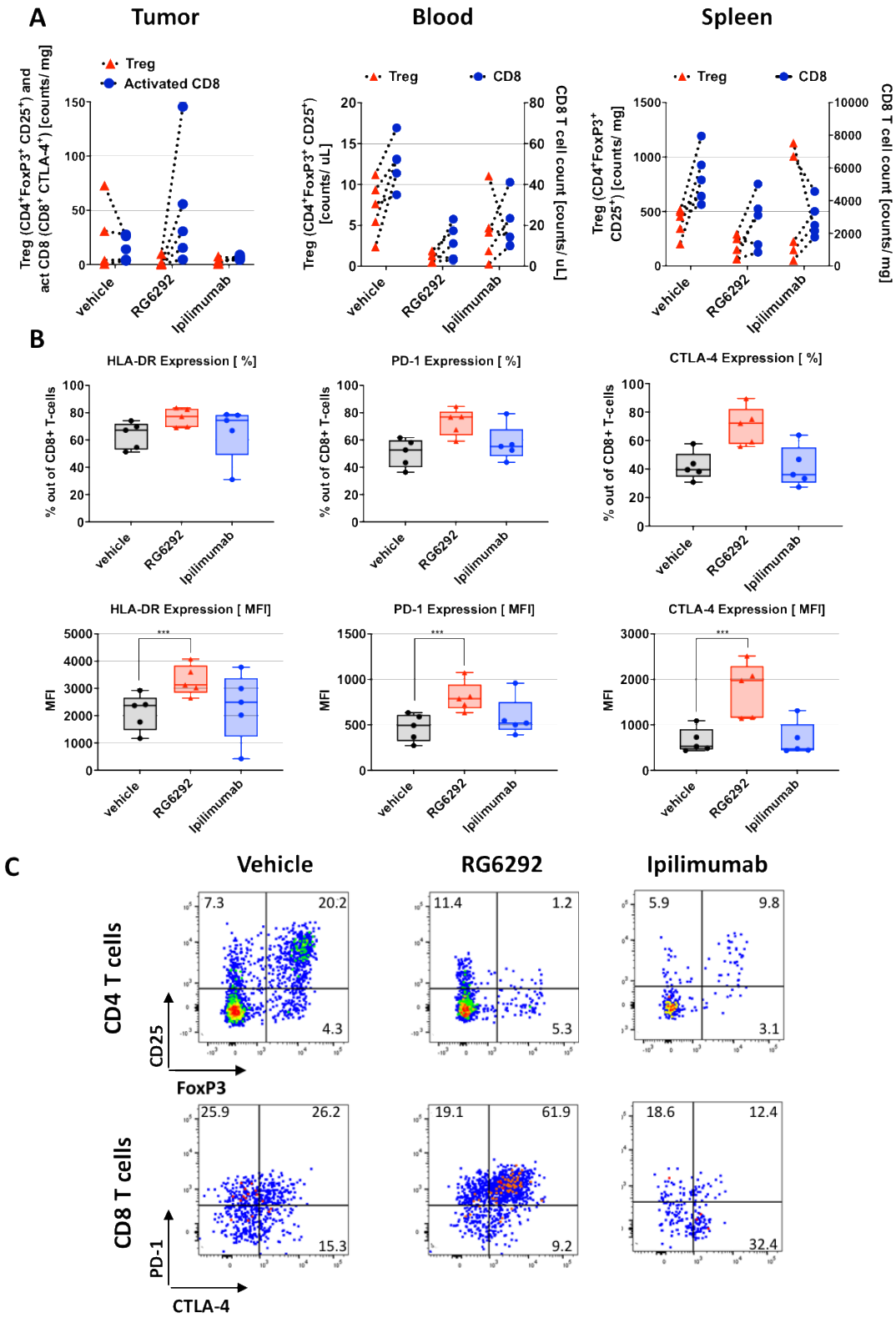

Figure 7.2. A single dose of RG6292 systematically depletes Treg cells in tumour bearing humanized mice whilst allowing accumulation of activated CD8+ T cells.

Stem cell humanized NOG mice were s.c. injected with BxPC-3 prostate adenocarcinoma cells in matrigel. Mice were injected i.p. with Vehicle, RG6292 [4 mg/kg] or Ipilimumab [10 mg/kg]. 72 hours after monotherapy injection, splenocytes, blood lymphocytes and tumor infiltrating lymphocytes were isolated and evaluated for counts of activated CD8 T cells (huCD45+, huCD3+, huCD8+ huCTLA-4+) and Tregs (huCD45+, huCD3+, huCD4+, huFoxP3+) as well as for markers of recent T cell activation. **(A)** Normalized counts were plotted for the respective treatment groups. Each symbol represents one animal, CD8 and Treg cells are connected for the same animals. Ipilimumab as well as RG6292 decreased the intratumoural Treg counts. An increase of intratumoural activated CD8 T cell count was only evident after administration of RG6292. **(B)** The % of marker positive cells and MFI were plotted for the respective treatment groups. Each symbol represents one animal. RG6292 increased PD-1, CTLA-4 and HLA-DR on intratumoural CD8 T cells. **(C)** Representative FACS plots showing CD25 expression versus FoxP3 expression in CD4 T cells and PD-1 expression versus CTLA-4 expression in CD8 T cells. Statistical analysis of RG6292 and Ipilimumab treated group against Vehicle group is indicated.